International Science And Technology Center

FINAL REPORT

Investigation of the possibility of the application of the under-critical microwave streamer gas discharge for the ignition of a fuel in the jet engine.

Project #1840p

June 1, 2000 – May 30, 2001

MRTI RAS
Moscow

REPORT DOCUMENTATION PAGE

Form Approved OMB No. 0704-0188

1. AGENCY USE ONLY (Leave blank)	2. REPORT DATE	3. REPORT TYPE AND DATES COVERED
	20-April-2001	Final Report

4. TITLE AND SUBTITLE

Investigation of a Possibility of Application of the Undercritical Microwave Streamer Gas Discharge for Ignition of Fuel in Jet Engines

5. FUNDING NUMBERS

ISTC Registration No: 1840

6. AUTHOR(S)

Dr. Igor Esakov

7. PERFORMING ORGANIZATION NAME(S) AND ADDRESS(ES)

Federal State Unitary Firm Moscow Radio-Technical Institute RAS (FSUF MRTI RAS)
Warshavskoe Shosse 132
Moscow 113519
Russia

8. PERFORMING ORGANIZATION REPORT NUMBER

N/A

9. SPONSORING/MONITORING AGENCY NAME(S) AND ADDRESS(ES)

EOARD
PSC 802 BOX 14
FPO 09499-0200

10. SPONSORING/MONITORING AGENCY REPORT NUMBER

ISTC 00-7006

11. SUPPLEMENTARY NOTES

12a. DISTRIBUTION/AVAILABILITY STATEMENT

Approved for public release; distribution is unlimited.

12b. DISTRIBUTION CODE

A

13. ABSTRACT (Maximum 200 words)

This report results from a contract tasking Federal State Unitary Firm Moscow Radio-Technical Institute RAS (FSUF MRTI RAS) as follows: The goal of presented project consists in experimental and theoretical investigations of the physics of the initiated undercritical streamer microwave discharge for creation of the principally new system of ignition of the fuel-mixture in the jet engine. Creation of the reliable system of ignition of the fuel-mixture in the jet engine that can ignite the fuel and also insure the second start the engine after its stop during a flight stays nowadays the important problem at supersonic and hypersonic speeds of flight. Experimental and theoretical investigations that are planned to be carried out in the frames of the project will allow to obtain the data about the properties of the this discharge in a gas flow (in the supersonic flow as well) at different characteristics of the microwave radiation, fuel types and flow parameters. They will also allow to obtain the evaluation of the temperature and to demonstrate the possibility of the ignition of the flammable mixtures with the use of the microwave discharge. The data obtained during the project will allow coming to the preparation of the investigations on the real jet engine. Results of the laboratory experiments and theoretical investigations are of great scientific importance for the development of the fundamental physics of gas discharges. The data obtained during the investigation of the Initiated undercritical streamer microwave discharge in the high-speed flow will allow to develop the principally new system of the ignition of the fuel-mixture in the jet engines. The system of the ignition based on it will realize the volume-type fuel ignition over the whole combustion-chamber cross-section including the case of stoppage of the engine in flight. Besides, results obtained in the course of the fulfillment of the project will be of great value for other problems of plasma-gasdynamics since the microwave discharge are of promising prospects of the application here. The project in full scale corresponds to the main goal of ISTC to give the scientists and specialists connected with the production of the weapons the possibilities for the scientific investigations in the peaceful areas promoting the solution of the international technical problems and supporting the transition to the market economy.

14. SUBJECT TERMS

EOARD, Propulsion, Engines and Fuels, Combustion & Ignition

15. NUMBER OF PAGES

16. PRICE CODE
N/A

17. SECURITY CLASSIFICATION OF REPORT	18. SECURITY CLASSIFICATION OF THIS PAGE	19, SECURITY CLASSIFICATION OF ABSTRACT	20. LIMITATION OF ABSTRACT
UNCLASSIFIED	UNCLASSIFIED	UNCLASSIFIED	UL

List of main authors

Kirill V. Khodataev, Scientific Head of the Project
Igor I. Esakov, Project Manager
Lev P. Grachev, Chief experimenter

Content

1. Introduction

Present work is a continuation of investigations carried out in the frame of special project SPS-97-4003 under the title "Experimental investigation of a Possibility of Application of the Microwave Streamer Gas Discharge for Ignition of Fuel in a Jet Engine" [1].

Distinctive feature of that work is an application of a microwave discharge ignited in quasioptical beam of electromagnetic (EM) waves. Such a discharge is ignited in a space area far from elements forming EM beam. In principle, it can be located far from other elements of a construction, i.e. it can be realized as though in a free space. EM beam is called "quasioptical" in a sense that it can have sizes about tens of wavelength of microwave radiation along its propagation and about some units of a wavelength in the transverse direction. So a discharge region can have typical sizes also about some units of a wavelength. The discharge is the pulse type with typical maximal pulse duration of some tens of microseconds. Such a discharge is as a rule substantially non stationary in a space. It has a tendency to propagate toward EM radiation from a place of its origin, covering larger and larger area of a microwave beam.

Properties of such a discharge revealed during our previous work are represented in a Fig.1.1. In this picture typical photos of microwave discharges at experimentally used wavelength λ=8.9 cm of EM field and tp=40 μs duration of the microwave pulse are represented in coordinates air pressure p and ratio of the amplitude of the microwave field E_0 to the critical breakdown amplitude E_c for a given pressure.

In the photos the direction of EM wave with TEM structure is from left to the right and a vector of the linear polarized electric field lies in a plane of the picture.

From the picture it can be seen that in the overcritical field at $\mathbf{E_0/E_{cr}>1}$ at **p**=50 Torr such a discharge is of the diffuse type and at higher pressures it is of the streamer type.

However during experiments it was revealed that a discharge of this type can be realized in substantially under-critical field ($\mathbf{E_0/E_{cr}}$<1). For this purpose the discharge has to be initiated, it means that local breakdown conditions are to be formed. In the undertaken works the discharge was initiated at the location of a small metallic ball into EM beam or of microwave vibrator (metallic cylinder) located parallel to an electric field vector.

The corresponding photos at $\mathbf{E_0/E_{cr}}$<1 are represented in Fig.1.1 also. In the picture the form of a discharge initiated by a ball is the diffuse one, since the discharge is realized at low **p**. At the same time the streamer under-critical discharge corresponds to normal atmospheric air pressure. One can see a vibrator to the right in the photo of the streamer under-critical discharge. It is made in the form of a metallic cylinder with spherically rounded ends, it is of 3 cm length and of 0.8 mm diameter.

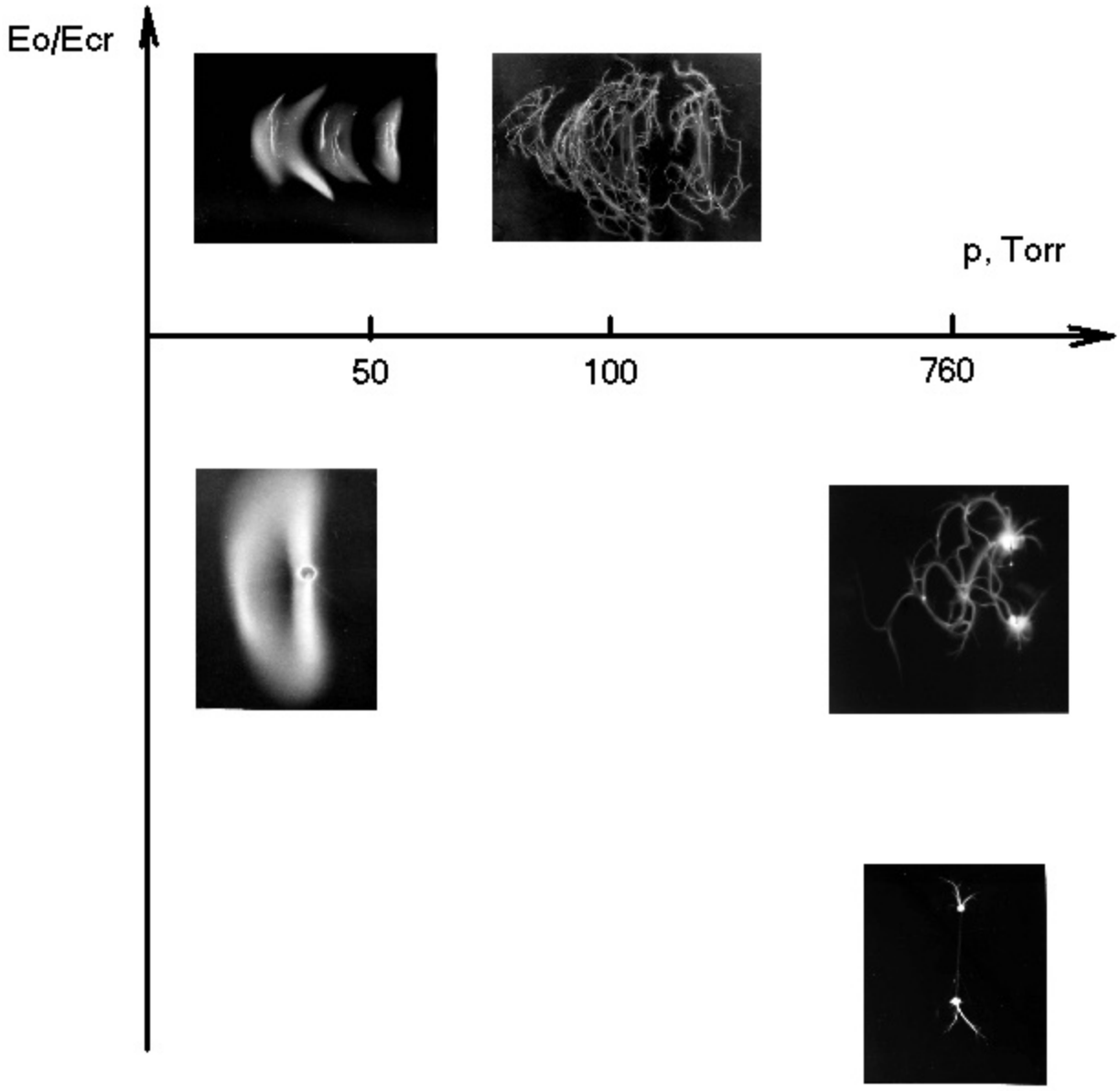

Fig.1.1. The types of the discharge dependence from electric field and gas pressure.

Streamer under-critical discharge in the integral photos does not practically differ from analogous discharges in the under-critical field and conserves main important for practical applications property to absorb well oncoming on it energy of EM wave. Investigations of this discharge have shown that being originated on the initiator's poles it propagates toward the radiation with a supersonic velocity of 10^5 cm/s scale.

Discharge looses the capability to detach from the initiator with the decrease of the amplitude of the EM wave in the microwave beam below some boundary value. A typical photo of such an under-critical discharge in the air of atmospheric pressure at $\mathbf{E_0/E_{cr}}<<1$ is represented in Fig.1.1 at bottom.

A gas temperature inside the streamer channels of the under-critical and deeply under-critical discharges was evaluated in the undertaken experiments. Its scale was some thousands of Kelvin degrees. In principle such value of the temperature can be enough for a flammable mixture ignition in a real scramjet. In the fulfilled work two

schemes of such ignition were proposed. They are represented in Fig.1.2 and 1.3. In the Fig.1.2 the scheme of the ignition with the application of the under-critical discharge is represented. The scheme of deeply under-critical discharge is shown at Fig.1.3.

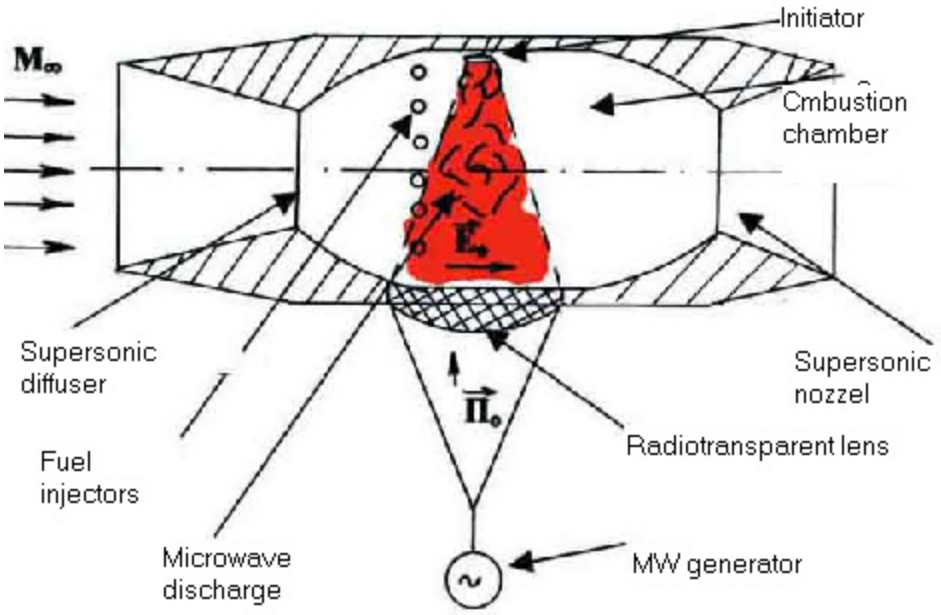

Fig.1.2. The scheme of the fuel ignition by means of under-critical discharge.

The present report is devoted to the further investigations of the possibility of the application of the microwave discharge in the quasioptical wave beam for the ignition of a fuel in a jet engine for both forms: the under-critical ($E_0/E_{cr}<1$) and deeply under-critical ($E_0/E_{cr}<<1$)

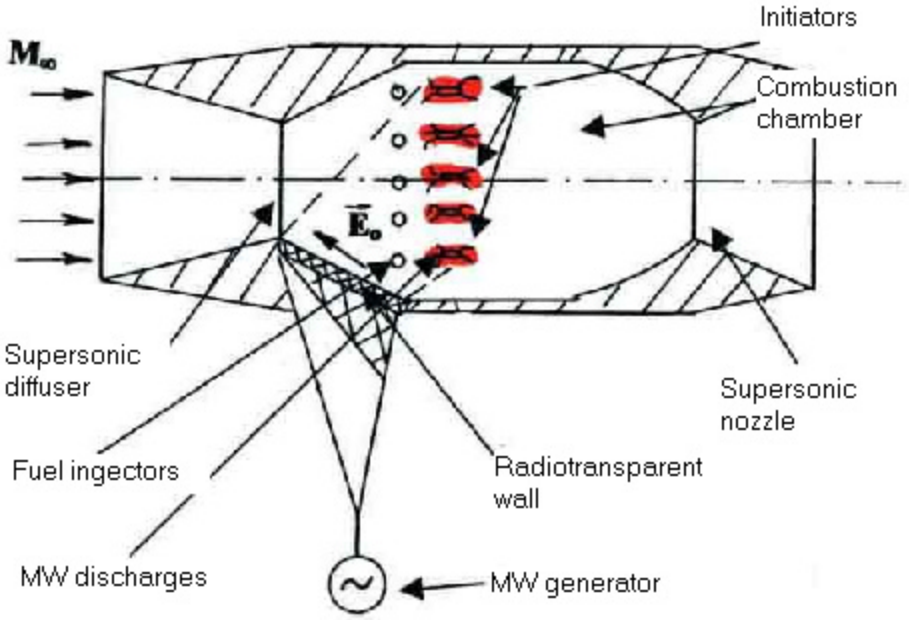

Fig.1.3. The scheme of the fuel ignition by means of deeply under-critical discharge.

Main goals of the work are the follows:

1. Experimental determination of the boundary between these two discharge forms of discharge at the plot of the microwave field amplitude and air pressure. Knowledge of this boundary value allows to calculate the microwave beam power that is necessary for realization of the fuel ignition according to schemes represented in Fig.1.2 or Fig.1.3.

2. Ignition of the under-critical and deeply under-critical streamer discharge in air flow including a supersonic flow. As it was noted above the velocity of the streamer channel's growth are of the scale 10^5 cm/s, hence a flow with much lower velocity (of the scale 10^4 cm/s) will not qualitatively change the discharge character. However, naturally only experiments can give the final answer to this question.

3. Conducting of the more precise experiments on measurement of a temperature inside the streamer channels and determination of energy release inside of them. Ultimately namely these values determine the possibility of the application of this type discharges for realization of the goals.

4. Demonstration of the ignition of a model flammable mixture by means of the under-critical and deeply under-critical discharges. This experiment has to evidently demonstrate the principle possibility of realization of the task set.

5. Experiments with different wavelengths of the microwave radiation for the clarification of the type of changes in the discharge properties, connected with this characteristic.

6. Theoretical accompanying of experiments and developing of physical models of the under-critical streamer microwave discharges on this basis. This work will allow to solve set of problems in different definite conditions, but not only in those where experiments have been previously conducted.

7. Designing of the proposals for further investigations are to be elaborated on the basis of conducted works. They have to be close to solution of some problems that are facing developers of jet engines.

2.Experimental setup

A scheme of the experimental setup is represented in the Fig.2.1 and its photos from different positions are represented in the Fig.2.2 and 2.3. In this section we will describe only those elements that were used practically in all experiments. Specific devices we will describe in details in corresponding sections.

The main part of the setup consisted of the equipment that was used in previous investigations. At the same time the set was significantly enlarged.

The microwave generator is included into the setup. It ensures the maximum of the power P of the EM wave (P=1 MW) putted into the hermetic chamber by the single pulse with the maximal duration t_p=40 μs. The wavelength equals λ=8.9 cm.

A waveguide route of the arrangement was supplemented by the waveguide switch. It allowed to connect up the new microwave generator with λ=12.5 cm to the

setup. It gives the maximal output power P=2.5 kW in the continuous mode of generation.

Two controlled attenuators are installed into the waveguide route of the arrangement, their total coefficient of the field amplitude attenuation equals to 50.

On the exit from the route the linear-polarized EM wave with TEM field structure was formed with the application of a lens system of the circle aperture of 60 cm diameter. It was radiated into the hermetic chamber along its axis.

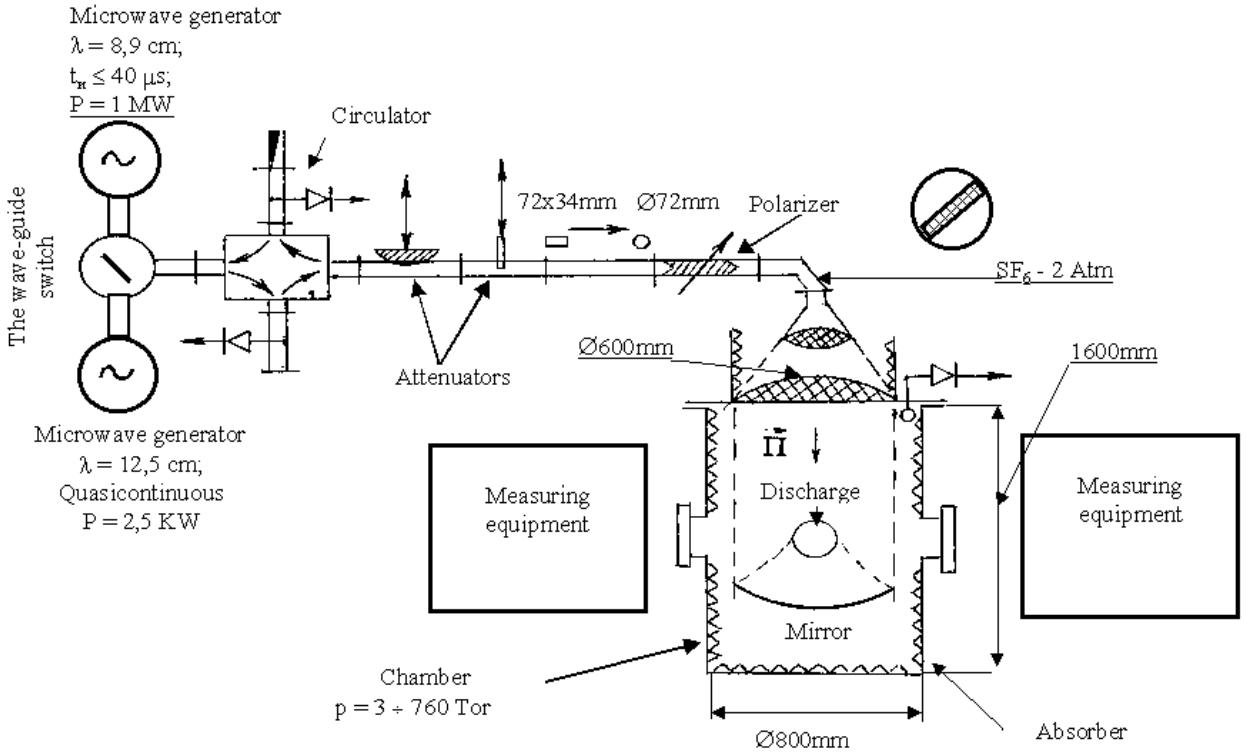

Fig.2.1. The scheme of the experimental installation.

A cylindrical chamber had internal diameter about 80 cm and a length about 2 m. It was possible to set the air pressure from 3 to 760 Torr in it, the pressure was measured with the accuracy ~1.5 Torr. A metallic mirror is installed in the chamber. The EM radiation is focused by the mirror on its axis in the chamber.

Value of the field in the EM beam focus at which the experiments were conducted was checked with a means of an inductive loop placed in the chamber. The microwave signal went from the loop to an amplitude detector, amplifier and to the oscillograph with memory. In frames of the setup modernization a special cycle of works was carried out for measurement of the field absolute value. The specially designed method of measurement allows to conduct experiments more precisely. This method of the absolute field calibration is described below in details.

It was possible to locate a metallic ball or a microwave vibrator in the area of the focus. The surface of their poles could be lighted by the ultra violet (UV) pulse that ensured the appearance of a small number of photoelectrons near it. Namely they start avalanche and then give a discharge.

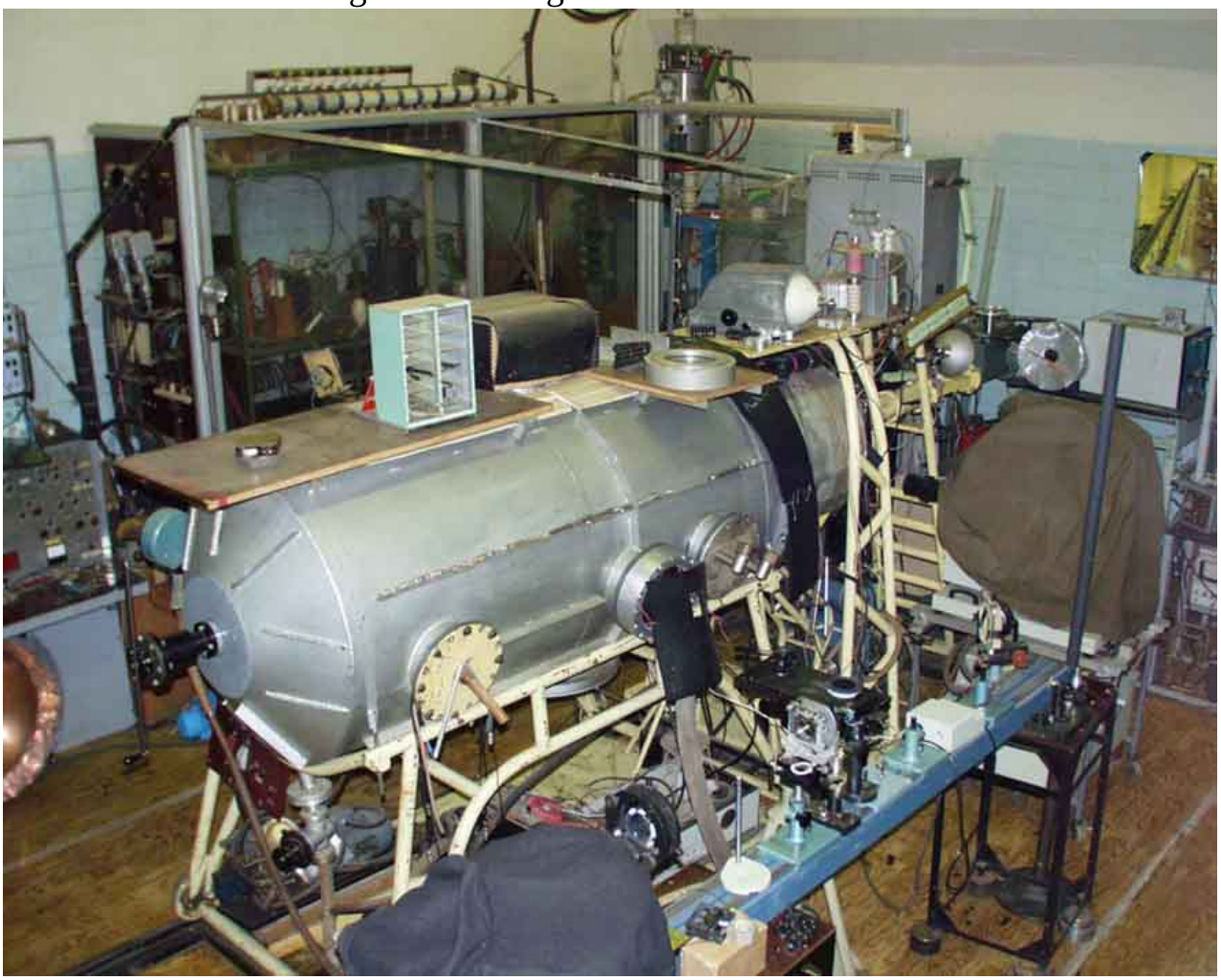

Fig.2.2. The general view on the experimental chamber.

The chamber was additionally completed by a device that allowed to create a supersonic emerged air jet in the focus area. In details it is described in a corresponding section.

3. The method of the measurement of a local absolute value of the microwave electric field

Before the description of experiments on determination of threshold that separates the under-critical discharge from deeply under-critical discharge we will describe works that allowed to conduct more precisely the quantitative measurements of a field in EM beam. In a theoretical part of this section we will introduce and determine some notions that later will be used in other sections of the report.

Determination of local absolute value of a field value in EM beam usually encounters with serious difficulties. Often one is limiting himself by the estimation of

these values on the basis of geometry of the focusing EM beam system and initial generator's power.

It seems that the amplitude of the field established in the focus can be calculated by use of so called Paschen curve by means of experimentally measured maximal air pressure at which its breakdown in this field is still realized [2]. However the situation becomes difficult for the analysis because of a small number of free electrons in air in the natural conditions. This circumstance gives a stochastic property to the breakdown process and experimental points "substantially do not lie" on the Paschen curve [3,4].

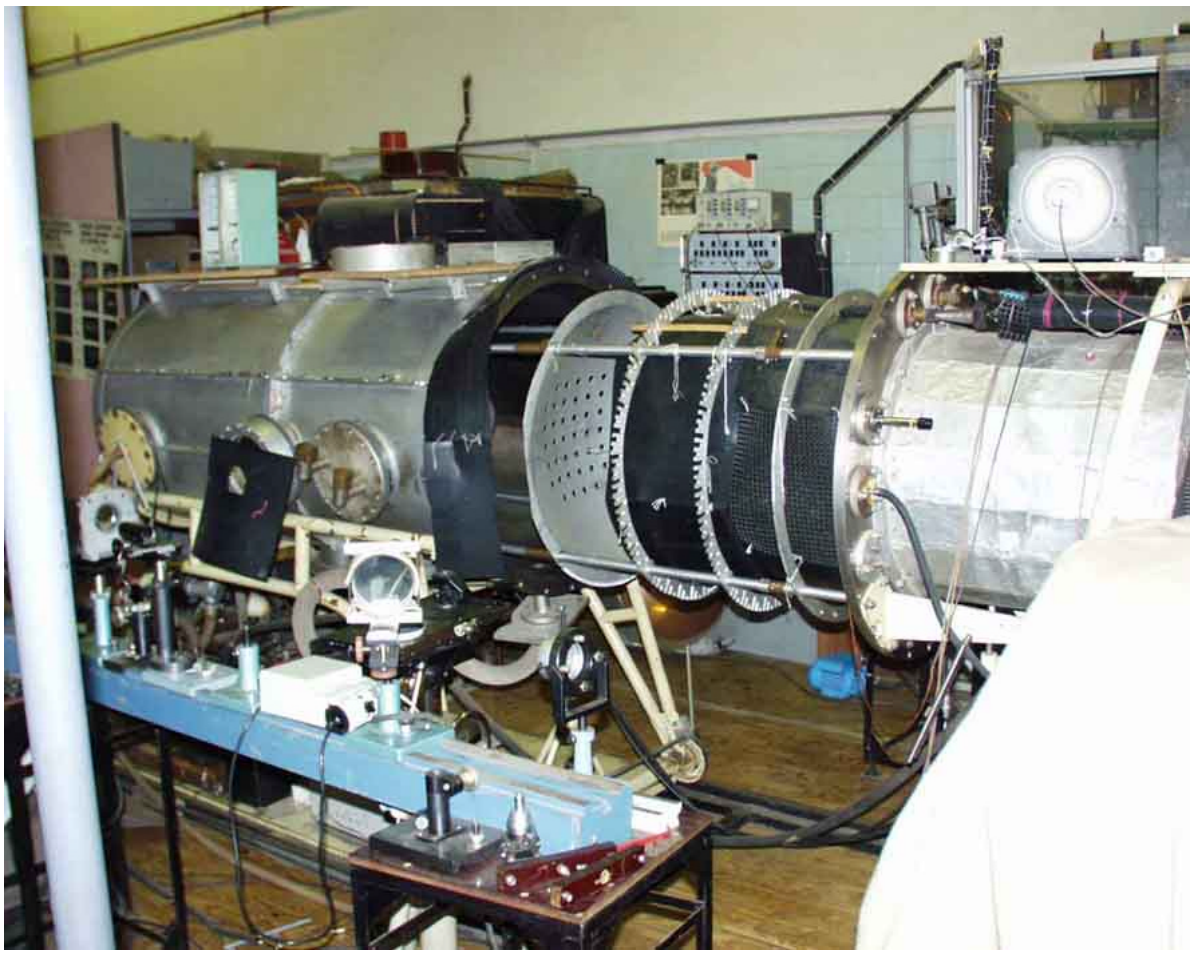

Fig.2.3. The view of the opened experimental chamber. One can see the spherical metal mirror for focusing of the microwave radiation.

The application of the penetrating radiation previously ionizing a gas (for example UV source) does not solve this problem because the property of the discharge at ionizing radiation can be changed unpredictably and qualitatively. This fact is most important in our experimental situation when such a source has to be located outside the EM beam about tens of centimeters far from the focus area and, hence, has to be powerful enough.

In the present investigations an original method free from the noted shortcoming was applied for determining of the local field level. In the experiment the routine "breakdown" methods was applied: the maximal air pressure at which a breakdown is

still possible at a given but unknown value $\mathbf{E_0}$ in some point is being determined. But into this point the metallic ball is located. Its diameter is substantially smaller than the wavelength of a microwave field. Its surface is lighted by the far source of the UV radiation synchronized with the microwave pulse.

Our experience showed that for ensuring of required number of free electrons necessary for a discharge initiation realized by photo-emission from the ball surface the UV radiation of enough low intensity is needed, when its influence on the gas is excluded. In this case the breakdown process can be calculated correctly since the disturbance of electric field caused by a ball is known and in close to a ball region can be calculated on the basis of electrostatics. The situation becomes complicated due to diffusion electron losses in the breakdown process. But this factor can be considered in famous conditions correctly.

3.1. Theory of an air breakdown in a microwave wave beam at presence of a metallic ball

Balance of electrons (electron concentration) in air in linear approximation can be described by the equation (at small ionization degree, when the process of dissociative recombination of electrons and positive molecular ions, $e + M_2^+ \to 2M$, is insignificant)

$$\frac{\partial n}{\partial t} = D\Delta n + (n_i - n_a)n, \qquad (3.1)$$

Here n – is electron concentration, n_i and n_a – frequencies of ionization and attachment in processes: $e + M_2 \to 2e + M_2^+$ - ionization (M=N_2, O_2), $e + O_2 \to O + O^-$ - dissociative attachment, and D is coefficient of a diffusion. In the case of our interest we can accept for the breakdown criterion the following condition

$$\partial n / \partial t = 0 \qquad . \qquad (3.2)$$

It means that the ionization is compensated by the electron attachment and diffusion losses of electrons from a breakdown area. Usually ionization frequency is approximated by the formula [5]

$$?_i = ?_a \cdot \left(\frac{E}{E_{cr}} \right)^{ß}, \qquad \beta=5.3, \qquad (3.3)$$

where E is local value of the field amplitude,

$$E_{cr} = 30p\sqrt{2\left(1 + w^2/n_c^2\right)}\ , \text{ V/cm} \qquad (3.4)$$

is the amplitude of the critical (breakdown) field, ω - circular frequency of EM field,

$$n_a = 6.4 \cdot 10^4 p; \quad \text{s}^{-1} \qquad (3.5)$$

is the frequency of attachment,

$$n_c = 4.10^9 p; \text{ s}^{-1} \qquad (3.6)$$

is transfer collision frequency of electron-neutral molecule collisions. Here and in analogous formulas air pressure p is expressed in Torr.

If a ball of radius a<<1/k (k=2π/λ - a wave number) is placed into the microwave field $\mathbf{E_0}$ the field amplitude is maximal on the ball's poles (where a vector of the external field $\mathbf{E}_0$ is perpendicular to its surface) and equals $3\mathbf{E}_0$. At the ball equator the field equals zero. Hence the best breakdown conditions are realized at polar areas of the ball. The electric field at the pole is directed along the external field E_o.

At taking away from the ball's pole along E_0 the field is being decreased up to E_0 by the law

$$E = E_0 \cdot \left(1 + \frac{2}{(r/a)^3}\right). \qquad (3.7)$$

where r is distance from the ball center.

The Eq. (3.7) is right if the body is small in comparison with a wavelength, the boundaries are far from the body quite enough and the situation is far from electric-dynamical resonance. In this case the field structure is insensible to the ball presence so it does not influence on the general field distribution and field initial level. The ball is creating only local deviation described by (3.7). The refraction wave generated by the ball is small enough and is possible be not taken into account.

The ionization process will start near the ball pole where the maximal electric field equals to $3E_0$ and exceeds the critical value. It is easy to see that at $3E_0/E_{cr}-1<<1$ the ionization area represents the thin layer near the pole. It allows to simplify the task and to find the stationary solution of Eq. (3.1) in a frame of the 1D approximation.

The breakdown at the ball presence comes to the one-dimension problem of searching of a stationary distribution of electron concentration $\boldsymbol{n}(\boldsymbol{r})$ that would satisfy diffusion equation (3.1) at the condition (3.2) in non uniform field of form (3.7). Moreover $\boldsymbol{n}$ has to become equal to zero on the ball's surface at r=a and to decrease to zero at taking away from it. The required values of a field $\mathbf{E_0}$ and pressure **p** are present at the obtained distribution as parameters.

The diffusion equation (3.1) is reformed into the Airy equation (in the result of linearization of the function (3.3) for ν_i near the ball's surface relative to a value **E)**:

$$\frac{\partial^2 j}{\partial z^2} + \frac{z}{b^2 B^2} j = 0, \qquad (3.8)$$

Solution of the equation (3.8) is known [6,7]:

$$j = ? \begin{cases} z^{1/2}\left[J_{1/3}\left(\frac{2z^{3/2}}{3bB}\right) + J_{-1/3}\left(\frac{2z^{3/2}}{3bB}\right)\right], z > 0 \\ \left(-z^{1/2}\right)\cdot\left[-I_{1/3}\left(\frac{2(-x)^{3/2}}{3bB}\right) + I_{-1/3}\left(\frac{2(-z)^{3/2}}{3bB}\right)\right], z < 0 \end{cases} \qquad (3.9)$$

where $J_{\pm 1/3}(x)$, $I_{\pm 1/3}(x)$ are the Bessel functions. It automatically satisfy the condition posed on the distant boundary $\rho\to\infty$ ($z\to-\infty$), since there it is exponentially small.
Here we introduce the follows dimensionless parameters

$b=\nu_a a^2/D$,

$\varepsilon_{0=}E_0/E_{cr}$,

$A=(3\varepsilon_0)^{\beta}-1$,

$B=2\beta(3\varepsilon_0)^{\beta}$

and variables

$\rho=r/a$,

$\varphi=n\rho$,

$z=bA - bB(\rho-1)$.

The condition of the ball's surface $\varphi(\rho=1)=0$ is satisfied at

$2z^{3/2}/(3bB)=2.338.$ (3.10)

The higher eigenvalues are disregarded because j is alternating in sign.

On the surface of a ball we have $z=bA$ and from (3.10) finally appears the required relation between E_0/E_k and ***p***

$$\frac{1}{\sqrt{b}} \equiv \frac{l_a}{a} = \frac{\left[(3e_0)^b - 1\right]^{3/2}}{7{,}2b\,(3e_0)^b} \quad . \tag{3.11}$$

Here

$$l_a = \sqrt{\frac{D}{n_a}} \tag{3.12}$$

is a diffusion length of the electron attachment which is the air pressure's function.

In (3.12) under D we have to mean an ambipolar diffusion coefficient

$$D = D_a = \frac{1.4 \cdot 10^4}{p}, \text{ cm}^2/\text{s}. \tag{3.13}$$

Indeed, if the UV radiation source maintains some electron concentration in a gas near the isolated body's surface at some electron temperature T_e then after a time

$t_d \gg 1/(4ps)$, (3.14)

where s is plasma conductivity, the potential of this body rises to a value about of several T_e. So the further entering of plasma electrons into a body can take place only by ambipolar type. With accounting of (3.4) and (3.13) the Eq. (3.12) for diffusion length of the electron attachment can be changed into

$l_a=0.33/p$, cm. (3.15)

The dependence (3.11) in coordinates $3E_0/E_{cr}$ and l_a/a is represented in the Fig.3.1.

From Eq. (3.11) follows also that at high ***p,*** i.e. at $l_a/a \to 0$, the breakdown takes place in the polar ball's areas as if in three times increased field. In this case the breakdown field is $E_0=(1/3)\,E_{cr}$. With the decrease of the pressure the electrons begin to diffuse intensively from the polar ball's areas, where the field is increased, so as the breakdown takes place at a value $\mathbf{E_0}$ that is approaching to $\mathbf{E_{cr}}$. In this case the presence of a ball only stabilizes the breakdown by emission of the initial photo-electrons near its surface. Note that at relatively low pressure, i.e. at high value of l_a/a, the presented theory is quantitatively inapplicable to the description because of assumption $(l_a/a)-1 \ll 1$ accepted at its formulation. The field of its applicability was

determined experimentally. For the illustration on the Fig.3.2 on the basis of (3.7) and (3.9) the graphs of dependencies: **E(r/a)** (Fig.3.2a) and **n[(r-a)/l_a]** (Fig.3.2b) were depicted. The latter corresponds to area near the ball's poles at parameter value $l_a/a=0.1$.

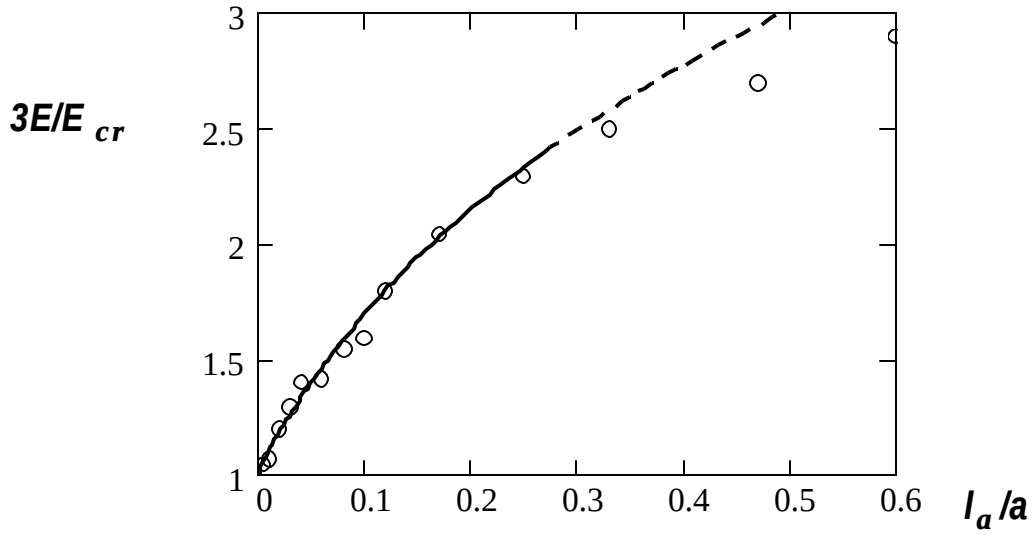

Fig.3.1. The dependence of the normalized breakdown field Ebr/Ecr from the attachment length. The line – Eq.(3.11), points – experimental data.

3.2. Experiments on the microwave air breakdown at a ball's presence

The scheme of the experiment is represented in the Fig.3.3.

The microwave radiation with flat phase front from the generator comes into the experimental chamber and is being reflected by the metallic spherically concave mirror.

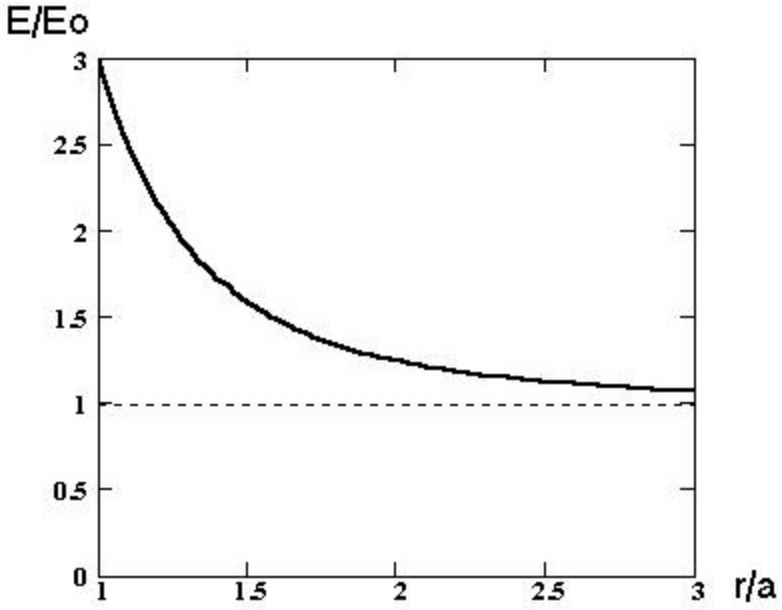

Fig.3.2a. The total electric field distribution on radial axis oriented along external electric field.

The focus point is located at distance Rmir/2 from the bottom of the mirror (the mirror's radius Rmir=45cm). The depth of the mirror equals to 15.8 cm, so the point of the geometric focus is located at a distance L=6.7 cm from its "cut'. Namely into this point the balls are being set.

The balls of diameter 2a=0.25 cm were hung in the focus of the converging beam of linearly polarized microwave radiation at λ=8.9 cm on the kapron string of 10^{-2} cm diameter perpendicularly to $\vec{E}_0$.

A mercury lamp with the radiation line in the UV range at 254 nm wave length was used in experiments as a source of UV radiation. Energy of a quantum of this radiation exceeds the work of escaping of an electron from the lead. Specially conducted measurements have shown that the UV source ensured presence of 10-100 photo-electrons near a ball's surface.

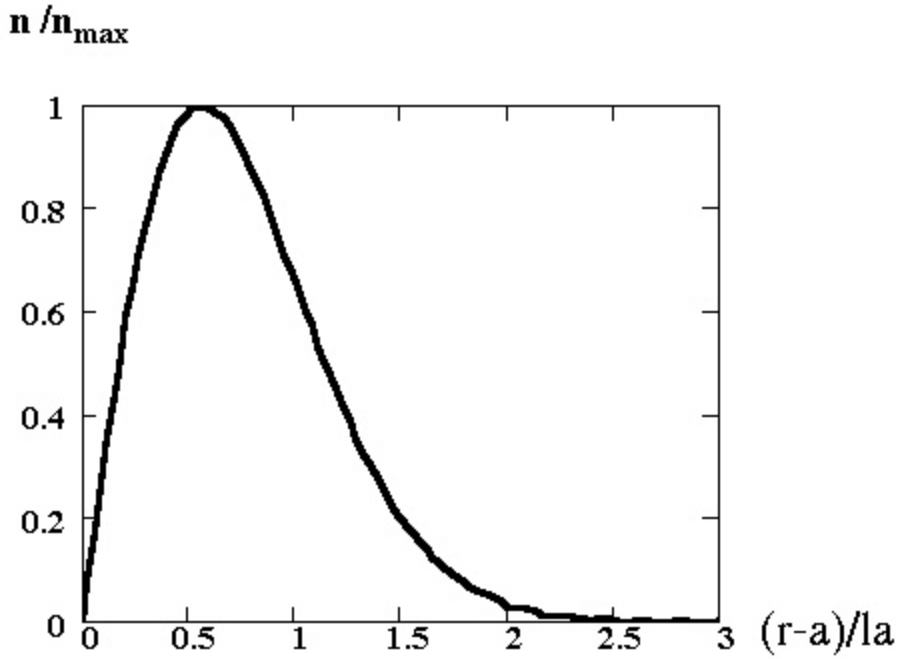

Fig.3.2b. The electron density distribution near the sphere surface at the pole. l_a/a=0.1.

During the control experiment the field's structure in the focus's area was visualized with a help of an electrodeless microwave discharge at low pressure.

In the Fig.3.4 the photo of a discharge is represented at p=50 Torr and the field's level in the focus $\mathbf{E_0}$ practically coincided with the breakdown level E_{br}. In the picture the focusing mirror is to the left, EM radiation falls on it from the right. The vector $\vec{E}_0$ lies in a plane of the image and is vertical. In the picture one can see the kapron thread along the axis of EM beam with traced measuring marks. The distance between marks equals to 1 cm. On the photo to the left one can see an additional tread of a small length fixed on the main measuring thread it indicates the location of the mirror's cut.

In the Fig.3.4 one can see that the field along the beam's axis is not uniform. One of its maximums is located practically in the calculated focus's point that is at the

distance L=7 cm from the mirror's cut. There are several of its maximums behind the focus. One can suppose that additional maximums are the result of the interference of waves falling on the mirror and focused, reflected from it. They characterize so called CSW (coefficient of the standing wave) of EM beam system.

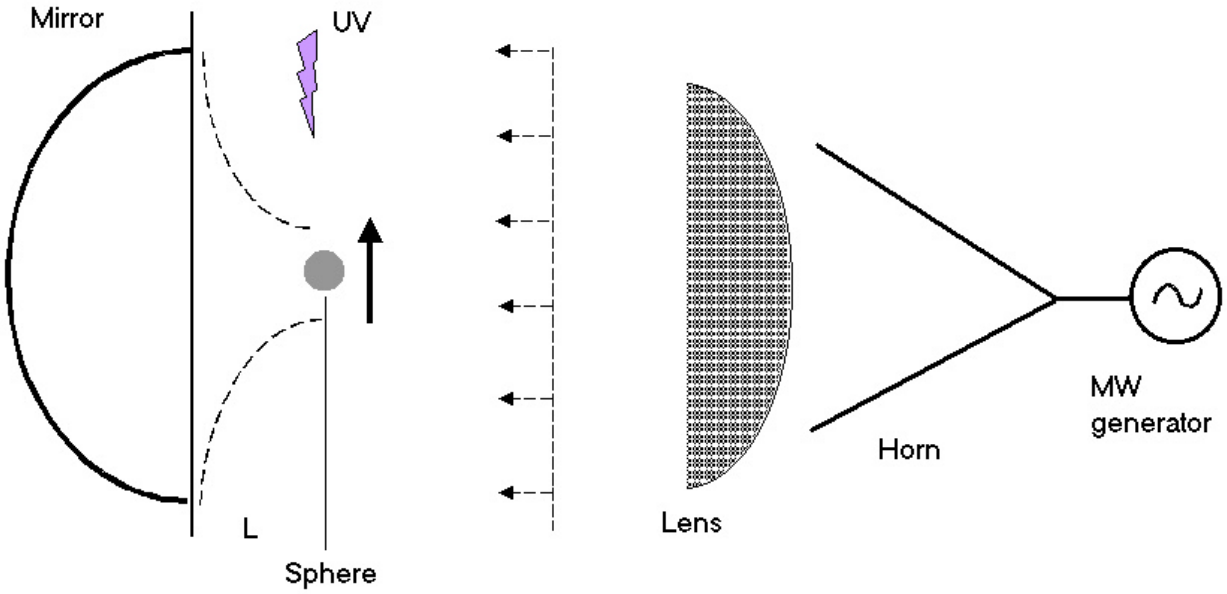

Fig.3.3. The scheme of the field amplitude measurement using the sphere

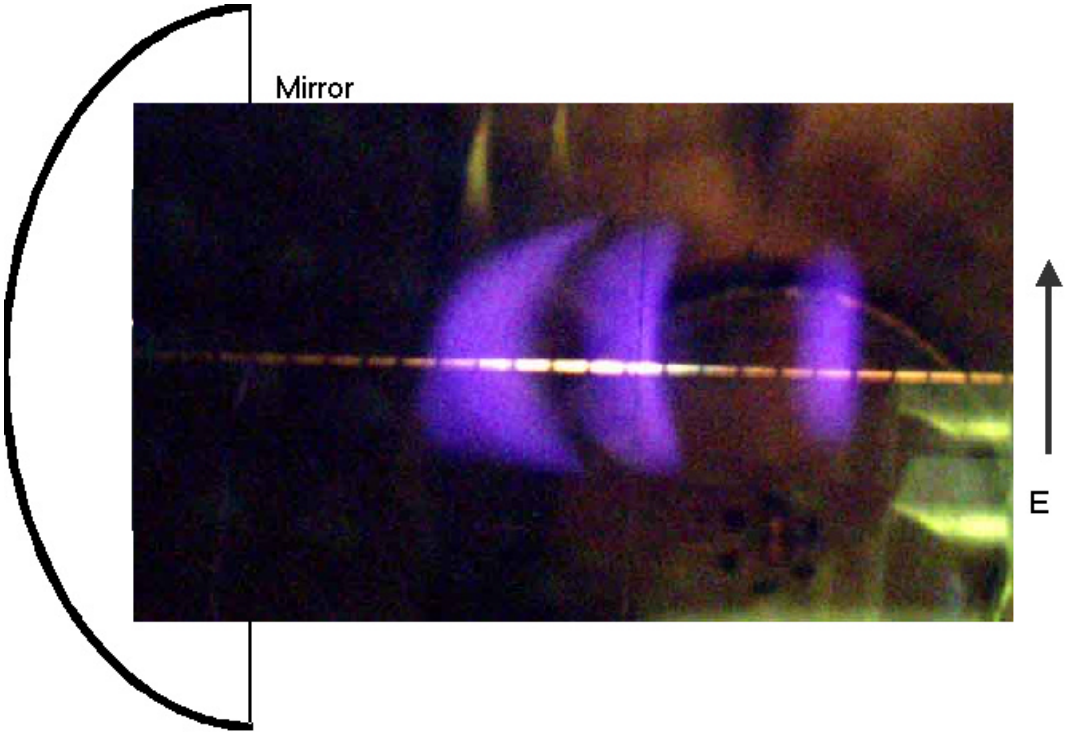

Fig.3.4. The photo of the discharge at comparatively low gas pressure in transverse direction relative to electric field. The marked string is seen.

In the Fig.3.5 the photo of the same discharge is represented but from the direction going along the vector $\vec{E}_0$. One can see the axis of the EM beam in the horizontal plane is somewhat inclined in respect to the constructive axis of the electrodynamic

system of the setup, along which the measuring thread is directed. In the experiment the balls were located in the real focus with the maximum of the field.

In the main experimental series with each ball the breakdown $\mathbf{E_0}$ was determined at the fixed **p** in a range from 3 to 420 ????.

Note also that at $E_0 < E_{br}$ the breakdown took place only at presence of the UV radiation. Results of measurements depicted by the points in the Fig.3.1 and Fig.3.6.

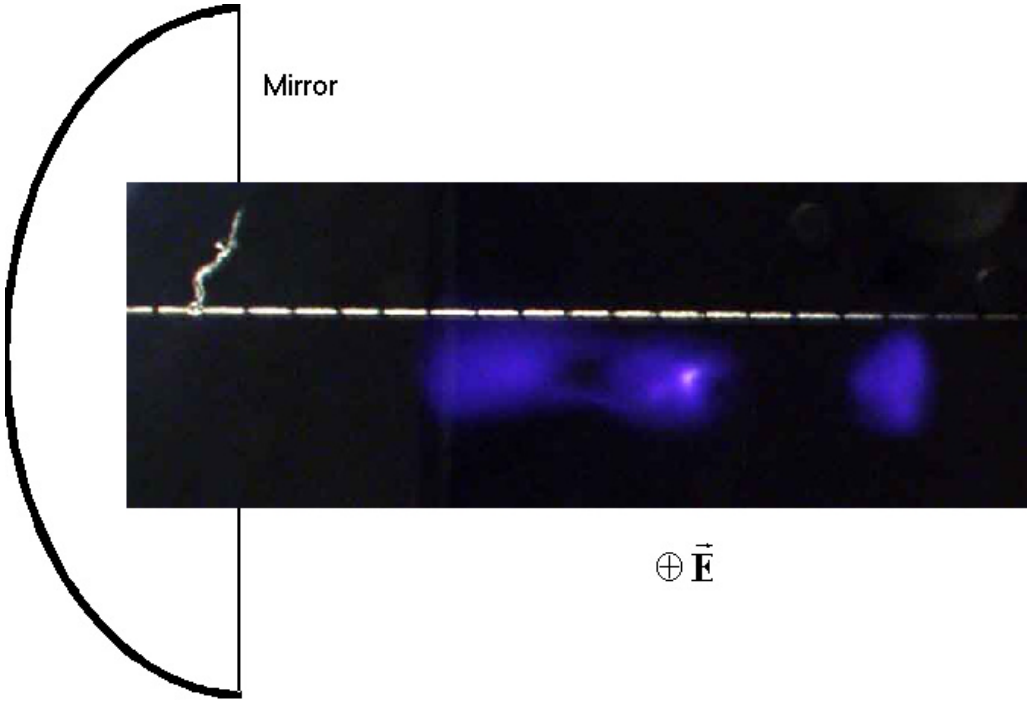

Fig.3.5. The photo of the same discharge that on Fig.3.4 performed along the electric field.

Experimental points at the Fig.3.1 have coordinates over abscissa axis calculated for the given ball, i.e. definite **a,** and determined **p** with the application of the equation (3.16). The field $\mathbf{E_{cr}}$ included into the value placed over the ordinate axis was calculated for this **p** by (3.5). The Fig.3.1 reflects that exposed above theory describes real processes well up to the value $l_a/a=0.35$. It is not valid at very low pressure and small ball as it was previously supposed.

In the Fig.3.6 a line **1** corresponds to a dependence $E_{cr}(p)$, obtained by (3.5), and a line **3** is the dependence $E_{cr}(p)/3$. In this picture a line **2** is the graph of the breakdown field $E_0=E_{br}$ calculated with the application of data from the Fig.3.1.

Experimental points for a ball with 2a=2.2 ?m in the Fig.3.6 are not black. In coordinates $(\mathbf{E_0, p})$ they lie practically on the same line. Previous estimates show that at a presence of a ball of such a big diameter the breakdown has to take place practically without electron diffusion influence in the tree times increased field.

That is why a line that approximate experimental points was specially coincided with a line **3**. Namely in this case experimental points obtained with a ball 2a=0.25 cm, that are black, lie on the calculated dependence **2**. One can see in the Fig.3.6 that a small ball at low pressures **p** does not decrease the level of the breakdown field –

the breakdown takes place at $E_0 \approx E_{cr}$. Relative difference between $\mathbf{E_{br}}$ and $\mathbf{E_{cr}/3}$ becomes smaller and smaller with the increase of **p**.

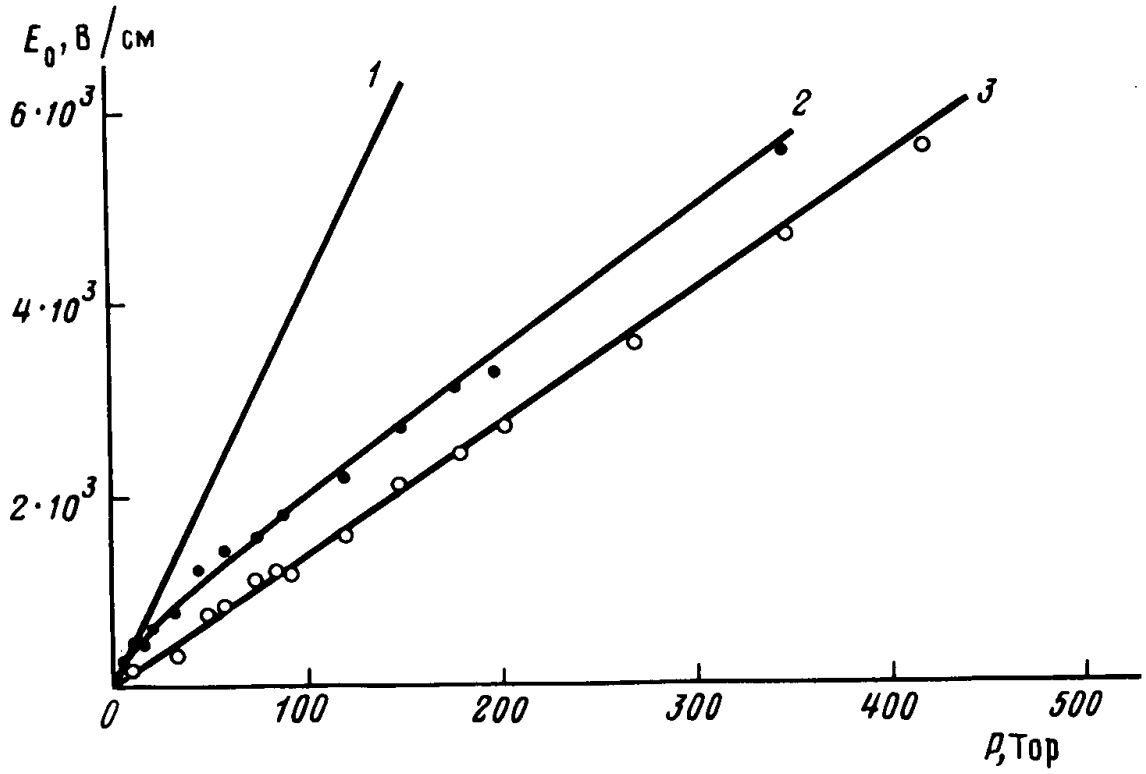

Fig.3.6. The breakdown field dependence on the gas pressure at metal sphere presence. 1 – critical field, 2 and 3 – breakdown field with a=0.125 cm and 1.1 cm. Experimental points: black circles – a=0.125 cm, empty circles – a=1.1cm.

3.3. Calibration of the field probe

Conducted experiments allowed to calibrate the field probe, i.e. connect its reading with the absolute field value in the focus of EM beam.

As it was noted before in our experiments a signal from the inductive loop was given to the amplitude detector, amplifier and the oscillograph with the electron-beam tube with memory. The signal's oscillogram at the maximal level of the microwave power putted into the chamber is represented in the Fig.3.7a. Its horizontal scan corresponds to a scale 10 μs/div and vertical – 1 V/div. The fluctuations on the signal's top characterize the accuracy of its amplitude measurements.

One can see from the oscillogram that the maximal signal's level was U=4V. In the Fig.3.7b the same oscillogram is presented with the horizontal scan 1μs/div. One can see only the front pulse's edge in it. The signal's fluctuations in it are the noise from the high power circuit of the magnetron feeding. It follows from the oscillogram that the microwave pulse front is much less 1μs .

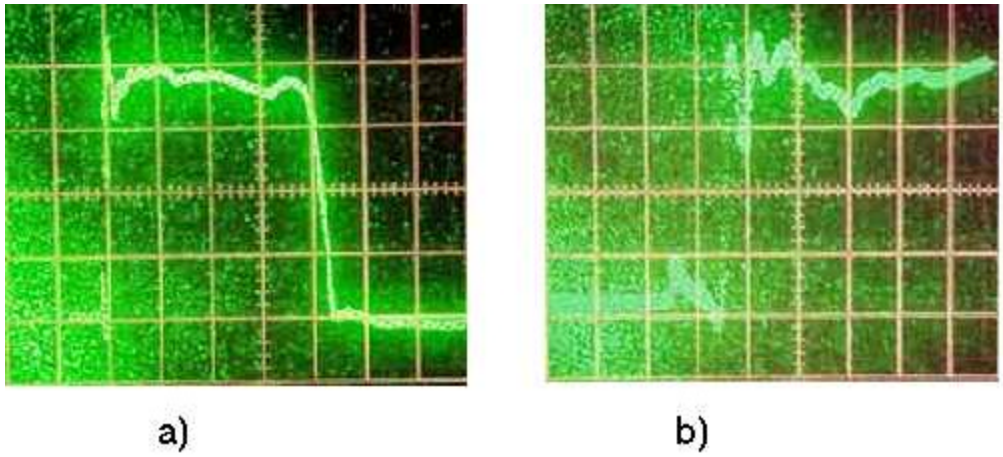

Fig,3.7. The microwave field envelop: a) – 10 μS/div, b) – 1 μS/div.

At the total entry of the attenuators into the wave guide the field level decreases and accordingly the signal's amplitude dropped up to U=0.1V. At the switching of the gain coefficient of the oscillograph's inlet the relative accuracy of measurement of the signal's amplitude can be kept the same, as on Fig.3.7a. It means that independently from sensitivity of the measuring circuit the level of a microwave noise is small.

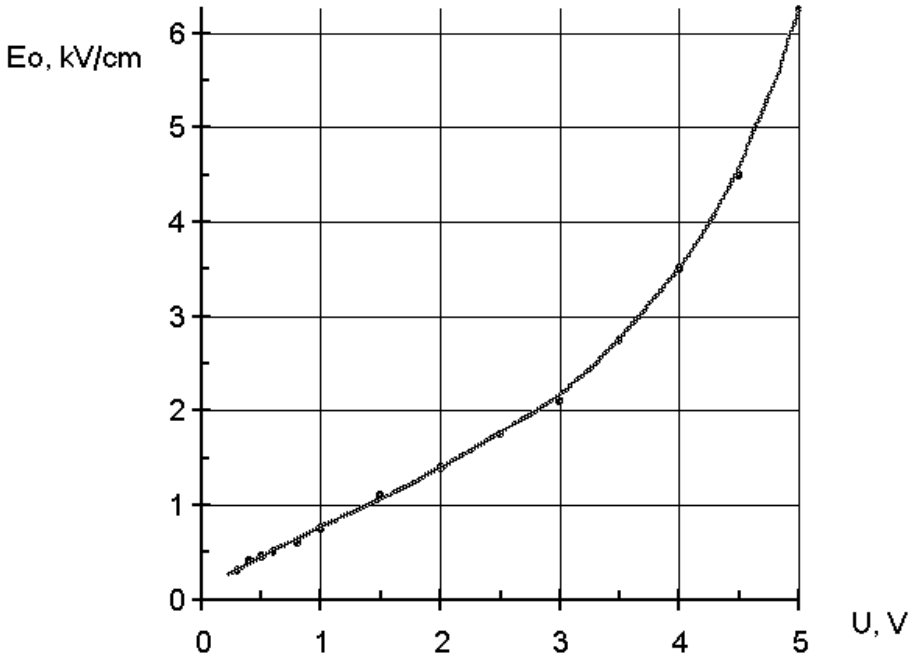

Fig.3.8. The measured dependence of the probe voltage U from the electric field amplitude at the focus.

In the Fig.3.8 the experimental calibration dependence $E_0(U)$ for the probe is represented.

In the Fig.3.9 are given the photos of probe's oscillograms that have been got at the same field amplitude. The first of them (3.9a) was obtained at high air pressure in the chamber when the discharge is absent. The second one (3.9b) is obtained at low

pressure **p** and consequently at presence of a discharge. One can see on the Fig.3.9b that the pulse's top in the second one is strongly disturbed. It is connected with the fact that on the probe mainly comes the radiation that is reflected by the mirror and has been passed the area of the discharge in the focus.

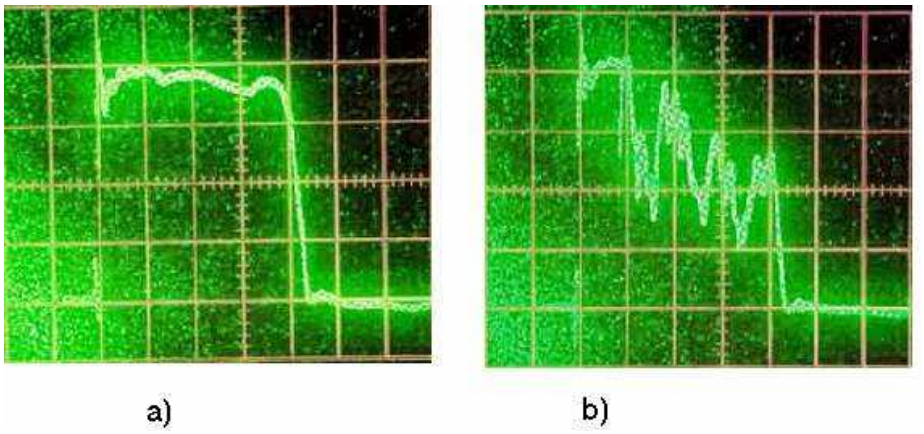

Fig.3.9. The probe signal without discharge (a) and with discharge (b).

It means that a signal coming to the probe at presence of a discharge brings an information about a discharge plasma and its dynamics during the microwave pulse.

4. The breakdown at the presence of the initiator

As it was noted earlier the streamer microwave discharge can exist and propagate in the field that is much less than the critical one. But creation of these discharges need the start initiation. The role of initiator can be performed by thin long metal body (which can be shaped as sphere, ellipsoid or cylinder) placed in the under-critical field.

4.1. The field arising on the top of a metal initiator

In the quasi-stationary approximation the spatial distribution of a field potential φ at presence of arbitrary distributed electrical permeability Σ is described by Puasson's equation

$$\Delta j + \nabla\Sigma \cdot \nabla j = 0. \qquad (4.1)$$

For the special case of a spherical symmetry of permeability distribution and azimuth symmetry of the electric field the Eq. (4.1) can performed in the 1D form by changing of variables

$$j(r,q) = f(r) \cdot \cos(q), \qquad (4.2)$$

where (r,φ,θ) – spherical coordinates.

Instead of the Eq. (4.1) we have now the 1D equation for f:

$$\frac{\partial^2 f}{\partial r^2} + \frac{2}{r} \cdot \frac{\partial f}{\partial r} - \frac{2}{r^2} \cdot f + \frac{1}{\Sigma} \cdot \frac{\partial \Sigma}{\partial r} \cdot \frac{\partial f}{\partial r} = 0. \qquad (4.3)$$

The electric field is defined by formula:

$$E = -\nabla j = -\nabla(f(r)\cdot\cos(q)) = -(\cos(q)\frac{\partial f(r)}{\partial r}i_r - \sin(q)\frac{f(r)}{r}i_q), \qquad (4.4)$$

The solution of Eq. (4.3) for the case of metallic sphere in homogeneous external field $E=E_z$ in spheroidal coordinates (r,φ,z) is performed on Fig.4.1

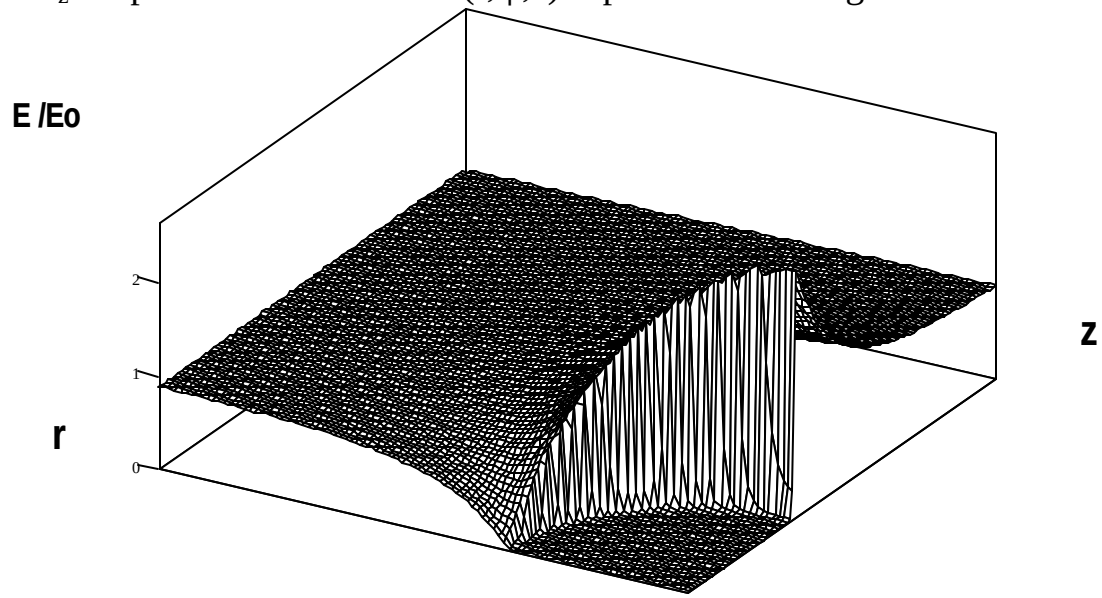

Fig.4.1. The spatial distribution of the field amplitude around the sphere.

The Eq. (4.3) is especially interesting because allows investigate the any permeability distribution with spherical symmetry.

For the metallic ellipsoid oriented along the external electric field the famous analytical solution (see Ref. [3]) can be used if the sizes of body is much small comparatively wavelength of microwave radiation.

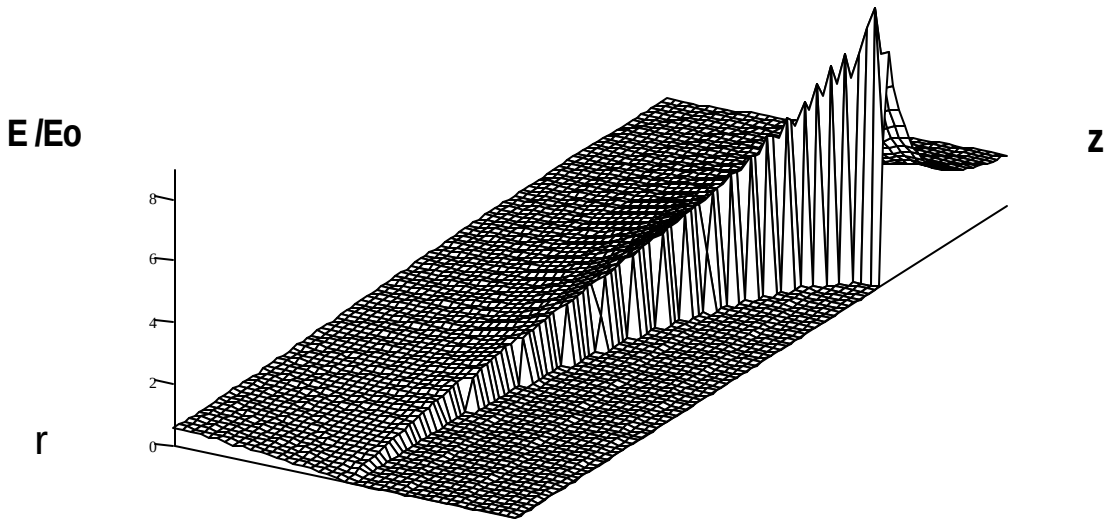

Fig.4.2. The spatial distribution of the field amplitude around the ellipsoid.

For the field on the pole the expression is simplified and we have the formula (4.6) for the increase coefficient Q [8]

$$Q(a/l)=\frac{\left(\sqrt{1-a/l}\right)^3}{Arth\left(\sqrt{1-a/l}\right)-\sqrt{1-a/l}}\cdot\frac{l}{a} \qquad (4.6)$$

The graphic of the Eq. (4.6) is given on Fig.4.3.

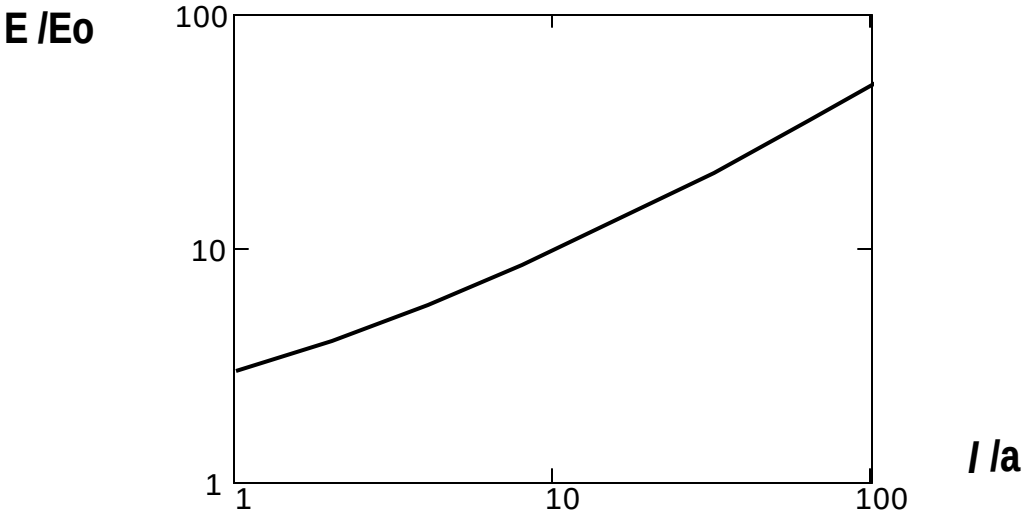

Fig.4.3. The increase coefficient Q dependence from the relation between ellipsoid half-length and radius of curvature at its pole

The approximate calculation of the field on the top of metallic thin cylinder gives the expression [9]

$$Q(a/l)=\frac{l}{a\cdot\left(\ln\left(\frac{8\cdot l}{a}\right)-2\right)} \qquad (4.7)$$

But the expressions (4.6) and (4.7) can describe the top field only if the length of the initiator is much less than half wavelength of microwave radiation. In the case of an equality between initiator length and half wavelength the increasing of the top field is significantly more because the electric-dynamical resonance. At the resonance the top field is limited by only so named radiation resistance and can be successfully described by expression (4.8)

$$Q(a/l)=\frac{E_{top}}{E_0}=\frac{2}{c\cdot a}\cdot\frac{l/p}{R_w}\approx 0.255\cdot\frac{l}{a} \qquad (4.8)$$

where

$$R_w\approx\frac{2.5}{c}$$

is well known the radiation resistance of the vibrator, which at the resonance approximately equals to 75 Ohms in practical force system of measurement. The factor in the numerator λ/π - is so named the acting length of a resonant vibrator.

For calculation of the field around the thin initiator of any length (both resonant and sub-resonant) placed in the external microwave field the integral equation (of second kind) is successfully being used. (The algorithm of the solving of the integral equation is described in the Ref. [10]). The formula (4.8) just is a consequence of this equation that was used for estimation of the inducted current in the resonant vibrator. The experimental dependence of E_{br} on the vibrator length for several values of its radius is shown on Fig.4.4.

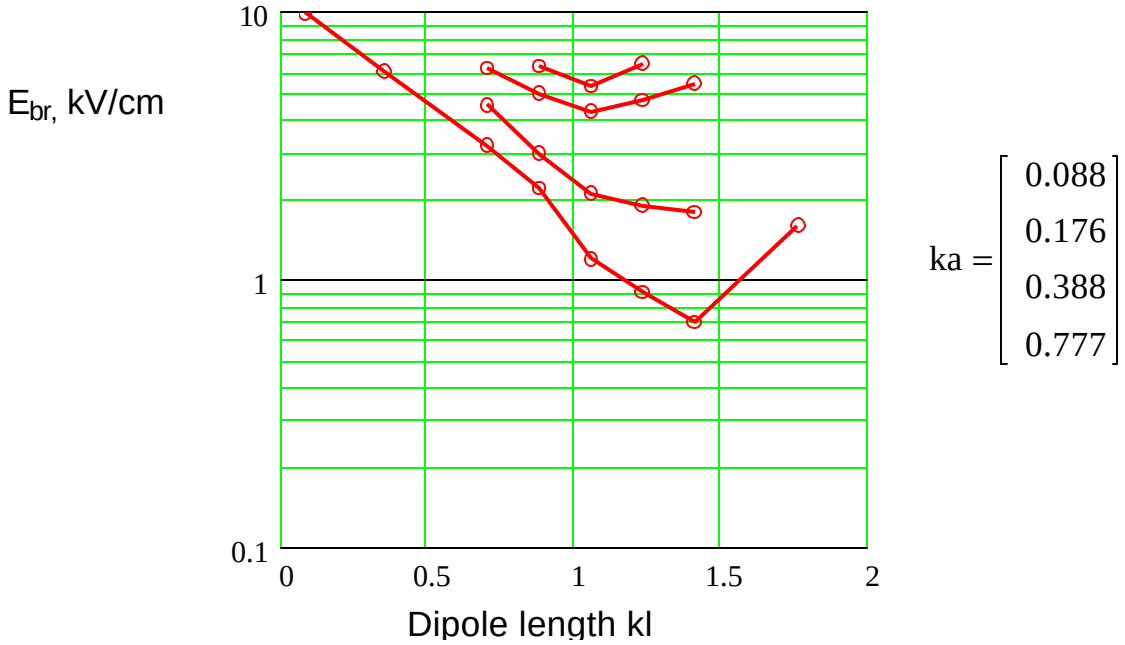

Fig.4.4. The experimental dependence of E_{br} on the vibrator length $\boldsymbol{l}$ for several values of its radius **a** (**k** – wave number)

The coefficient Q can be increased up to very high value if the radius of curvature at the pole is small enough. But diffusion of electrons on the initiator can increase the field E_0 needed for breakdown at the presence of the vibrator.

4.2. The electron diffusion influence on the breakdown field at presence of an initiator

By the same way as in the case of the sphere that have discussed in the chapter 3 the diffusion influence on the breakdown field is more strong in the case of a long body.

Using the same method of calculation as at the chapter 3 one can get the expressions that is analogical to (3.11)

$$\frac{l_a}{a} = \frac{\left[(e_{br})^b - 1\right]^{3/2}}{7{,}2b\,(e_{br})^b} \qquad (4.9)$$

where $e_{br}=(E_{top}/E_{cr})_{br}$. The Eq. (4.9) with (3.4) and (3.12) taking into account gives the needed equation $F(E_{br},p,a)=0$

$$\frac{0.33}{a \cdot p} - \frac{\left[\left(Q\left(a/l\right) \cdot Eo_{br}/E_{cr}(p)\right)^{b} - 1\right]^{3/2}}{7{,}2b\left(Q\left(a/l\right) \cdot Eo_{br}/E_{cr}(p)\right)^{b}} = 0. \qquad (4.10)$$

The Eq.(4.9) in common with (3.12) allows to get the universal dependence of $(E_{top}/E_o)_{br}$ on the product of pressure **p** on the initiator radius **a** for any length of initiator (see Fig.4.5). The same dependence for spherical initiator is shown on Fig.3.2a. It is clear from Fig.4.5 that diffusion influence on the breakdown with initiator is insignificant if the product **ap**>10 cmTorr.

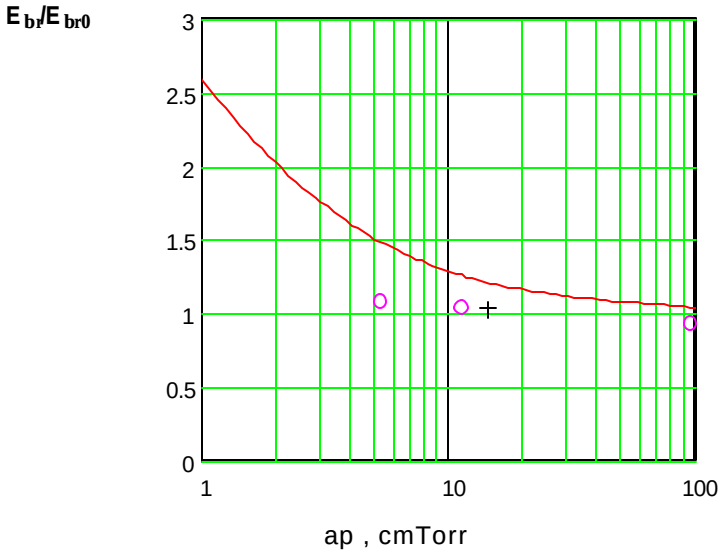

Fig.4.5. The breakdown field E_{br} related to one without the diffusion influence E_{br0} dependence from product **ap**. Experimental points: circles – a=0.25 cm, cross – a=0.019 cm.

The solution of E_q. (4.10) (that follows from E_q. (4.9)) in common with expressions for Q let to find the needed dependencies. Fig.4.6 shows the breakdown field E_{br} dependence on the pressure for initiator of 2 cm length (it is so named sub-resonant initiator) at wavelength 8.9 cm. The initiator is shaped as cylinder with semi-sphere on the ends. The dependencies are given for several values of cylinder radius. Consequently the same dependence for the resonant initiator with length that equals to half of wavelength is shown on Fig.4.7. One can see that resonant initiator with the same radius allows to get discharge at the more pressure (approximately at 2-3 times). It is important because a very thin initiators is less rack to heating by the microwave current inducted in the external field. The values of the increasing coefficient Q for resonant length in dependence on **a**/l (l–wavelength) achieved by E_q. (4.8) and by integral equation is compared with experimental data on Fig.4.8. The measurement data for two wavelength (8.9 cm and 12.5 cm) are present on the picture. It must be noted that the experimental points for 12.5 cm wavelength are submitted by supposition of E_o=100 V/cm.

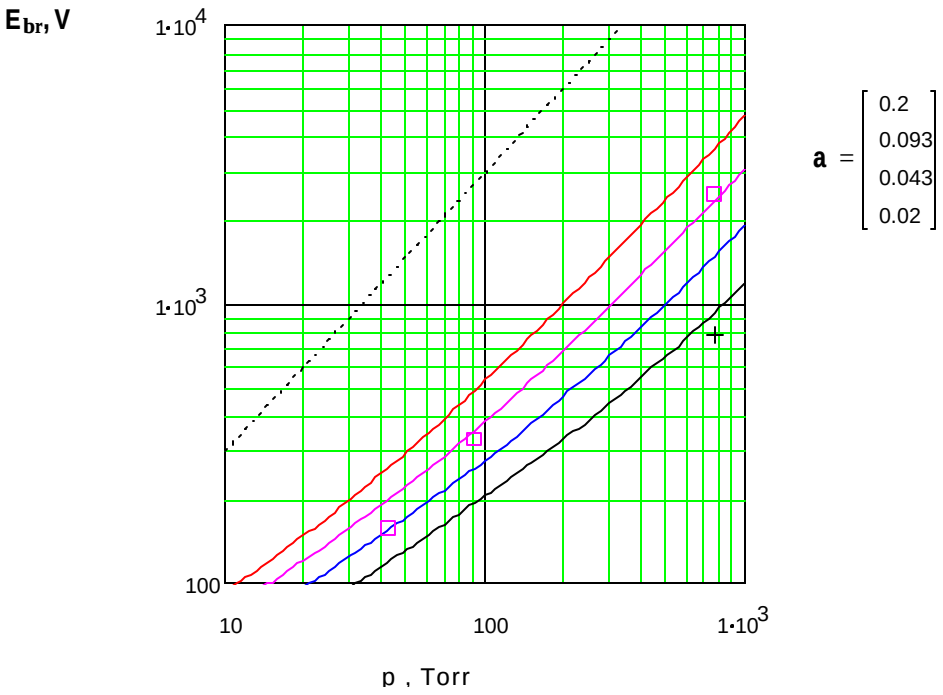

Fig.4.6. The dependence of the breakdown field E_{br} from the pressure with different values of the radius of curvature **a** at the top of the **sub-resonant** initiator which are shown on the right and corresponds to solid lines from above downwards. The dot line is the critical field (3.4). The experimental points: box - **a**=0.125 cm, cross - **a**=0.019 cm. λ=8.9cm

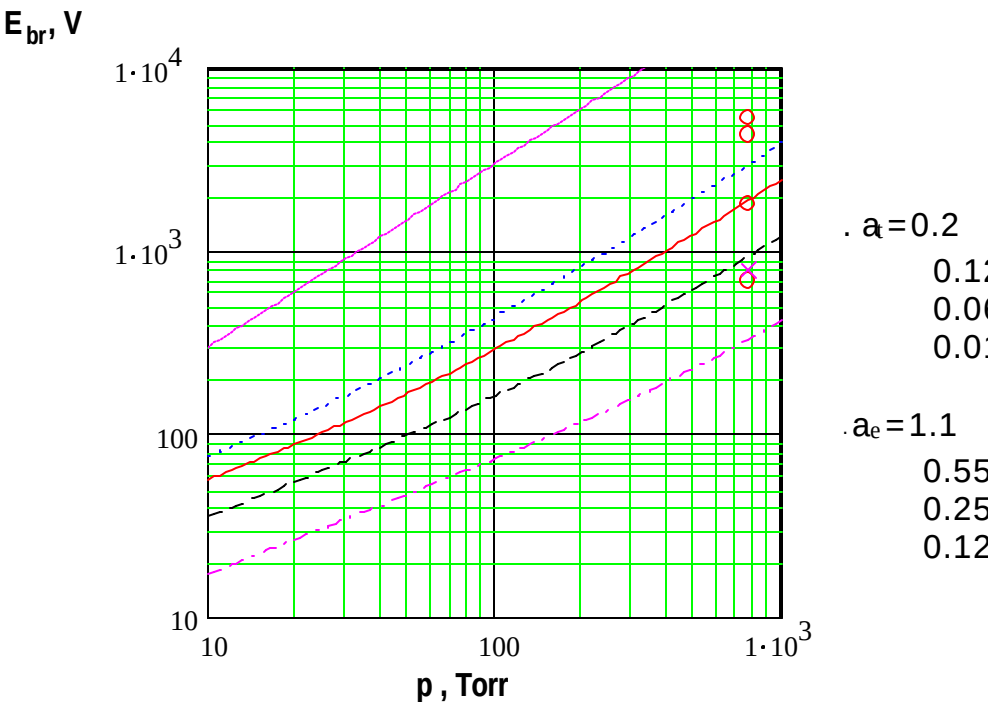

Fig.4.7. The breakdown field E_{br} dependence from air pressure p at different radius a of cylindrical initiator of the resonant length. The lines are the solution of Eq. (4.10) together with (4.8). a_t – parameter of the theoretic curves, a_e – of the experimental points.

It is two time smaller the value which corresponds to power output of the generator. The comparison of the theory with experiment points on Fig.4.4-4.7 gives the satisfactory consent.

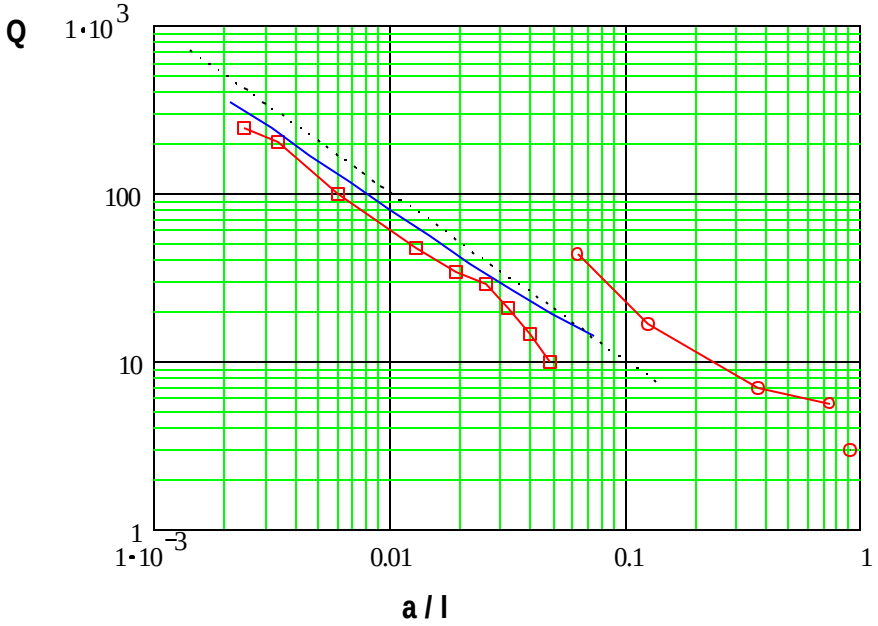

Fig.4.8. The coefficient of field increasing $Q=E_{top}/E_0$ dependence on aspect ratio a/l for resonant length of initiator. The blue solid line – the values calculated by integral equation, the black dot line – the estimation (4.8), circles and boxes – the values measured at λ=8.9 cm and 12.5 cm accordingly.

5. Boundaries of the existence of the initiated under-critical streamer microwave discharge in the "separated" and "attached" forms in respect to parameters of the gas and of the microwave field.

Investigations fulfilled in the frame of the work showed that the streamer microwave discharge in the quasi-optical EM beam can be ignited in the under-critical field as well, for example, by the placing of the microwave vibrator into it. Experiments showed that if the level of the initial field E_0 is insignificantly smaller than level of the critical field E_{cr}. Then the discharge, being originated near the vibrator's poles, separates itself from them and, also as in the case of the overcritical field, begins to act "independently" in the form of the growing and branching streamer channels. It is evident that the upper boundary of the existence of the under-critical discharge in respect to the field coincides with the level $E_{0=}E_{cr}$. With the decrease of E_0, i.e. with the increase of the under- criticality level, defined by parameter

$$\psi=E_{cr}/E_0, \qquad (5.1)$$

the discharge loses its ability to separate from the initiating vibrator, being attached to its poles during the whole microwave pulse. This discharge we will call the deeply under-critical discharge (or the attached discharge).

The targets of the experiments, described below, were:

- the study of a change of the under-critical discharge properties in respect to the level of the parameter ψ of the initial field;
- the determination of the boundary separating different kinds of discharges (under-critical and deeply under-critical) at the plot (E_0, p), and
- the study of the typical features of the deeply under-critical discharge at the increase of ψ .

5.1. Conditions of the experiment at λ=8.9 cm

The microwave generator with λ=8.9 cm was applied. The amplitude of the electric component of the initial field in the focus can be varied from 0.95 to 2 kV/cm. It was measures on the basis of the signal from the inductive loop with the application of the calibrating curve, represented in the Fig.3.8. Experiments were carried out in the mode of the single microwave pulses. The pauses between them were nor less than of one minute.

The initiators (metallic ball of the diameter 2a=0.5 cm or - cylindrical vibrators which are parallel to $\vec{E}_0$) were placed in the EM beam focus. Vibrators were made of the copper wire with the diameter 2a=0.08 cm and of length 2*l*=2 or 3 cm, and of the dur-aluminum with the diameter 2a=0.25 cm and of length 2*l*=1, 2, 3 and 4cm. The surface of the ball and of the vibrators could be illuminated by the UV radiation as it was described above. The signal from the inductive loop changes its value even at absence of the discharge if the vibrator is located into the focus, so the measurements of the established field were made at the absence of the vibrator.

The pictures of the discharge area were obtained at the exposure time considerably greater than those of the microwave pulse duration. On the photos below the radiation propagates from right to left. The electric field $\vec{E}_0$ is directed vertically. The sizes of the ball or of the vibrators can be used as the scale for the picture.

5.2. Results of the experiments

In the Fig.5.1 and Fig.5.2 the photos of discharges with the initiators of 2 and 3 cm length correspondingly are represented in the form of the matrixes. The columns (from left to right) in the matrixes correspond to the definite pressure p, the rows (from above downwards) correspond to the definite field amplitude E_0.

In the Fig.5.1, starting from the left side p=60, 100, 150, 200, 300 & 400 Torr, and starting from the upper side E_0=0.95, 1.2, 1.4, 1.6, 1.8 & 2 kV/cm. The maximum value of p is limited by the possibility of the air breakdown at the application of the vibrator at the maximum field level E_0=2 kV/cm applied in the experiments. By means of the vibrators with the length and diameter, which are mentioned above, the breakdown of air at this level of the field was realized only at p < 400 Torr.

Values of p and E_0 in the rows and lines in the Fig.5.2 are analogous to those indicated for the Fig.5.1, but the rows correspond to pressure values p=60, 100, 150, 300,400 & 760 Torr. Note that in the experiments the breakdown took place at the placing of the vibrators into the beam and at switched on the UV radiation source at each microwave pulse. It means that near the relatively "sharp" edges of vibrator the creation of initial electrons is ensured by the auto-emission.

From the exposed photos in the Fig.5.1 and Fig.5.2 follows that the initiated discharge at small values of ψ does not differ by the form from the discharge in the over critical field independently from the vibrator's length. It represents the typical tangle of plasma channels. For example the fragment of the picture of such discharge is represented in the Fig.5.3a in a larger scale. It corresponds to p=150 Torr and $E_{0=}$2 kV/cm, i.e. ψ=3. The length of this discharge toward the radiation is about 5 cm. At the duration of the microwave pulse 40 μs it corresponds to the propagation of the discharge front toward the radiation $V_{fr}=1{,}25\cdot10^5$ cm/s, or to the average velocity of the growth of its streamer channels $V_{str}=2{,}2\cdot10^5$. These velocities, naturally, lie in the ranges of velocities measured earlier in [11].

In analogy to the diffuse discharge form, represented in the Fig.5.4b, we will suppose that the streamer discharge at the boundary field value forms the plasma loop during the time of the microwave pulse. This loop connects the ends of the ionizing vibrator. At a smaller field value only the unconnected channels, going from the channel ends, are formed. At a higher field value are formed the channels, growing towards the radiation.

The typical example of the discharge that can independently develop is represented in the Fig.5.5a at the field's amplitude close to the boundary value. This discharge was performed at the following parameters $2l$=2 cm, at p=150 Torr and E_0=1.2 kV/cm. At the photo one can. It demonstrates evidently the principle of the independent development of the streamer microwave discharge in the under-critical field.

At the increase of the parameter ψ the volume density of the streamer channels, i.e. their number, decreases. It can be caused by both the physics of the processes in the under-critical discharge and the decrease of the area of the EM beam with the allowed ψ for this discharge form in our definite experimental conditions.

From the represented matrixes follows also that at the maximum values of ψ realized in the experiments the character of the discharge is substantially different. For example, in the Fig.5.3b, in comparatively larger scale than in the Fig.5.2, the photo of the discharge is represented. It corresponded to p=150 Torr and $E_{0=}$0.95 kV/cm, i.e. ψ=6.3. One can see on it, that the streamer channels go from the vibrator's poles. But during the whole microwave pulse they stay as if they are attached to them.

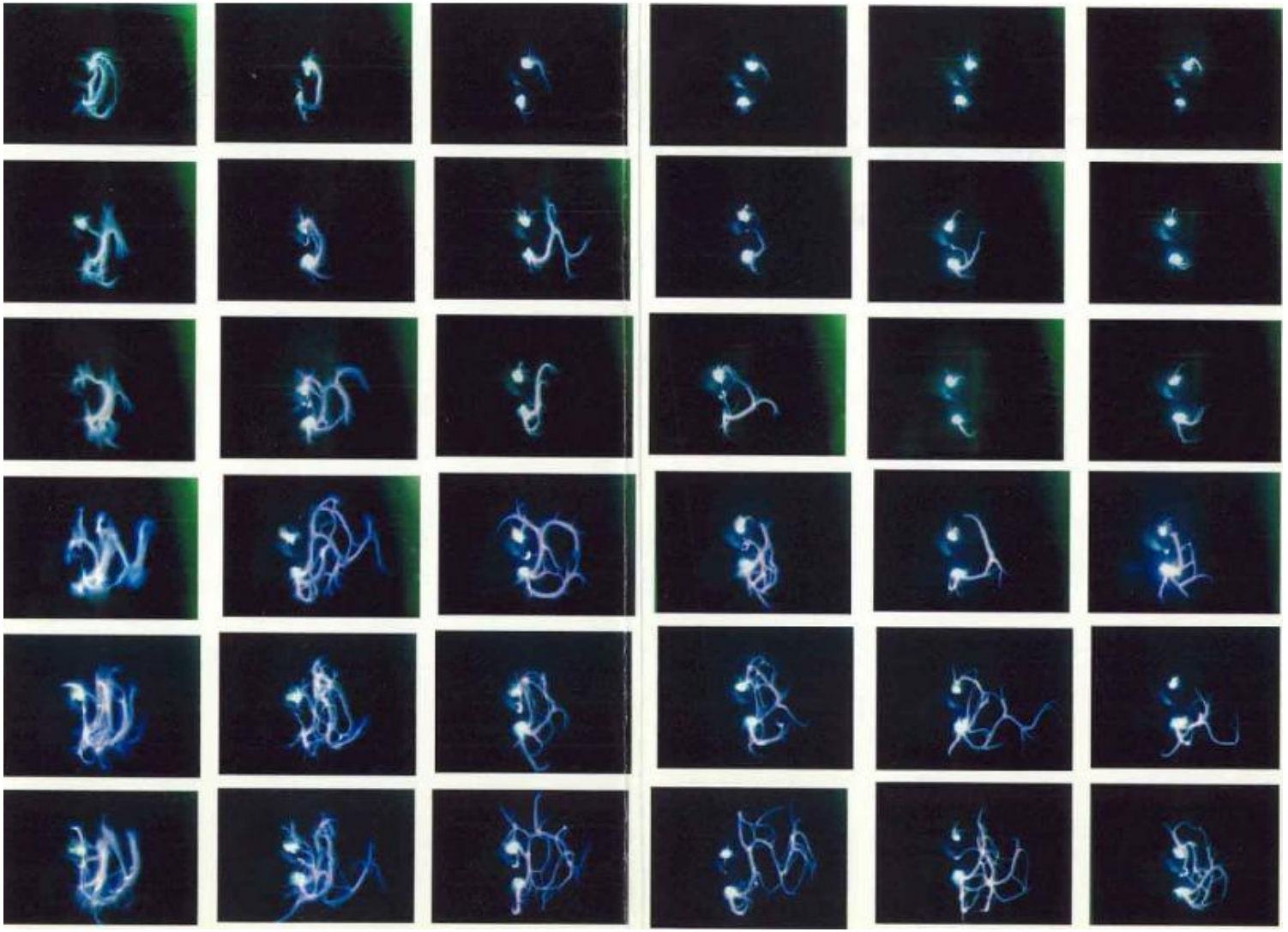

Fig.5.1. The photo of initiated discharge at the length of the initiator 2***l***=2 cm., columns (from the left side) - p=60, 100, 150, 200, 300 & 400 Torr, rows (from above downwards) - E_0=0.95, 1.2, 1.4, 1.6, 1.8 & 2 kV/cm.

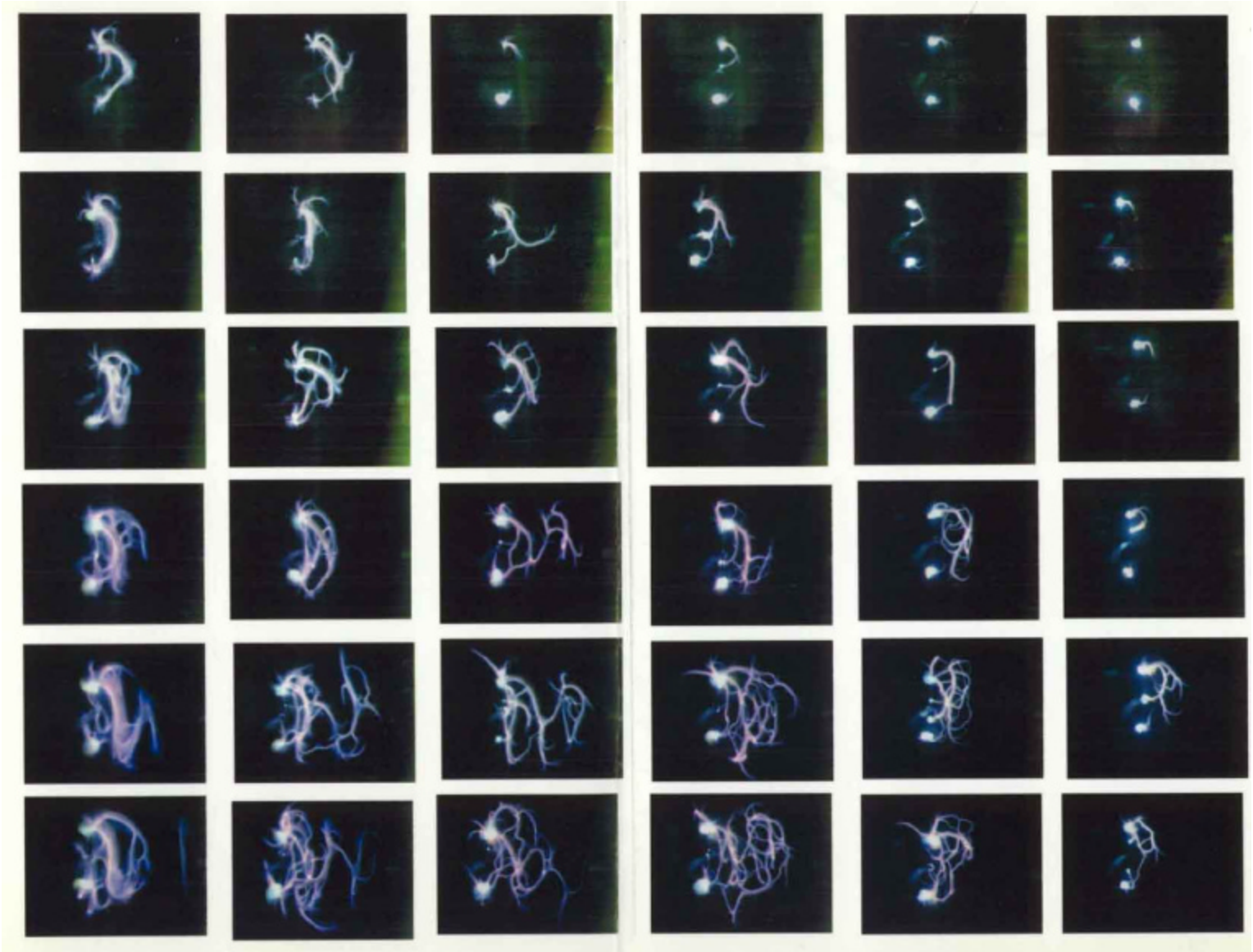

Fig.5.2. The same as on Fig.5.1 but the length of the initiator 2***l***=3 cm and p=60, 100, 150, 300,400 & 760 Torr

By the Fig.5.1 and Fig.5.2 the boundary of the transition from the independently developing under-critical discharge to the attached deeply under-critical discharge in respect to air pressure over E_0 or ψ can be defined. First let us define the criterion which will be used for the determination of this boundary.

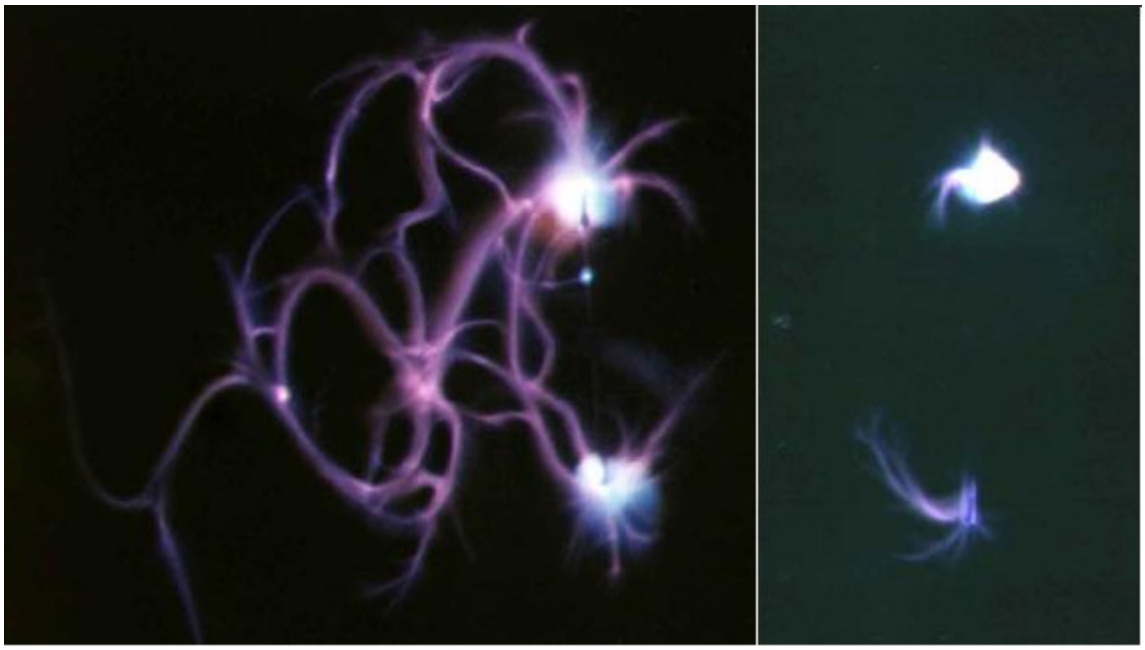

Fig.5.3. The photo of two form of initiated discharge. a)-typical tangle of the plasma channels (p=150 Torr and $E_{0=}$2 kV/cm, i.e. ψ=3). b) – attached discharge (p=150 Torr and $E_{0=}$0.95 kV/cm, i.e. ψ=6.3).

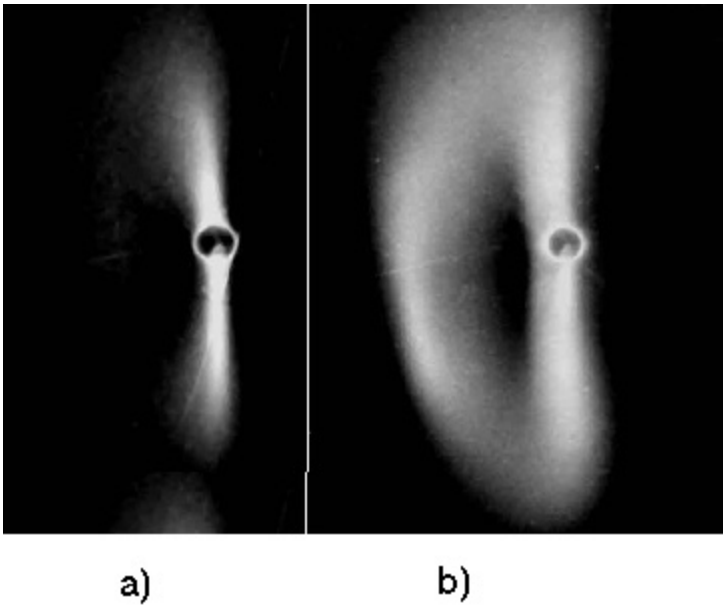

Fig.5.4. The typical photo of initiated diffuse microwave discharge. The discharge is initiated by the ball with diameter 2a=0.5 cm. p=20 Torr, E_0=0.8 kV/cm. Duration of the microwave pulse equals to: a) - 20 μs b) – 40 μs.

It is known that the microwave discharge in the EM beam being in the diffuse form does not come out of the area $E_0 \geq E_{cr}$. It means that in difference to the streamer discharge it does not propagate to the area of the under breakdown fields.

It such a discharge will be initiated in the under-critical field, than it is localized only in the area of the strengthened field, being attached to the initiator. For example, in the Fig.5.4a the discharge photo is represented. The discharge is initiated by the ball with diameter 2a=0.5 cm, at p=20 Torr, $E_{0=}$0.8 kV/cm and the duration of the microwave pulse equals to 20 μs. It is typical diffuse microwave discharge. The investigation of its dynamics showed, that being originated on the ball's poles it spreads along the $\vec{E}_0$ in the result of the ionization-field process. In so doing it reaches the size about λ/2, and then it forms the diffuse plasma loop directed to the side of radiation (Fig.5.4b).

One can see in the Fig.5.1 and 5.2 that in the definite range of ψ the streamer discharge can also form the loop attached to the initiator's ends and directed to the side of the radiation. It can consist of one or several streamer channels. In the Fig.5.5a such a discharge is represented. It is taken from the matrix represented in the Fig.5.1 at p=100 Torr and $E_{0=}$1.2 kV/cm.

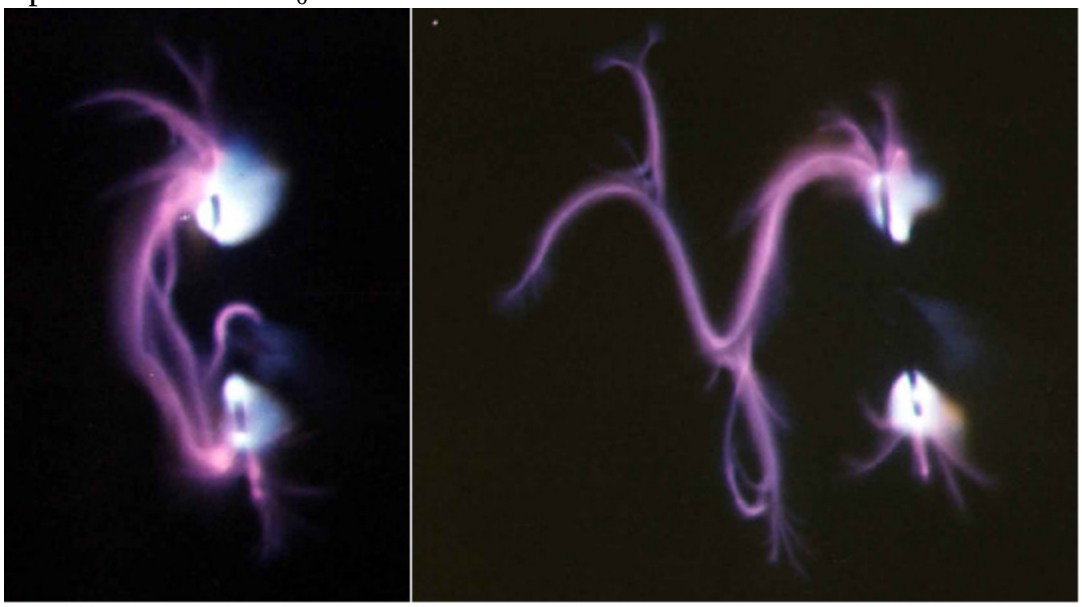

Fig.5.5 a) The streamer's loop attached to the initiator's ends, p=100 Torr, $E_{0=}$1,2 kV/cm 4.7. b) The streamer sinusoid going from the below end of the initiator toward the radiation, p=150 Torr, E_0=1,2 kV/cm. The length of the initiator – 2cm.

Comparably linear parts of this sinusoid, inclined to $\vec{E}_0$ at approximately at 45^o, in essence represent the initiating plasma vibrators that ensure the following consequent development of the discharge. Hence the property of the discharge to consequently form the plasma ionizing microwave vibrators is its main property, i.e. the main property of the independent developing non attached streamer microwave discharge.

The measurements, executed by means of the photo in the Fig.5.5b, show that the length of the streamer sinusoid is about 10 cm.

Hence the average velocity of the growth of the whole streamer V_{str} is no less than $2.5 \cdot 10^5$ cm/s. This value practically coincids with the value V_{str} evaluated above by the application of the Fig.5.3a for the discharge with the developed spatial structure at small level of the under-criticality. So, as it follows from [12], the fulfilled experiment shows that if the under-critical discharge has the capability to be separated from the initiator then at the pressure of hundreds Torr the velocity of growth of the streamer discharges, in its composition, can not be less than 10^5 cm/s. In the fields at values less than some definite value of the boundary field the discharge simply stops to "propagate", so the notion of velocity looses a sense. The values of the boundary field experimentally obtained for each pressure p by means of analysis of the results represented in the Fig.5.1 and Fig.5.2 using the accepted criterion are shown in the Fig.5.6.

In this picture the points correspond to the vibrator with 2L=3 cm, and crosses to those with 2***l***=2 cm. From the Fig.5.6 follows that the boundary values of the field are practically independent of the vibrator's length. It is natural, since by its sense it is the characteristic of the discharge, namely, and has not to depend on the method of its initiation. The experimental points are rather well fit the linear line in the coordinates used in the picture.

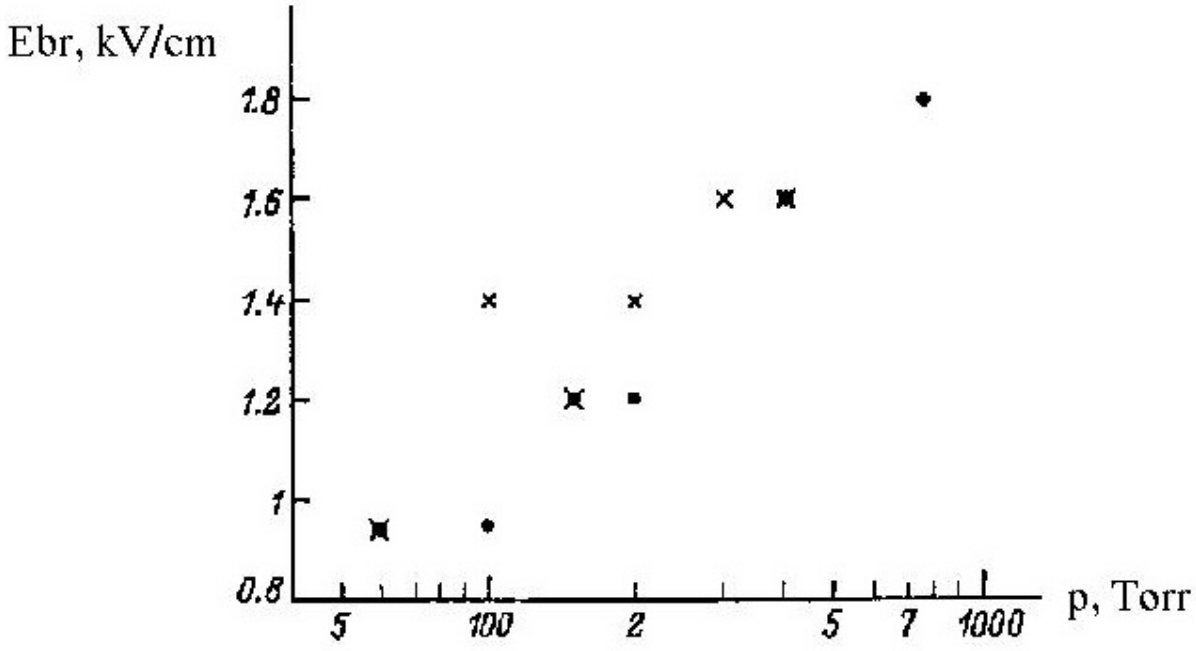

Fig.5.6. The analysis of results represented in the Fig.5.1 and Fig.5.2. The boundary field values experimentally obtained for each pressure p. The points correspond to the vibrator with initiator length 2 ***l***=3 cm, crosses - to those with 2***l***=2 cm

In the Fig.5.7 in the coordinates E_0 - p by the line 2 is shown the dependence of the boundary value E_0 of p that approximates the experimental points. The line 1 in this picture represents the dependence $E_{cr}(p)$. Above it there is the area I of the discharges

in the over critical field. In the area II between 1 and 2 the under-critical separating discharges are realized. Below the curve 2 there is the area III of the deeply under-critical attached discharges.

From the Fig.5.7 follows that the length of the area II in respect to E_0 increases with the rise of p. For example at the atmospheric pressure the discharge in the separating form is realized up to the level of the under-criticality ψ=17. Hence for its ignition, at other equal conditions, can be applied the microwave generator with the power about 300 less than those necessary for the ignition of the over critical discharge.

Extrapolation of the curve 2 to the side of low p gives its crossing with the curve 1 at p=20-30 Torr. This fact is in good agreement with the experimental results represented in the reference [13]. It was shown in it that the streamer discharge in air can be realized only at p>25 Torr. Namely the streamer discharge, in difference to the diffuse one, has the ability to propagate to the area of the under breakdown fields. But the microwave streamer mechanism accounts the developing of the thermal-ionization instability in the discharge plasma, i.e. the substantial increase of the gas temperature inside the streamer channel with the corresponding exclusion of molecules from its near axial regions.

---

1. Final report of special project spc-97-4003. “Experimental investigation of a possibility of application of a microwave streamer gas discharge for ignition of fuel in a jet engine".
2. A.D.MacDonald. Microwave Breakdown in Gases. John Wiley & Sons, Inc., New York – London – Sydney, 1966.
3. Karfidov D.M., Lukina N.A., Sergeychev K.F. Fizika plazmi, 1981, T. 7, V.2, p.312.
4. A.S.Zarin, A.A.Kuzovnikov, V.M.Shibkov. "Svobodnolokalizovanniy microwolnoviy razrjad v vozduhe". Moskva, 1996.
5. W.Sharfman, T.Morita. IEEE Trans., AP-12, 6, 709,1964; W.Sharfman, T.Morita. Appl.Phys., 33, 2016, 1964.
6. R.O.Kuz'min. Besselevi funkcii. ONTI. 1935.
7. ?.?.????????. ?????????????? ?????????????? ???? ? ??????. ? ?????, «? ????», 1967, ???. 299.
8. L.D.Landau, I.M.Lifshic. Electrodinamika sploshnih sred. Moscva. "Nauka". 1982. P.32.
9. L.D.Landau, I.M.Lifshic. Electrodinamika sploshnih sred. Moscva. "Nauka". 1982. P.37.
10. L.A.Vanshteyn. Volni toka v tonkom cilindricheskom provodnike. ZGTF, 1959, T. XXIX, V.6, p. 689-699. ZGTF, 1961, T.XXXI, V. 1, p. 29-44.
11. L.P.Grachev, I.I.Esakov, G.I.Mishin, K.V.Khodataev. Skorost' fronta stimulirovannogo microvolnovogo razrjada v volnovom puchke. ZGTF. T.65, V.5, p.21-30.

12. L.P.Grachev, I.I.Esakov, G.I.Mishin, K.V.Khodataev, and V.V.Tsyplenkov. Evolution of the structure of a gas discharge at a microwave focus as a function of pressure. Tekh. Fiz. 39 (1), January 1994.
13. L.P.Grachev, I.I.Esakov, G.I.Mishin, K.V.Khodataev, and V.V.Tsyplenkov. Photografic record of the development of a high-pressure discharge in a wave beam. Sov. Tech. Phys.Lett. 18(11), November 1992, 737-739.

6. Deeply under-critical microwave discharge

Experiments described in the previous part showed the following consequence of the structure's change of the "attached" deeply under-critical streamer microwave discharge. Near the maximum level of the field, limiting the region of its realization, the discharge streamer channels are capable to form loops. These loops connect the ends of the initiating vibrator. With the increase of the value of the under-critical field this channels, going from the ends, do not connect into loops anymore.

At the further decrease of the microwave field's level they become shorter and shorter, localizing itself near the ends of the initiator. In this section we will describe the investigations of the initiated deeply under-critical discharge at very low level of the electric field. They were carried out with the relatively low-powerful generator with λ=12.5 cm. This wavelength is usually used in the everyday devices. The comparison of measurement results achieved for generators with wave length 8.9 cm and 12.5 cm have allowed to find also the discharge characteristics dependence on the radiation's wavelength.

6.1. Conditions of the experiment at λ=12.5 cm

Since the generator with λ=12.5 cm was for the first time applied in this setup, the preliminary works were carried out for the study of its characteristics and the field parameters that can be achieved in the discharge area.

Its basis represents the magnetron with the λ=12.5 cm, which outputting power is controlled in a definite range. The level of the operating signal is under the control. It determines the duration of the microwave pulse t_u, magnetron's output power P_{gen}, anode current of the magnetron I_a and its voltage U_a.

The operation scheme allows to control the duration of the microwave pulse from t_{pul}=0.25 s to practically continuous mode of the generator's work. The minimum duration of the pulse is limited by the velocity of the rise of the magnetron's output power starting from the moment of its switching on. Namely during this time it comes to its stable, constant value.

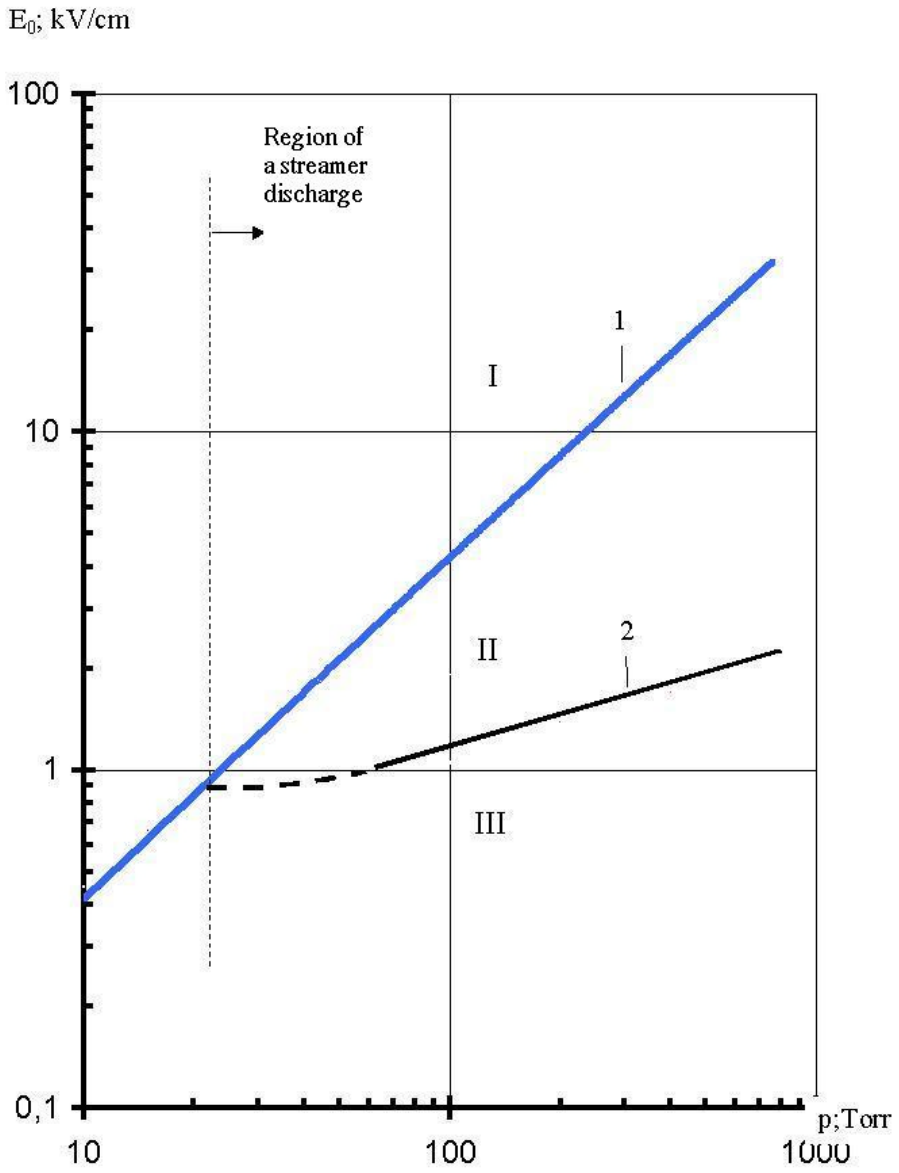

Fig.5.7. The areas of existence of the differ types of the microwave discharge in the coordinates (E_0, p). Line 2 shows the dependence of the boundary value E_0 of p that approximates the experimental points. Line 1 - E_{cr} (p). Area I - over critical discharges. Area II - the undercritical separating discharges. Area III - the deeply-undercritical attached discharges.

In the Fig.6.1 the experimentally obtained points I_a in the allowed range of the U_a variation are represented, the approximating them dependence $I_a(U_a)$ is represented too. This dependence corresponds to a famous law "power of 3/2": $I_a=\mu\cdot U_a^{3/2}$; at the perveance value $\mu=2.33\cdot10^{-6}$. This value of the perveance lies in the conventional range of values for such class devices. In Fig.6.2 the experimental dependence $P_{gen}(I_a)$ is represented.

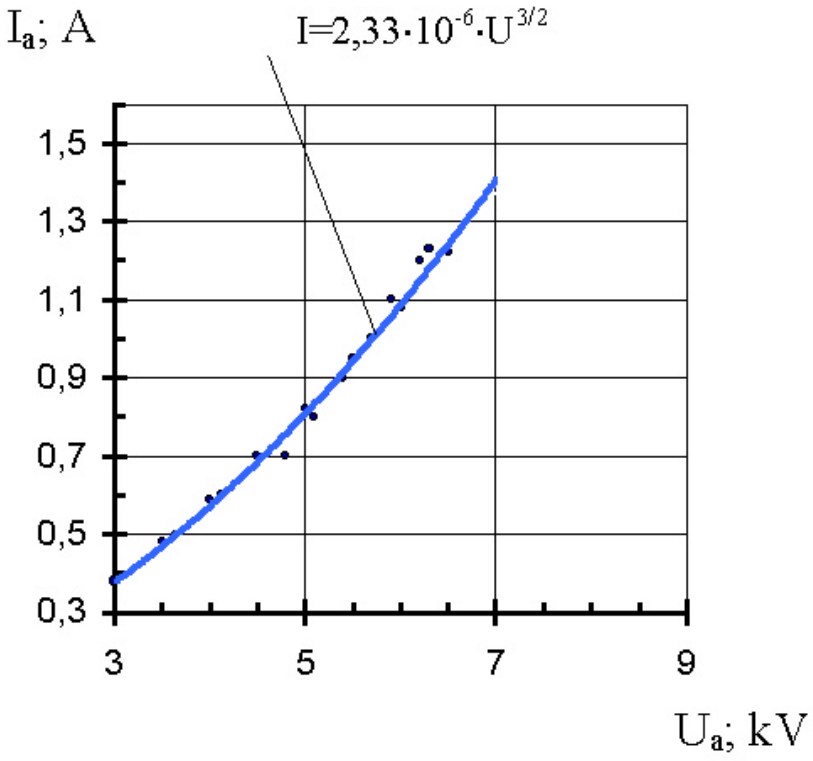

Fig.6.1. Anode current of the magnetron I_a in the allowed range of the anode voltage U_a. Points – experiment, solid line - the approximating dependence $I_a(U_a)$

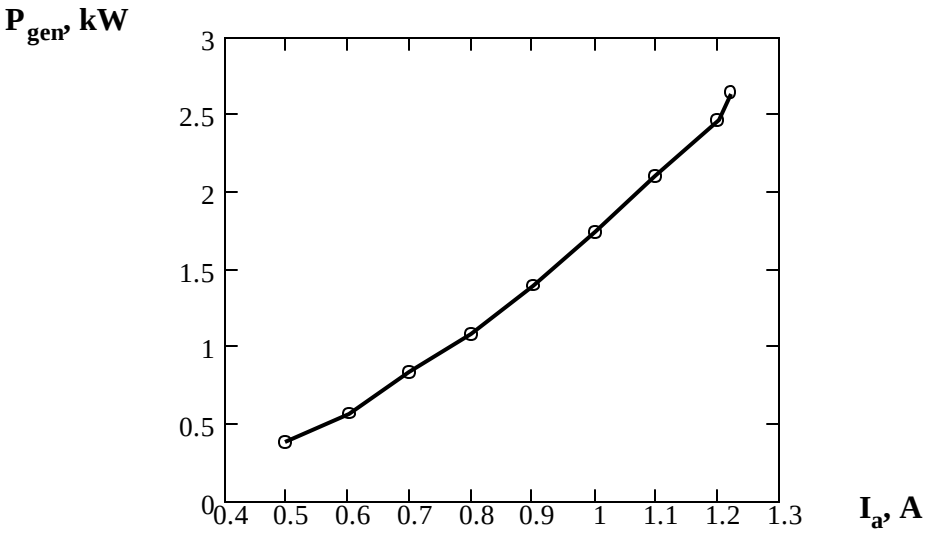

Fig.6.2. The generator power dependence on the anode current (λ=12.5 cm).

It was obtained at the continuous mode of the generator's work by means of the measuring wave-guide calorimeter. From this dependence one can see that the maximum output power of the generator is P_{gen}=2.6 kW, and the minimum one is 0.38 kW.

The efficiency coefficient of the generator in dependence of the anode current is given on Fig, 6.3.

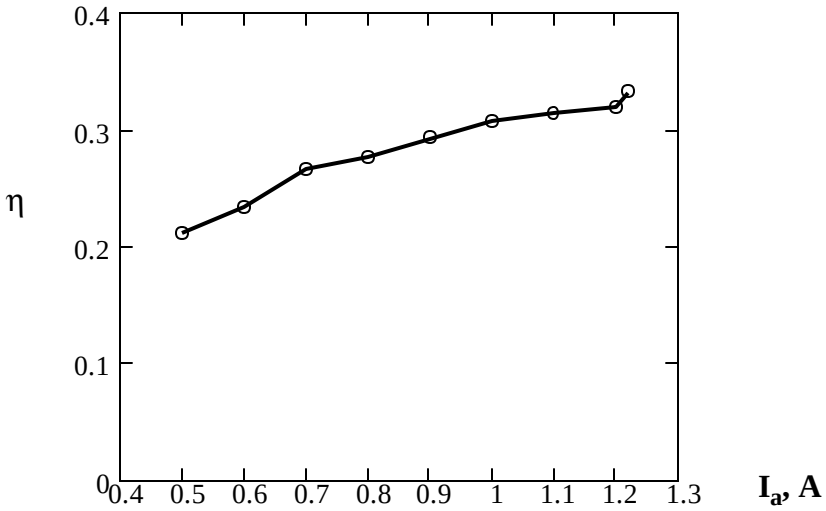

Fig.6.3. The efficiency coefficient of the generator (λ=12.5 cm) in dependence on the anode current.

In the main experiments the generator was connected with the wave-guide by the switch as it is shown in the Fig.2.1. Thus the EM wave with linear polarization was going from generator's outlet into the wave-guide path of the setup. In the focus of mirror the cross section amplitude distribution can be described approximately by the law

$$E = E_0 \cdot e^{-(x/a)^2 - (y/b)^2}, \qquad (6.1)$$

where mutually orthogonal axes x and y have the origin in the focus of the EM beam. The axis x is directed along the vector $\vec{E}_0$, and the typical sizes are a=7.3 cm and b=3.5 cm.

By the application of the obvious equation for the EM energy flux

$$P = c\frac{E_0^{\ 2}}{8p} \cdot \frac{pab}{2},$$

which are true for the EM wave with the TEM structure, one can estimate the maximum field's amplitude in the focus E_0. At the limit $P \to P_{gen}$ (the losses in wave-guide path and quasioptical antenna system is not taking into account) $E_0 \to 220$ V/cm. (In reality the coefficient efficiency of the wave-guide path is approximately equal to ~ 0.2-0.4).

From the Fig.5.7 follows that at λ=8.9 cm its maximal value E_0 lies in the area III, i.e. in the area of deeply under-critical discharges. And only the experiments can show if it will be at λ=12.5 cm in the same area.

6.2. Breakdown at the presence of the vibrator at l =12.5 cm

In the paragraph 4.1 the formula (4.8) is represented. It connects the field's value E_v on the tops of the conducting resonant vibrator, being placed parallel to the vector

$\vec{E}$ of the EM field, with the undisturbed amplitude of this field E_0. For the vibrator with the diameter 2a and the length $2l$=6.2 cm ≈ λ/2 this field is equal

$$E_v \approx \frac{3.2}{a_{[cm]}} \cdot E_0 . \qquad (6.2)$$

From the (6.2) follows that the field on the vibrator's tops can be made in principle arbitrary big by decrease of the vibrators diameter. In particular, it can be greater than the critical breakdown field E_c, related to the established air pressure p.

There is the difference between the vibrator and the ball: the maximum field of the latter according to (3.7) does not depend on its diameter while it is much less than wave length and equals to $3E_0$. However, as it has been studied theoretically in chapters 3 and 4, at the decrease of the diameter of a ball or of a vibrator the electron diffusion from the area of strengthened field can influence the breakdown process. In the frames of the present investigation the special experiment was carried out for the evaluation of the diffusion influence on the breakdown process.

6.3. Experiment on the air breakdown initiated by the resonant vibrator

The experiment was carried out at the placing of the wire vibrators into the focus of the EM beam parallel to $\vec{E}_0$. All vibrators were of the same almost resonant length $2l$=6.2 cm, but of different diameters and materials. Different conductors and their compositions were used. The breakdown was realized at the same duration of the microwave pulse t_{pul}=0.25 s and the same maximum pulse generator's output power $P_{gen=}$2.64 kW. In the experiments with each vibrator the maximum pressure p was determined at which the breakdown was still possible. At the necessity the surface of the vibrator could be illuminated by the pulse UV radiation source, described above.

Results of the experiment are represented in the Fig.6.4. The blue squares in it correspond to the vibrators made of aluminum, the lilac triangles - of copper, black points - of iron, and red crosses - to those of tin-plated copper. In this picture the dependence $p_{br=}C/(2a)$ is depicted. The coefficient of the proportionality C in it is calculated by the data on the experimental values of p_{br} for the vibrator with 2a=0.12 cm. One can see that the experimental points are rather well fit for Eq. (6.2) dependence.

In experiments we managed to realize the air breakdown up to the atmospheric pressure, or at the under-criticality level ψ=138. At the same time at the application of the vibrator with $2a=1.5\cdot10^{-2}$ cm according to (6.2) the breakdown of air can be achieved up to 6 atm. So we see that the diffusion influence is rather substantial, and the data represented in the Fig.6.3. can be used as the reference points at the developing of the diffuse theory of the microwave breakdown at the vibrator's presence. Also it is necessary to pay attention to the fact, that in this experiment the parameter l_a/a , introduced in the part 3.1, stays the same for each experimental point.

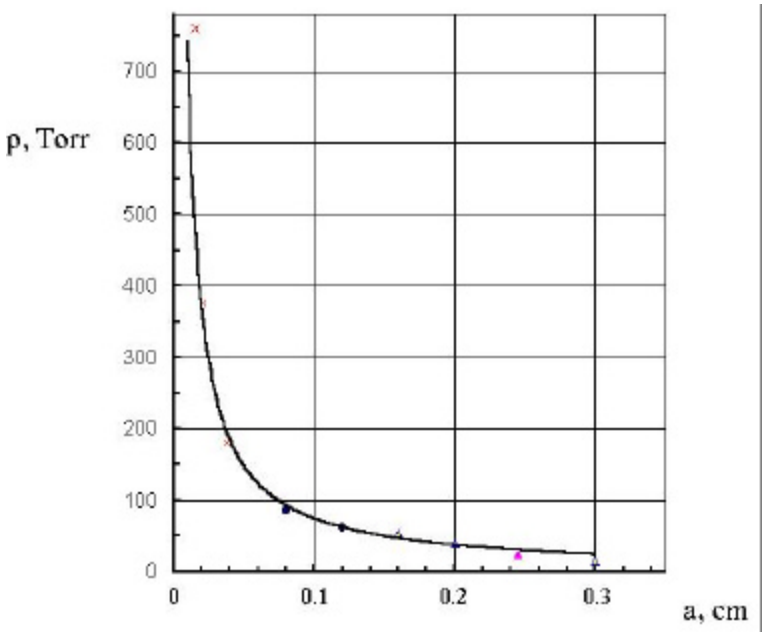

Fig.6.4. Results of the experiment with resonant vibrator at wave length 12.5 cm. The blue squares correspond to the resonant vibrators made of aluminum, the lilac triangles - of copper, black points - of iron, and red crosses - of tin-plated copper. Solid line -- the dependence $p_{br}=k/(2a)$. The coefficient k is calculated by the data on the experimental values of p_{br} for the vibrator with 2a=0,12 cm.

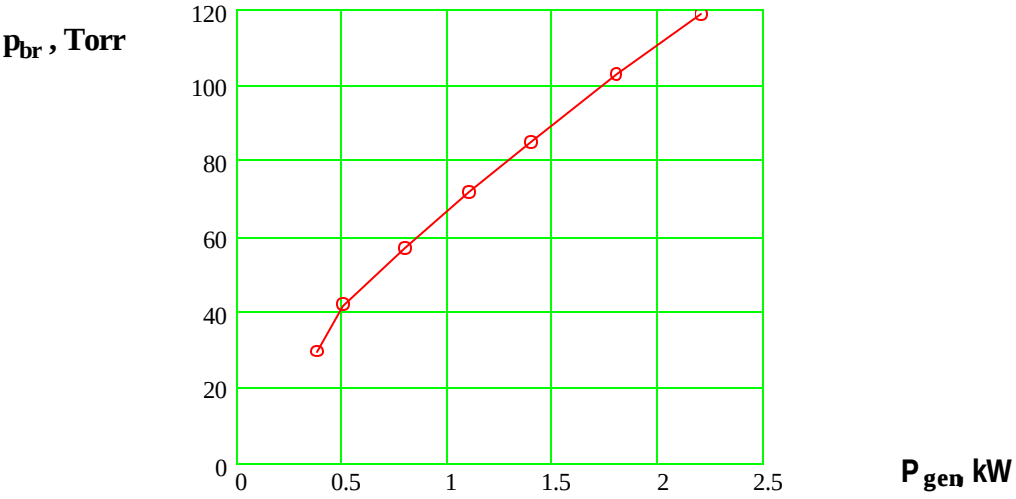

Fig.6.5 The experimental dependence p_{br} of the microwave beam power P_{gen} . The microwave pulse duration $t_{pal=}$1 s. The vibrator (length $2l$=6 cm, its diameter 2a=0.12 cm) is placed into the focus of the EM beam.

In the Fig.6.5 the experimental dependence p_{br} of the microwave beam power P_{gen} is represented. It corresponds to the microwave pulse duration $t_{pal=}$1s. It was obtained at the placing of the vibrator with $2l$=6.2 cm and 2a=0.12 cm into the focus of the EM beam. In the Fig.6.6 the same dependence is given in coordinates $E_{0\,br}(p)$.

In this picture the values E_{0br} were calculated on the basis of the experimental data P_{gen} with the account of the beam geometry and coefficient efficiency of he wave-guide path. In the same picture the dependence Eq. (4.10) for applied vibrator with the account of Eq.(4.8) at coefficient efficiency of waveguide path 0.4 is represented also. Obviously, by application of the vibrator as the discharge initiator it is possible to realize the microwave breakdown in the fields with very deep under-criticality.

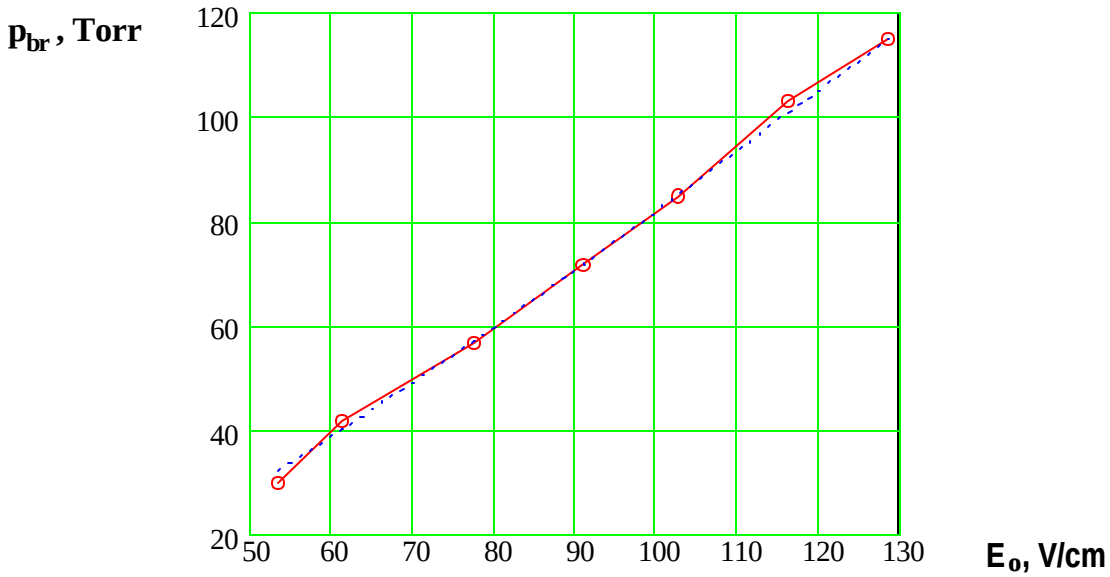

Fig.6.6. The breakdown air pressure in dependence of the unperturbed electric field amplitude at resonant vibrator (radius a=0.06 cm) presence. Solid line with points – the experiment data achieved from measured relation $\mathbf{p_{br}(P_{gen})}$ showed on Fig.6.4 at supposition that relation between microwave power passing through the focus spot to the generator power equals to R_{path}=0.4, dot line – the same theory function achieved from Eq. (4.10) and Eq.(4.8).

6.4. Deeply under-critical microwave discharge

In Fig.6.7 the typical photos of the discharges initiated by the vibrators are represented. These vibrators were earlier applied for obtaining of the dependence represented at the Fig.6.4 at the air pressure p=9 and 54 Torr. The vibrators in photos are located in the EM beam's focus and are parallel to the vector of the field $\vec{E}_0$. One can see there the capron thread used for vibrator's mounting.

Vibrator in Fig.6.7a has a diameter 2a=0.3 cm and the discharge burns at p=9 Torr. In respect with the Fig.5.7 it corresponds to the pressure area where at λ=8.9 cm the attached diffuse microwave discharge is realized. From Fig.6.7a). it follows that also at λ=12.5 cm the discharge is the diffuse one, and during the whole microwave pulse with the duration t_{pal}=0.25 s it is localized only near the poles of the vibrator initiating discharge.

Vibrator in Fig.6.7b has a diameter 2a=0.12 cm and the discharge burns already at p=54 Torr. In respect with the Fig.5.7 it belongs to the pressure area where at λ=8.9 cm the attached microwave discharge is realized in the streamer form. From the

Fig.6.7b follows that also at λ=12.5 cm the discharge is the "attached" one. One can see in the picture that it is ignited only near the lower initiator's end. Evidently it is connected with the level of the field which was reached as close as possible to the breakdown one during the experiment. From the picture is unclear if this discharge is the streamer type or not. In these experiments the duration of the microwave pulses was long, so it did not allow identify the discharge structure. The same phenomenon was observed at higher pressures also. At higher values of pressure the discharged area was stronger "pinned" to the vibrator's end.

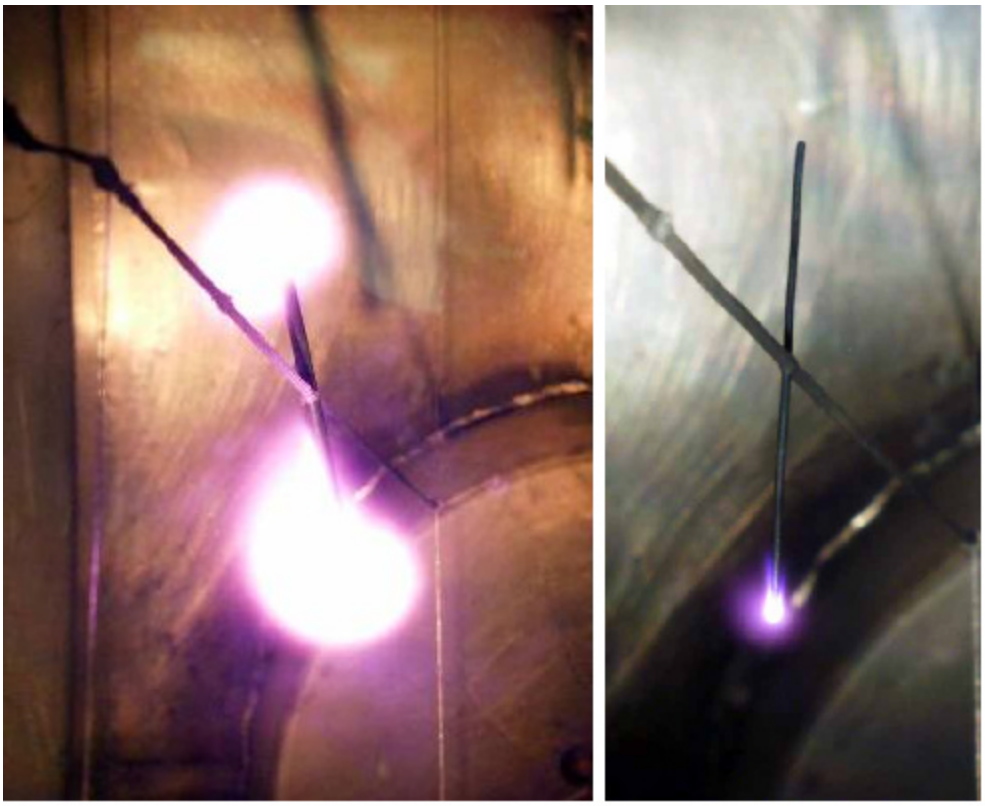

Fig.6.7. The typical photos of the discharge initiated by the vibrators. The vibrator are located in the EM beam's focus and are parallel to the vector of the field $\vec{E}_0$. Air pressure: a) p=9 Torr, b) p=54 Torr.

7. Estimation of the temperature inside the streamer channels of the under-critical initiated discharge in the "separating" and "attached" forms

The gas temperature **?** $_a$ inside the streamer channels of the under-critical and deeply under-critical discharges during the preliminary experiments was estimated. It was of the several thousands Kelvin degrees scale. In case of the initiation of such discharges by the microwave vibrator the streamer channels are originated on its tops and are in contact with it for several microseconds. It is evident, that in the contact's region of so high temperature streamer with the vibrator's surface the latter can be

heated and this can lead to its vaporization. This possibility was tested in a special experiment.

7.1. Estimation of the gas temperature inside the streamer channels in respect to the EM field level

In the described experiments the setup was equipped by the generator with λ=8.9 cm. The aluminum vibrators of the same diameter 2a=0.25 cm but of different length 2***l***=1, 2, 3, 4 cm could be placed into the EM beam focus. The vibrator's ends were spherically curved. Experiments were carried out at the atmospheric air pressure.

The photo detection of the discharge was made with each of the vibrators, in so doing the electric field level coincided with the boundary breakdown level $\mathbf{E_{br}}$. These boundary field values are represented in Fig.7.1 in the coordinates (E_0,2***l***). In this picture the experimental points are connected by the approximating curve. Let us note that the boundary electric field measured during this experiment is equal to 0.6 kV/cm for the resonant length 2***l***=4 cm. In the present experimental conditions the electron diffusion influence on the breakdown process was small because product $a\Lambda p >> 1$.

From the Fig.7.1 follows that with the length of the vibrator the under-criticality of the discharge Y increased from $\Psi \cong 6$ at 2***l***=1 cm up to $\Psi \cong 50$ at the resonance vibrator's length 2***l***=4 cm. In its turn, as it follows from the Fig.5.7, the discharge in this case has to have both forms, the “separating” and the “attached” one, it means that it has to be the under-critical and deeply under-critical as well.

In the Fig.7.2a-7.2d the corresponding photos are represented. From then one can really find that at 2***l***=1 and 2 cm ($\Psi \cong 6$ and 12, respectively) the discharge is the under-critical one (Fig.7.2d and c), and at 2***l***=3 and 4 cm (i.e. $\Psi \cong 27$ and 50) – is the deeply under-critical (Fig.7.2b and a).

From these photos follows that in all the cases the vibrator's surface was vaporized. The reference datum for the aluminum vaporization temperature is 2300 °? . So the experiment has revealed that up to very deep level of the under-criticality the initiated microwave discharge insures the temperature inside the channels no smaller than this temperature. Besides, the rate of power input to the vibrator pole's surface is very high and substantially exceeds the rate of its cooling due to the thermal conductivity mechanisms. In the result the heating of the vibrator material surface up its vaporization temperature takes place during the time Δ**t** which do not exceed several microseconds.

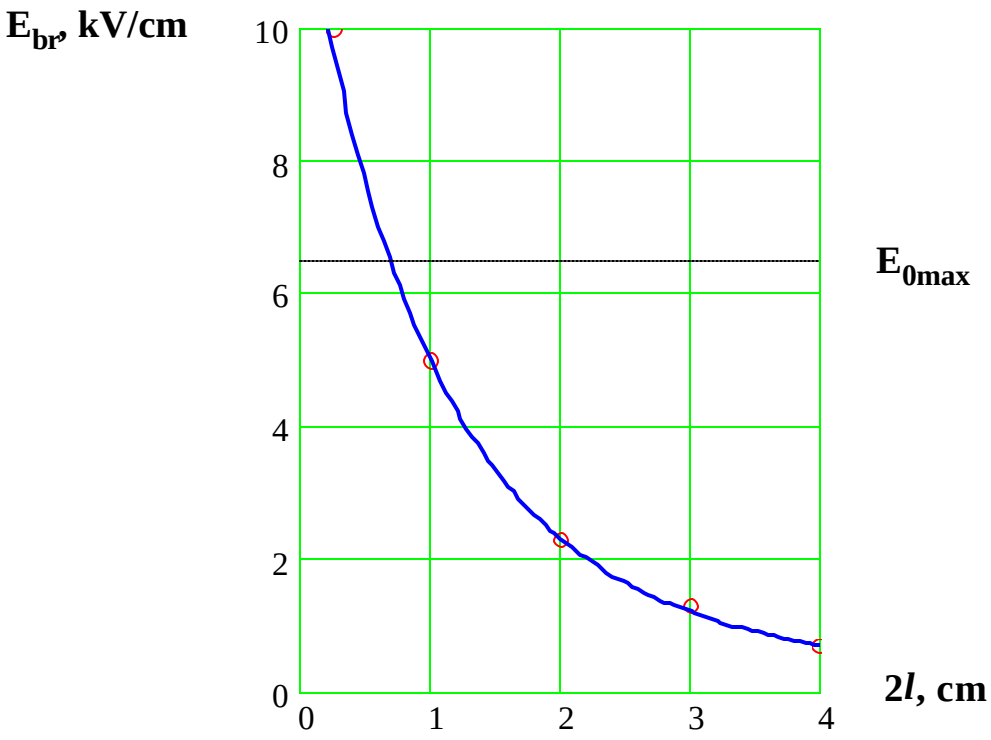

Fig.7.1. The breadown field $\mathbf{E_{br}}$ in depence on the vibrator length $2\boldsymbol{l}$. $2\mathbf{a}$=0.25 cm, p=760 Torr.

Let us make qualitatively the energy estimations for the streamer of the resonance length $2\boldsymbol{l} \cong \lambda/2$=4 cm of the under-critical "separating" discharge at p=760 Torr and at the experimental boundary under-criticality of this discharge form Ψ=17, that follows from the Fig.5.7. In experiments the diameter of the streamer's cross section did not exceed 2a=0.1 cm. Let us suppose that at the final stage of the development of this streamer channel's section the gas temperature in it rose for $\Delta T=2.5\cdot10^3$? . If to assume that the density of molecules in the streamer's channel $\mathbf{n_a}$ could not considerably decrease during the heating process, then for the heating of the gas inside the streamer the required energy is

$Q \cong (5/2)\cdot k\cdot\Delta T\cdot n_a\cdot 2\boldsymbol{l}\cdot\pi a^2 \cong 0.1$ J,

where $k=1.38\cdot10^{-23}$ J/K – is the Boltzmann constant, $n_a=2.43\cdot10^{19}$ cm^{-3}. The density of the EM energy flux in the TEM wave, at the given level of the under-criticality, in the region of this plasma vibrator is

$? =(E_c/\Psi)^2/(2Z_0) \cong 4.4\cdot10^3$ W/cm^2,

And its effective area is

$S_{ef} \cong (\lambda/2)^2$=16 cm^2.

Hence, the rate of the EM energy absorption by this vibrator is

$P=? \cdot S_{ef} \cong 7\cdot10^4$ W,

And time of the release of the required amount of energy is

$\Delta t=Q/P \cong 1.5$ μs.

In reality such a vibrator can absorb the EM energy during the time, which does not exceed the time of growth of another nearest plasma resonance vibrator. The

latter takes out the first one from the resonance. The growth average time of such vibrator

$t_{????} \cong (\lambda/2) / V_{str} \cong 4\ \mu s$,

where $V_{str} \cong 10^6$ cm/s is the mean velocity of the streamer's channel growth estimated during the experiment. One can see that the obtained numbers have the reasonable order of the magnitude.

The fields of deeply under-critical discharge are considerably smaller. The rate of power input to the streamer channels can be increased up to the full duration of the microwave pulse, but the channel's length in this case is significantly smaller.

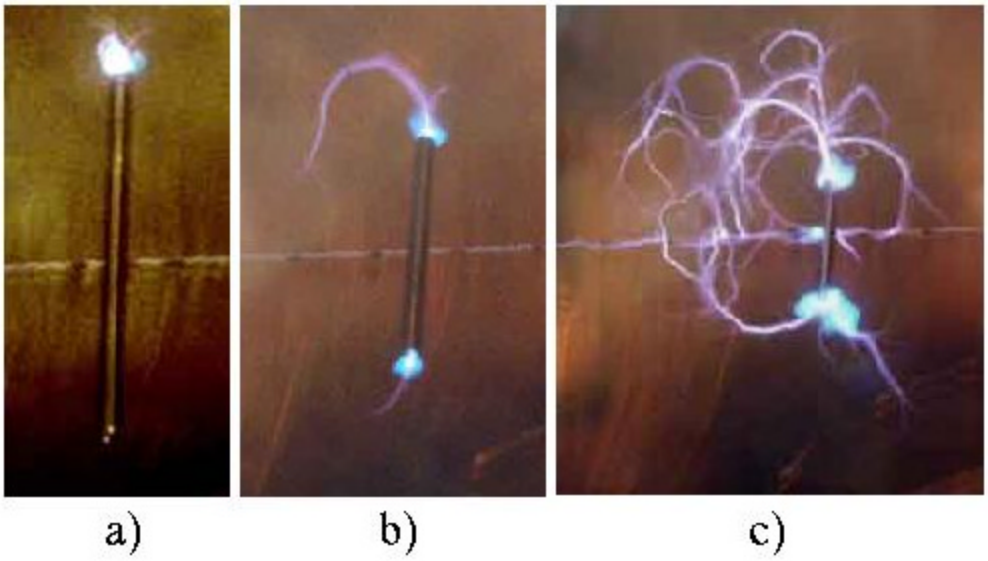

Fig.7.2. The views of initiated discharges with different degree of undercriticality. The vibrator's length 2l equals: a) – 4 cm, b) – 3 cm, c) 2 cm, d) 1 cm. p=760 Torr. The field values correspond to the Fig.7.1.

7.2. Estimates of the gas temperature inside the streamer's channel in respect to air pressure

In these experiments the setup was equipped by the generator with λ=8.9 cm. Into to the EM beam focus the aluminum vibrator of the diameter 2a=0.25 cm and of the length 2***l***=1 cm was placed. The vibrator's ends were spherically curved. The photo detection of the discharge region was carried out in the range of pressure from 9 to 760 Torr.

At each pressure the field was established at the level coinciding with breakdown field $\mathbf{E_{br}}$. In the Fig.7.3 these boundary field values in the coordinates (E_0,p) are represented, they are connected by the approximating curve.

In the Fig.7.4a–7.4e the discharge photos at p=9, 30, 120, 300 and 760 Torr, respectively, are represented at the boundary breakdown field levels.

One can see from them at discharges at p=9 and 30 Torr are the diffuse and the attached to the vibrator's poles. As a matter of fact, it again confirms the above represented data that the discharge in the streamer form is realized only at **p** greater than several tens Torr, and only being in this form it can "separate" from the initiator.

In the Fig.7.4c-e the discharges are already the streamer type and are capable for the independent development. At the same time the vaporization was observed only in the Fig.7.4d and 7.4e. It means that at p=120 Torr (Fig.7.4c) the discharge is in the streamer form, but the temperature, realized in the streamer, or the energy, transferred to the surface, is not enough for its heating and vaporization.

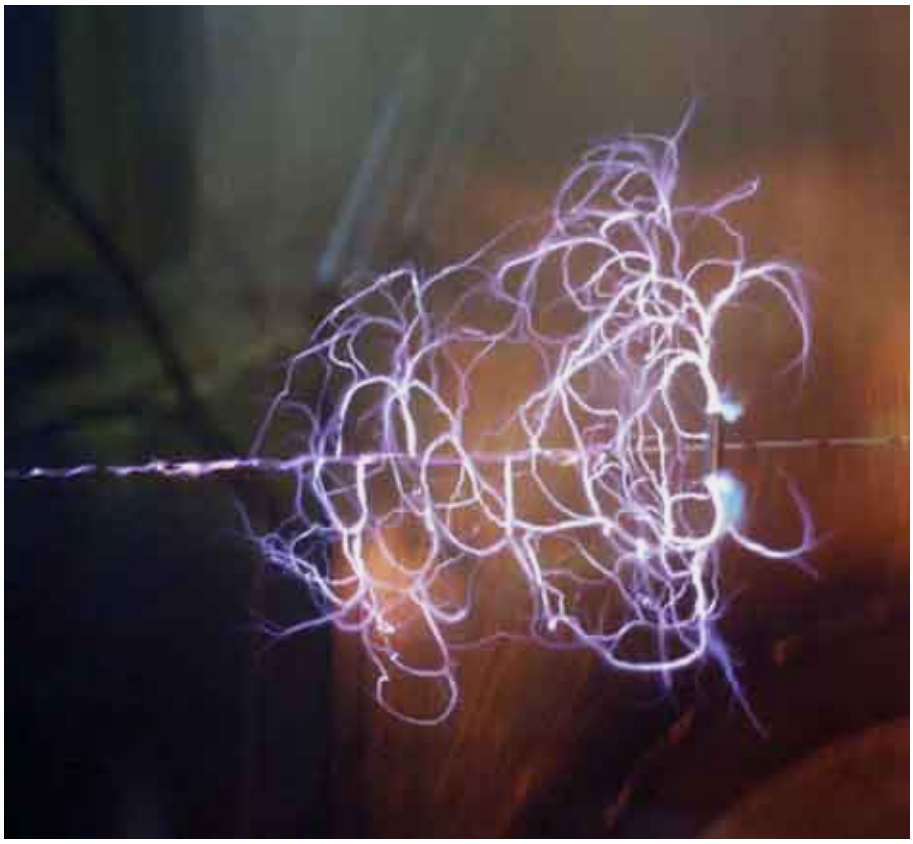

Fig.7.2d. The vibrator's length equals to 1 cm.

In the conditions of the experiment the vaporization of the surface on the initiator's poles began only at p > 250 Torr. Only starting from this pressure the gas temperature inside the streamer plasma channels has the value no less than $2.5 \cdot 10^3$ K, and energy coming to the vibrator's surface is enough for its vaporization. This experiment did not give the answer to the question about the value of the temperature inside the streamer channels in the range from 30 to 250 Torr.

7.3. The discharge at λ=12.5 cm

As it was pointed out above the pulse duration of the generator with λ=12.5 cm in the conditions of the experiment, could not be smaller than t_{pul}=0.25 s.

On this reason the thermal effects connected with the high temperature of the discharge were considerably greater than in experiments with λ=8.9 cm in spite of the relatively small power of this generator. (Let's remind, that generator 8.9 cm has the high power but the very short pulse duration-t_{pul}=40 μs).

In the Fig.7.5a the photo of the discharge region near the lower end of the initiating copper vibrator with $2\boldsymbol{l}$=6 cm and 2a=0.05 cm at p=160 Torr and E_0=220

V/cm is represented. One can see in it the intense vaporization of the vibrator's material and the convection upside elongation of the heated area. Remind that the copper's vaporization temperature is 2360 °C.

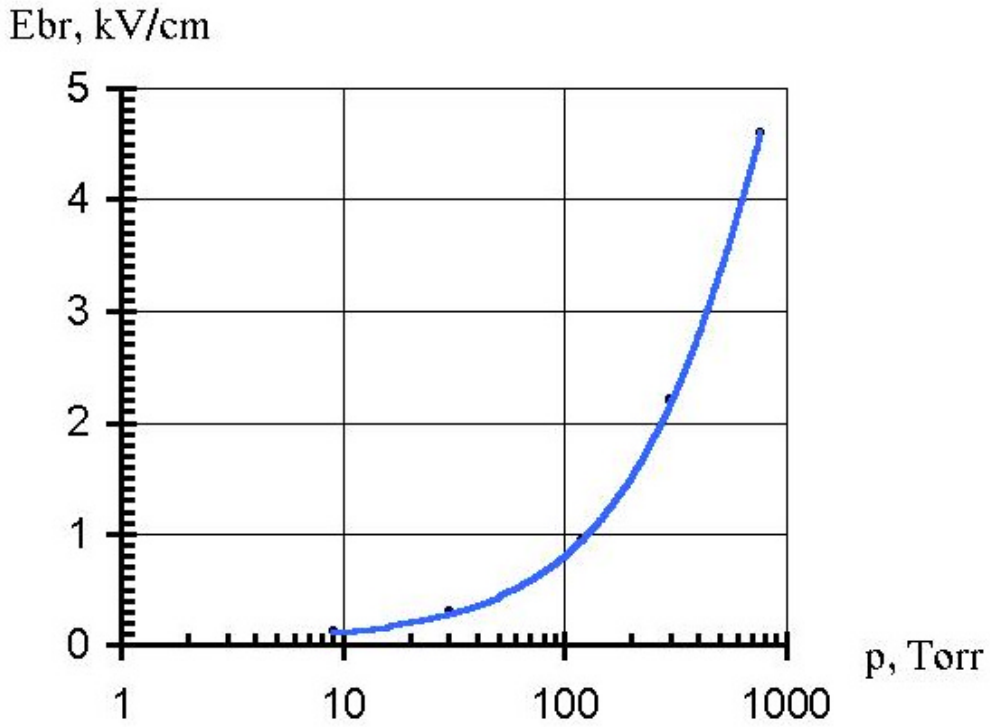

Fig.7.3. The breakdown field values Ebr in dependence on the air pressure. The vibrator length equals to 1 cm, 2a=0.25 cm. The line - approximating curve.

In the Fig.7.5b the photo of the discharge region near the upper end of the initiating tin-plated copper vibrator with 2***l***=6 cm and 2a=0.015 cm at p=330 Torr and E_0=220 V/cm is represented. In it is also detected the vaporization of the vibrator's material and the convection upside elongation of the heated area. Note that for the thin vibrator the vaporization has the catastrophically character. For example, in the Fig.7.6 the photo of the end of this vibrator after the single discharge is represented. One can see that this end is substantially melted, it had absolutely lost its initial form.

So in the real constructions, especially at high levels of the field's under-criticality, i.e. at small diameters of the initiating vibrators and long duration of the discharge in the "attached" form, it is necessary to account the considerable heat loads toward the initiator's surface.

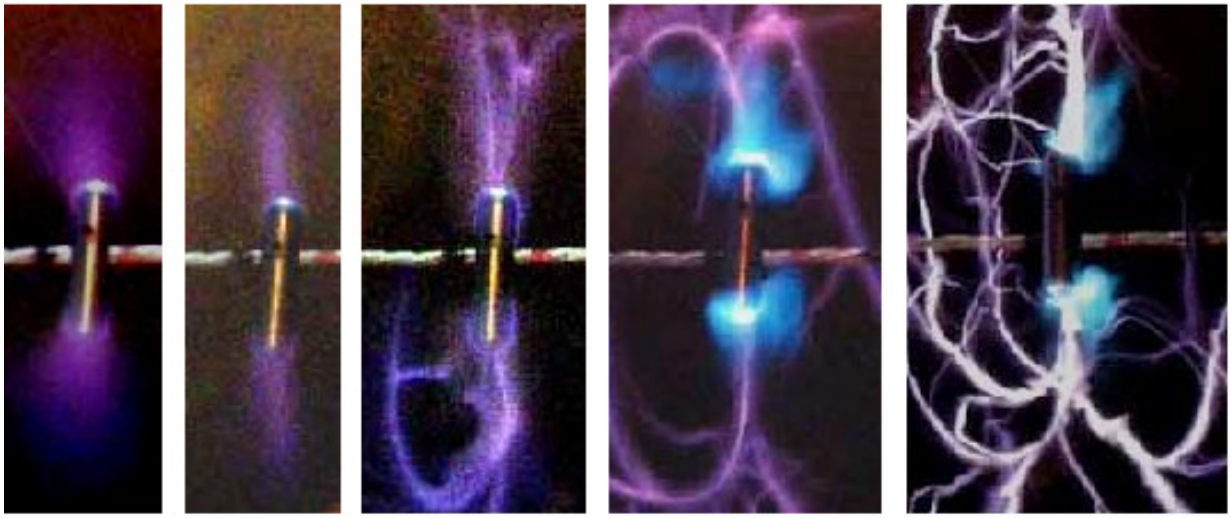

a) b) c) d) e)

Fig.7.4. The discharge photos at different air pressure: a) - 9, b) -30, c) – 120, d) - 300 and e) - 760 Torr, the boundary breakdown field levels correspond to Fig.7.3.

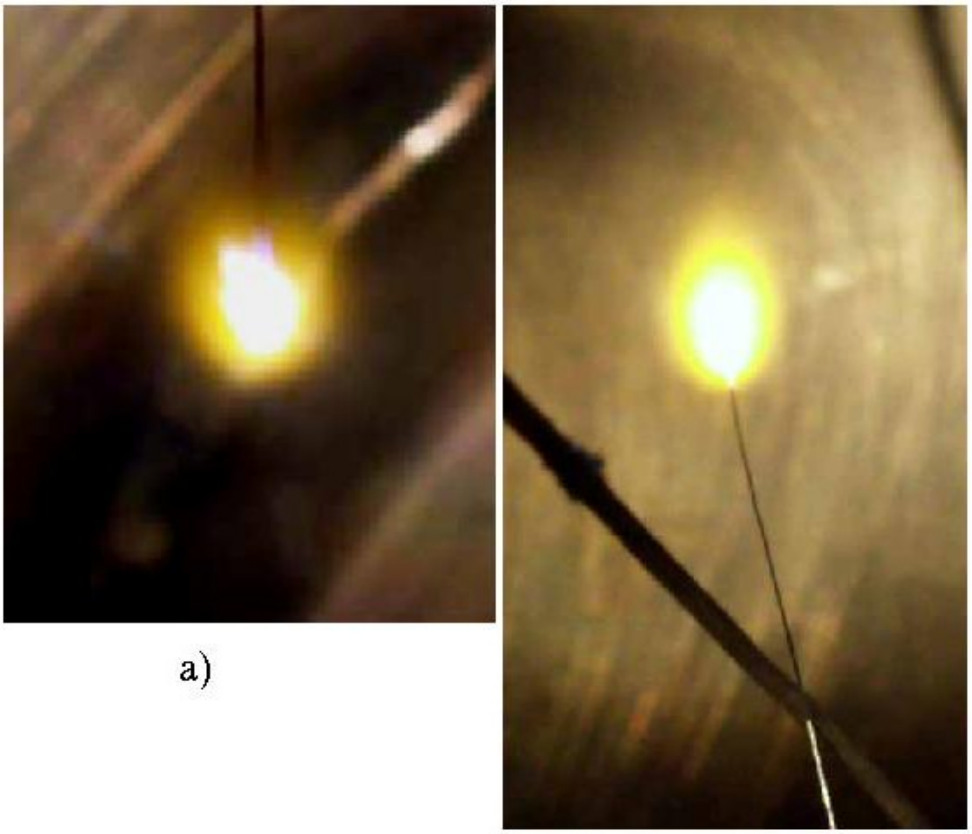

a)

b)

Fig.7.5. The photo of the discharge region near the end of the initiating copper vibrator with $2l$=6 cm, E_0=220 V/cm. a) - 2a=0.05 cm at p=160 Torr, b) - 2a=0.015 cm at p=330 Torr**.**

8. Demonstration of ignition of the model flammable mixture

Previous experiments have shown that the microwave discharge is of the streamer form at the high pressure in the undercritical and deeply undercritical fields. In these cases the temperature of plasma streamer channels that form the discharge has the scale no less than 2000 °K. In principle the realization of such temperature is enough for the fuel ignition. In the experiments, described below, this possibility was straightly tested. During the tests we used the mixture of butane-propane and of hydrogen with air. For the ignition of the model flammable mixtures we applied the initiated microwave pulse discharges in the under critical and deeply under critical forms at λ=8.9 and 12.5 cm.

Fig.7.6 (14) The photo of the end of the vibrator after the single discharge, as on the Fig.7.5b.

8.1. Experimental conditions

The scheme of the test with the undercritical "separating" discharge is represented in Fig.8.1, and with deeply undercritical "attached" discharge is in the Fig.8.2. For example, in the Fig.8.3 the photo is represented that illustrates the location of different elements of the schemes in the tests with the under critical discharge.

In the experiments the discharge was initiated by the vibrator that was located in the focus of the EM radiation parallel to the vector $\vec{E}_0$ of the field. Vibrator was fixed by the braid $2\cdot10^{-2}$?m thick, made of the glass fibers. The vibrator pierced the braid

and remained on it due to friction force. The braid was drawn perpendicular to the vector $\vec{E}_0$ of the field. In the Fig.8.3 to the right from the center one can see the vibrator, the braid for its fixing, and two vertical braids by which this braid was mounted.

Flammable gases were given from the balloon of the high pressure. To the outlet valve of it the system of the inputting of the flammable mixture to the place of the ignition was connected.

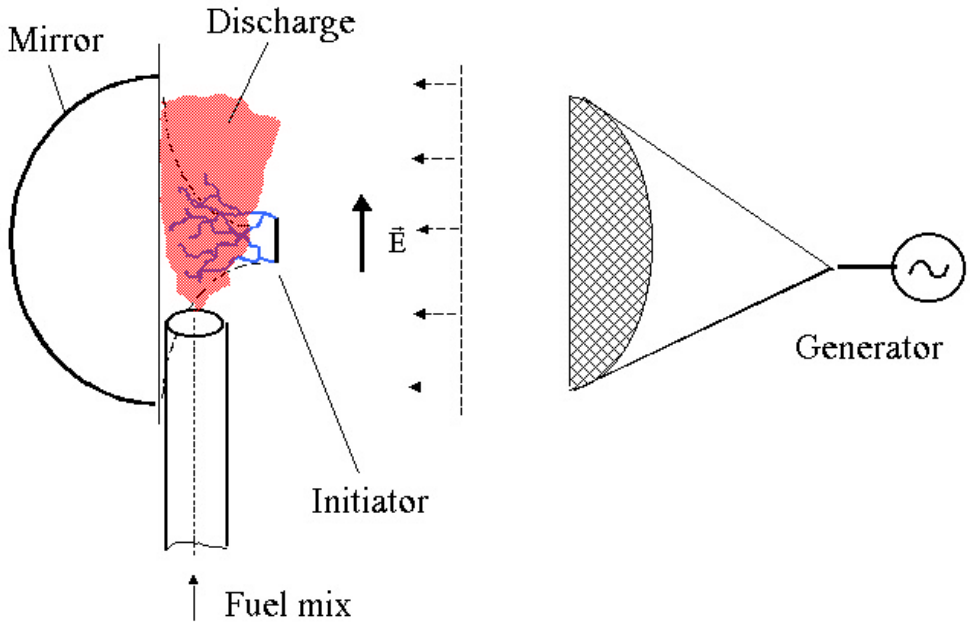

Fig.8.1. The scheme of the test with the undercritical "separating" discharge

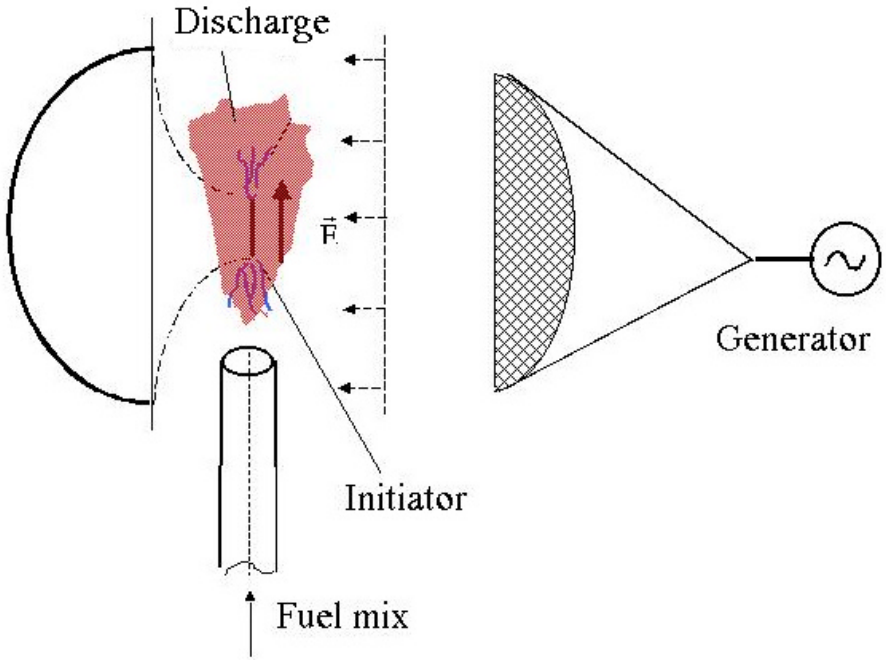

Fig.8.2. The scheme of the test with the deeply undercritical, "attached", discharge.

This system consisted (consequently from the balloon) of the mixer, in which the gas was mixed with air in the required proportion, flexible hose and the outlet quartz pipe. The quartz pipe had the outside diameter 2 cm, inside diameter 1.6 cm. Its length was 15 cm. The pipe was fixed so that its axis was collinear to the vector $\vec{E}_0$ and it crossed the axis of the EM beam. Its open outlet end was 5.5 cm below the axis of EM beam. In experiments with the undercritical discharge the pipe was pressed down to the mirror's edge, i.e. its axis was at 7 cm from the vibrator in the direction of the focusing mirror (see Fig.8.3). In experiments with deeply under-critical discharges the tube was located directly under the initiator, and its axis was aligned with the vibrator's axis.

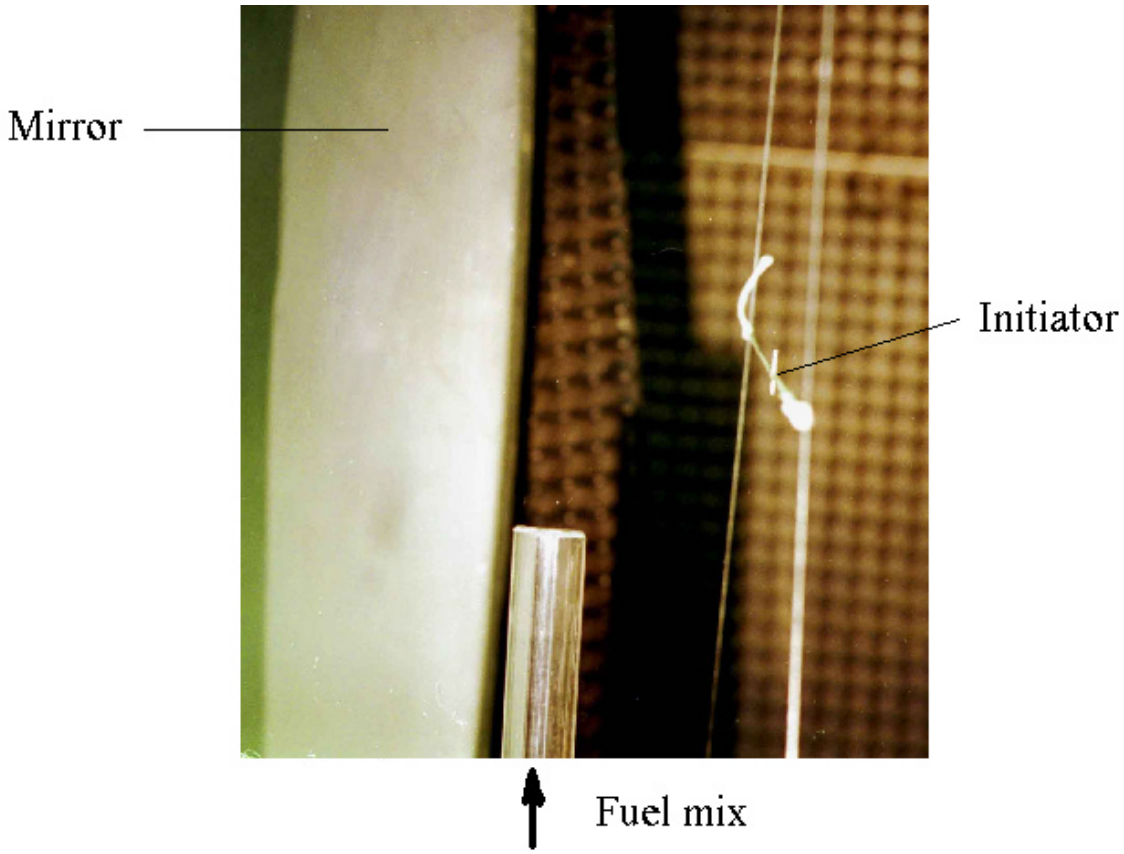

Fig.8.3. The photo of location of different elements in the tests with the under-critical discharge (see Fig.8.1)

These experiments were carried out in the atmospheric air. For this purpose the cylindrical part of the vacuum chamber was detached from the immobile flange and moved behind the focusing mirror (see Fig.2.3). Below the quartz pipe, brining the flammable mixture to the focus area, the ventilator was placed. It ensured the vertical airflow of several m/s through the discharge area.

8.2. Experimental results at l =8.9 ?m

In the Fig.8.4a the photo of the undercritical discharge without giving of the flammable mixture at E_0=6.5 kV/cm is represented. The discharge was initiated by the vibrator with 2a=0.25 ?m and 2L=1 ?m. One can see from the photo that during

the microwave pulse the discharge propagated in the direction of the focusing mirror and it crossed the axis of the quartz pipe. In the Fig.8.4b is represented the photo of the EM beam focus area at the discharge presence in the same conditions with the flow of the flammable mixture. One can see that the discharge has ignited it. In the experiment the mixture continued to burn after the end of the microwave pulse, i.e. it executed the role of the ignition key or a "match".

In the Fig.8.5a the photo of the deeply undercritical discharge without giving of the flammable mixture at E_0=1.5 kV/cm is represented. The discharge was initiated by the vibrator with 2a=0.25 ?m and approximately resonance length 2L=4 ?m.

One can see that the discharge is the "attached" one, i.e. the discharge areas are localized near the vibrator's poles. In the Fig. 8.5b one can see the photo of the focus area at the simultaneous presence of the discharge, with the given above characteristics, and the flow of the flammable mixture. On can see that the discharge has realized its ignition. In this case the discharge also executed the role of the ignition key or a "match".

8.3. Results of experiments with l =12.5 ?m

In the Fig. 8.6a the photo of the microwave discharge at E_0=220 V/cm and duration of 0.25 s is represented. The discharge was initiated by the resonance vibrator with 2L=6 ?m.

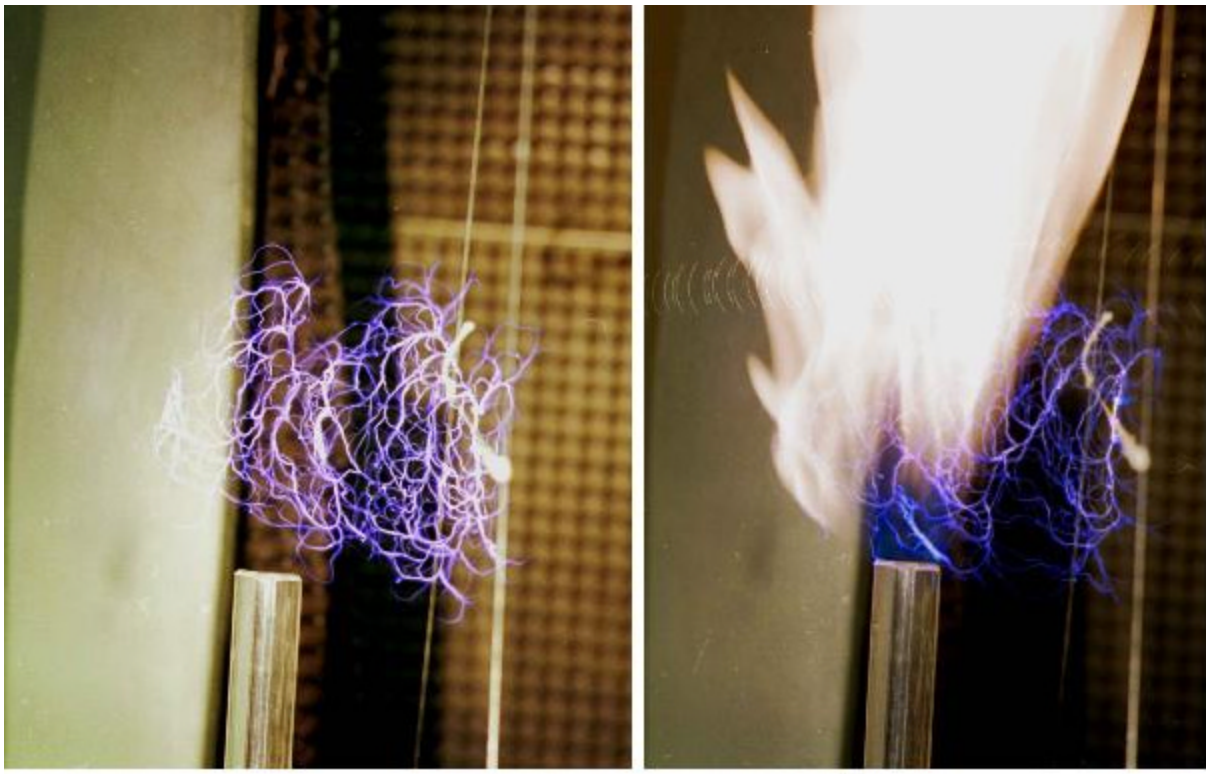

a) b)

Fig.8.4 The photo of the undercritical discharge, initiated by the vibrator with 2a=0.25 ?m and 2L=1 ?m (E_0=6.5 kV/cm,): a) - without flow of the flammable mixture, b) - conditions with the flow of the flammable mixture.

During the fulfillment of this experiment we revealed the difficulties connected with the impossibility to shorten the pulse duration $\mathbf{t_{pul}}$ at the application of the present microwave generator. From one hand for the atmospheric air breakdown in such deeply undercritical field is necessary to use the vibrator with the minimum possible diameter **2a**, up to tenth part of the mm (see the graph in the Fig.6.4). From another hand at the given $\mathbf{t_{pul}}$ the "ohm" energy released in the vibrator's central part at the absence of the discharge leads to its "blowing". At the switching the discharge on the energy release takes place now at the vibrator's poles. As the result they are destroyed (see Fig.7.7), and it is necessary to change the broken vibrator for the new one after each microwave pulse leading to the discharge ignition.

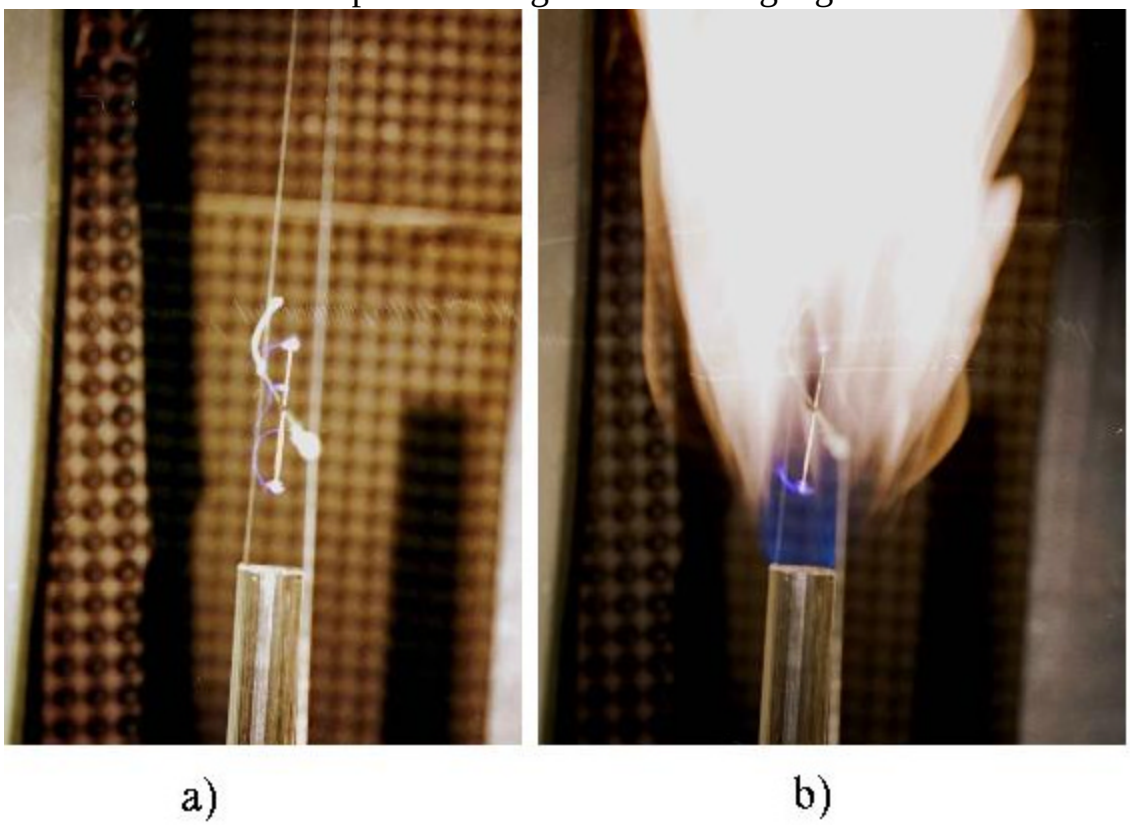

Fig.8.5 The photo of the deeply undercritical discharge, initiated by the vibrator with 2a=0.25 ?m and 2L=4 ?m (E_0=1.5 kV/cm,): a) - without flow of the flammable mixture, b) - conditions with the flow of the flammable mixture

One can see in the Fig.8.6a that at the given conditions the discharge has been ignited only near the upper end of the vibrator. It is the typical case that is realized in the experiment. It has the following explanation. At the starting segment of $\mathbf{t_{pul}}$ the "ohm" heating of the vibrator takes place, also the heating of air takes place in its vicinity. Isobaric heated air, having the smaller density, moves up due to convection, this facilitates the breakdown conditions namely near the upper end of the vibrator. One can see tracks in the Fig.8.6a, they are made by the heated "pieces" of the vibrator, starting from its end in the discharge area.

In the Fig.8.6b is represented one of the photos of the EM beam focus area at the simultaneous presence of the discharge, in the discussed above conditions, and of the

flammable mixture. One can see that the discharge has realized the ignition of the flammable mixture. Also in these experiments it has a role of the ignition key or a "match", i.e. the mixture continued to burn after the end of the microwave pulse.

In the Fig.8.6c another possible experimental situation is represented. From the given photo one can see the tracks, made by the destroyed material of the vibrator's surface. Shining vibrator's "pieces" start from its end, and then they "explode" with the creation of a fan of the new tracks. From our point of view this phenomenon can be used in the one-time-use devices for the flow of the flammable mixture with large transverse cross section. The mixture would be ignited along the way of each of such tracks.

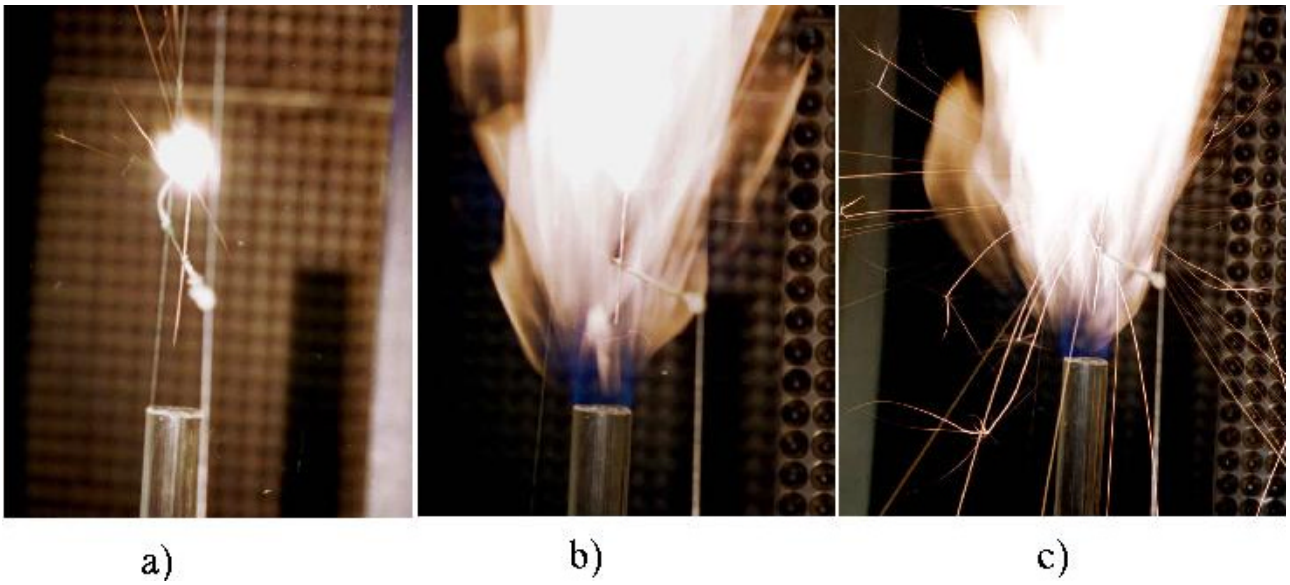

Fig.8.6. The photo of the microwave discharge at E_0=220 V/cm and duration of 0.25 s is represented. The discharge was initiated by the resonance vibrator with 2L=6 ?m.

9. Streamer undercritical microwave discharge in the supersonic flow

In the real engine the microwave discharge has to be realized in the high-speed flow of the flammable mixture. As it was noted above the undercritical microwave discharge is of the streamer type in gases at high pressure. The streamer channels of its composition have their typical velocity of growth that lie in the range 10^5 – 10^6 cm/s. It is naturally to suppose that at the ignition of such discharge in flows with considerably smaller velocities the discharge properties will not change. And, nevertheless, within the framework of the given work the experiment on the ignition of the streamer undercritical discharge in the supersonic airflow was executed. Thus the change of its appearance was recorded and the influence of a flow on border of a microwave field, that is separating the discharges in the undercritical and deeply undercritical forms, was estimated.

9.1. Experimental conditions

The scheme of the experiment is represented in the Fig. 9.1.

Discharge was ignited in the submerged air jet. The jet was formed at the outlet of the dielectric pipe of 5.4 cm diameter and of 81 cm length. The pipe's axis crossed the EM radiation focus and was collinear to the vector $\vec{E}_0$. Outlet of the pipe was opened into the chamber and was standing at 10 cm from the focus. The external pipe's end was sealed from the atmosphere by the polyethylene tereftalate diaphragm by 20μ thick. From the external side near the surface of the film the wire by 0.01cm diameter and by 3 cm length (made of Ni-Cr alloy) was located. The wire was included into the circuit of the discharge of the high voltage capacitor. The chamber was preliminary pumped out up to some pressure value $\mathbf{p_k}$. During the switching on of the high voltage capacitor circuit the wire was blown up and it destroyed the film diaphragm. From this moment the atmospheric air flowed into the chamber. The pressure in the chamber was increased with measured rate 0.38 Torr/ms.

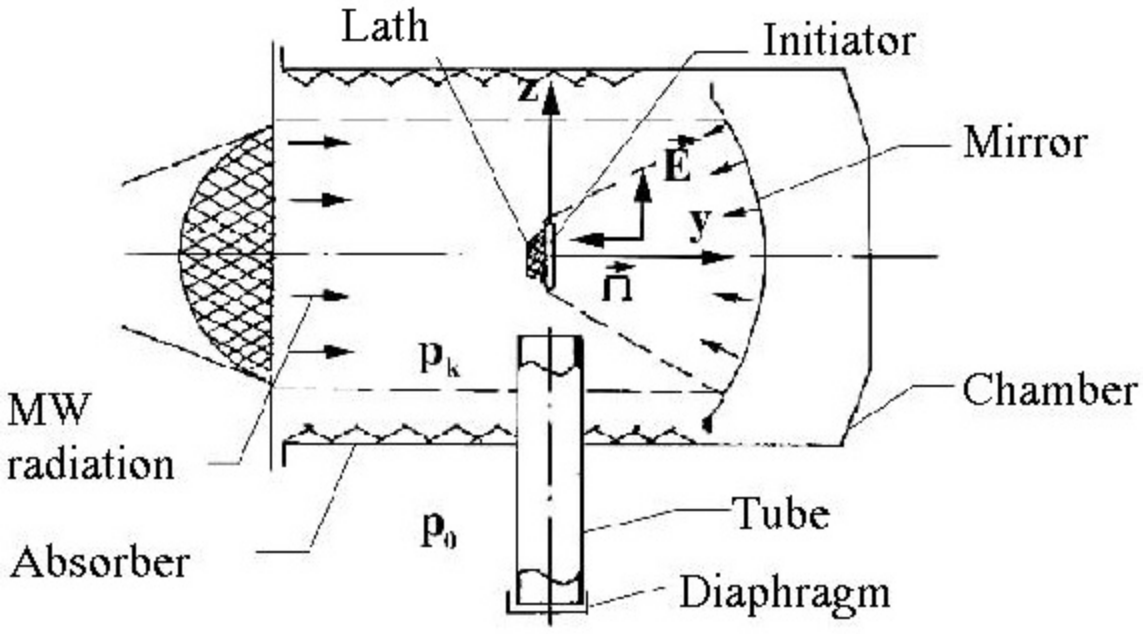

Fig.9.1. The scheme of the experiment.

In experiment the initial pressure $\mathbf{p_k}$ was always smaller than the external atmospheric one more than by 1.9 times. In this case the axially symmetric air jet was formed at the outlet of the pipe at the flow Mach number ? > 1. If in the beginning of the leak-in process the critical flow in the outlet pipe's cross section is realized, then in this cross section the flow parameters: velocity of the flow V_{out}, the air temperature T_{out}, the static pressure p_{out} and the density of molecules n_{out} , are equal to 310 m/s, 250°K, 400Torr and $1.632\cdot10^{19}$ cm^{-3} correspondingly. The jet parameters in the area of the focus depend on the ratio p_{out}/p_k.

For example at p_k=300 Torr the static air pressure in the jet equalizes with $\mathbf{p_k}$ at the increase of the jet's diameter in respect to its outlet diameter for 2%. At cross-section of the jet the flow is the supersonic one. Its Mach number is M=1.23, velocity of the flow is V=370 m/s and the density of molecules in the flow is $n_p=1.3\cdot n_k$, where $n_k=10^{19}$ cm^{-3} is the concentration of molecules in the immobile air surrounding the flow at this pressure $\mathbf{p_k}$.

At p_k=100 Torr in the jet's cross section, where its static pressure is equalized with $\mathbf{p_k}$, the jet's diameter is increased in respect to its outlet diameter for 30%. In this case the velocity of the flow is V=500 m/s at $n_p=1.8\ n_k$, where $n_k=3.4\cdot10^{18}cm^{-3}$. Here we have to note that at the equality between the pressure in the jet and the pressure in the chamber, because the flow is colder, the molecule density in the jet is higher than in the immobile air surrounding the flow. So the conditions of air breakdown inside the jet are stricter, i.e. for the discharge ignition in the flow the greater field is required.

The discharge initiating vibrator was located in the focus of the EM beam parallel to $\vec{E}_0$. It was made of the copper wire 0.08 cm in diameter and by 4 cm legth. The vibrator was fixed in the middle of the batten (see Fig.9.1) made of the

organic glass, 2.5 cm width and 0.6 cm thick. The batten crossed the focus perpendicular to the radiation's direction. Its wide side was parallel to $\vec{E}_0$. The batten had facets in its transverse section in order to decrease its influence on the airflow in the area of the expected discharge, as it is shown in the Fig.9.1. The initiating vibrator was fixed to the flat side of the batten, facing the mirror focusing the EM field.

In experiments some time D**t** was kept up between the moment of the film blowing up and the moment of microwave's pulse giving. This value D**t** was beforehand estimated by using of the expected velocity of the flow. Thus we accounted that the flow has been already formed in the area of the focus, but the reflections of the jet from the opposite chamber's wall has not appeared yet. This wall stayed at 45 cm from the focus. The more precise values of the time D**t** was found during experiments, because it was difficult to forecast the velocity of destruction of the diaphragm. It was found in experiments that D**t** is necessary for varying in the range of several ms.

9.2. Experimental results

During experiments we made photos of the discharge area, the forms of the discharge with and without flow were compared.

In the Fig.9.2a the discharge without flow is represented at p_k=300 Torr and E_0=6.5 kV/cm. One can see that the discharge in this case is represented by the typical "tangle" of the streamer channels. The length of the discharge area toward the radiation is about 10 cm.

In the Fig.9.2b the photo of the discharge is represented at the same $\mathbf{p_k}$ and $\mathbf{E_0}$, but with the jet at Δt=10 m?. In the photo on can see from below the outlet end of the pipe that formed the jet. It is illumined by the flash of the blowing up wire, that destroy the diaphragm sealing the pipe. One can see the tracks made by the wire and diaphragm "fragments", they drifted by the airflow.

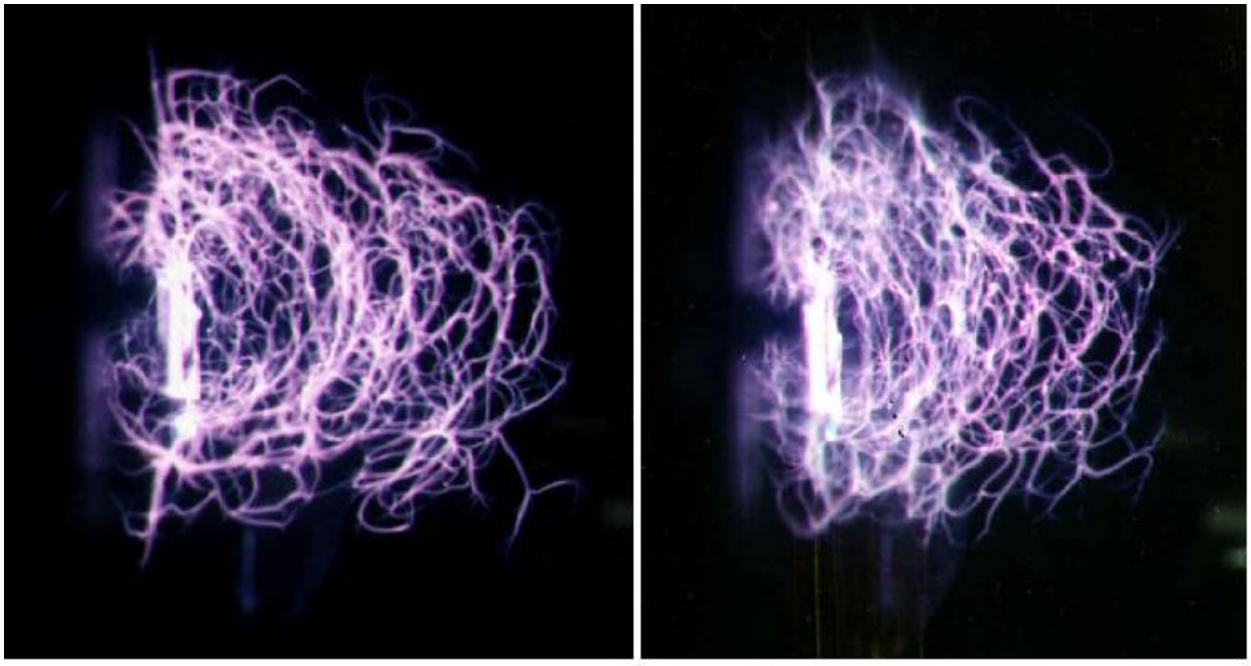

Fig.9.2. The discharge at p_k=300 Torr and E_0=6.5 kV/cm. a)- without flow, b)- with the flow

They in some way visualize the jet's boundaries. One can see that the discharge's form in the presence of the flow practically have not changed. The distance covered by the discharge in the direction of the focusing mirror at the presence of the jet also practically have not changed. We see that in conditions of this experiment, as it was expected, the discharge in the flow practically was not different from the discharge in the immobile air.

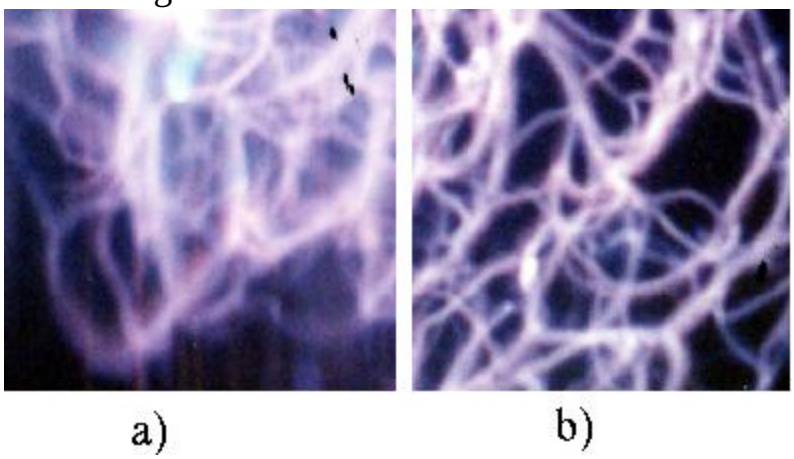

Fig.9.3. Large scale photos of the streamer discharge parts in the flow (a) and in immobile air (b)

In the tested geometry the discharge was in the flow only at the initial stage of its development, then it propagated to the mirror, focusing EM radiation, in the immobile air. In the photo it is reflected by the "blur" along the flow of the streamer channels placed in the area of the supersonic airflow. Outside the jet they

have distinct boundaries. In the Fig.9.3, in the magnified in respect to the Fig.9.2 scale, the photos of the streamer discharge parts are presented, approximately perpendicular to $\vec{E}_0$, in the flow (a) and in immobile air (b). From the picture one can see that the diameter of the streamer outside the jet is about 0.1 cm, but in the jet its size along the flow is much more.

The estimate shows that its enlarging is mainly the result of the streamer channel's plasma "afterglow", because the drift of molecules in the plasma channel's area during the microwave pulse does not exceed 0.1 cm. Indeed, the qualitative analysis of the high-speed photo scanning of this type discharge has shown that the time of the inputting of energy to any part of the streamer discharge by the EM wave, exciting the discharge, has a scale of 1÷2μs [8]. In conditions of the Fig.9.3 at V=370 m/s the molecules of air will be drifted with the flow no greater than for 0.1 cm.

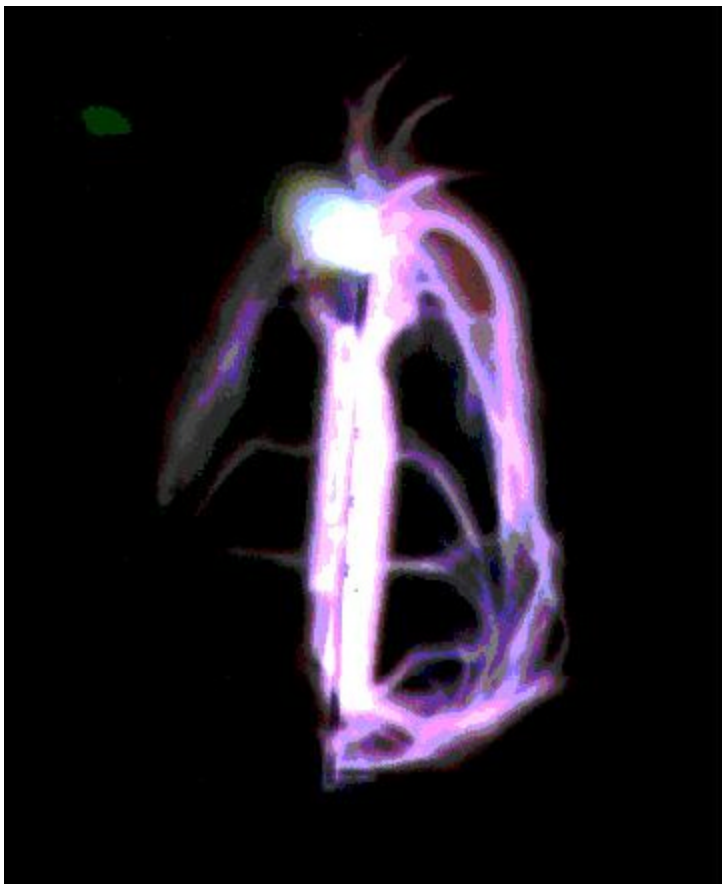

Fig.9.4. The photo of the discharge attached to the initiator. The streamer channel creates the loop connecting the vibrator's ends. p=100 Torr and E_0=1.7 kV/?m

In the Fig.9.4 is represented the photo of the discharge attached to the initiator at p=100 Torr and E_0=1.7 kV/?m. This discharge is close to the upper in respect to the field boundary that separates the area of deeply undercritical attached microwave discharges from the area of the undercritical discharges that can be separated from the initiator. In the photo there is the streamer channel that creates the loop connecting the vibrator's ends.

In the Fig.9.5 the discharge photo at the same **p** and $\mathbf{E_0}$, but in the supersonic flow at Δt=10 ms is represented. One can see that the discharge is qualitatively changed. In difference to the Fig.9.4 deeply undercritical discharge in the flow has a form of the system of luminescent turbulent channels stretched along the flow. The character of changing of the structure of this discharge has the qualitative explanation.

Fig.9.5. The discharge photo in the supersonic flow (compare with Fig.9.4). Δt=10ms, p=100 Torr and E_0=1.7 kV/?m

As it was indicated at the analysis of the Fig.9.2b the energy inputting time to the different parts of the undercritical discharge has the scale of units of μs. During this time the region of the energy release moves toward the radiation. In the deep undercritical field the discharge is attached to the area in the vicinity of the initiator during the whole microwave pulse. The gas in this area can be heated considerably higher. In this case the presence of the gas in the region of the energy release is limited in the first place not by the rate of the streamer channels growth, but by the time of the molecule motion along the vibrator. At the experimental velocity V=500m/s and the vibrator's length 2L=4 ?m this time equals to tents of μs. Evidently that in this case the average heating of the region near the vibrator is significantly higher that for the discharge in the undercritical case. The heating of the gas leads to the decrease of the molecule concentration in this region and in the

wake behind it, and also to the change of the discharge character. This is the discharge of the absolutely another type and it requires the special study.

10.The numerical modeling of the initiated undercritical discharge

The complete understanding of the investigated processes is possible only in the comparing of the experimental measurements with the theoretical simulation results. It is namely simulating because the investigated process is too complicated and nonlinear for design the analytical theory. This is modeling indeed as the researched process is rather complicated and is not linear.

The model of the undercritical discharge must be able to describe both the gas ionizing and heating in the discharge channel with wide diapason of temperature of gas and separately of temperature of the electrons and microwave field with the finite wavelength at the presence of the very thin discharge channel and initiator. In general case the Maxwell equation the thermodynamically not equilibrium plasma gas dynamical equations in 3D geometry must be used. But it is too complicated model for achieving of the practical results. Therefore the row of simplifications had been applied. Firstly it is supposed that microwave field is periodical in time: $E \sim \exp(-i\omega t)$. So the field can be described by the Helmholtz's equation which will be used below. For simplicity we will suppose that the electric field has a linear polarization and is directed along the body of initiator.

10.1. Calculation of the microwave field at presence of the initiator

If the initiator diameter is not too small comparatively to a wavelength the field can be calculated by direct solving of Helmholtz's equation. The special 3D code for solving of the Helmhotz's equation with Sommerfeld's boundary conditions has been designed for calculation field around a thin conducting body [1]. The example of the Helmhltz's equation solution for cylindrical body with semi-sphere at the tops with perfect conductivity and with almost resonant length (half wavelength) is shown on the Fig.10.1. The spatial distribution of the microwave field amplitude for the case of the 2D symmetry is presented in this figure. One can see that at the top of the cylinder the field amplitude is many times more than the amplitude of the external field. The electric field on the surface of the body is orthogonal to the surface and has the sharp peak on the initiators top.

But direct calculation of the Helmhotz's equation in the case of extremely small radius of the body demands a too large time of computation just on the recent PC. For a very thin (relatively to conductor length and wavelength) conducting filament one can use the semi-analytical method of calculation. In general the calculation of a current inducted in a thin wire of finite length by external microwave field is the traditional old task of the electrodynamics. A current inducted in the wire can be described by the integral equation of 1-st kind prepared by Pocklngton [2] from the Helmhotz's equation (10.1).

$$E_0(z) = -ik \int_{-kL}^{kL} I(z')G(z,z') \cdot dz', \qquad (10.1)$$

where

L,a – half length and radius of the conductor, $k=2\pi/\lambda$ – wave number.

$$G(z,z') = \frac{\exp(ikR)}{k^3 R^3} \cdot \left((1-ikR) \cdot \left(2 - 3\frac{a^2}{R^2} \right) + k^2 a^2 \right),$$

$$R = \sqrt{a^2 + (z-z')^2}.$$

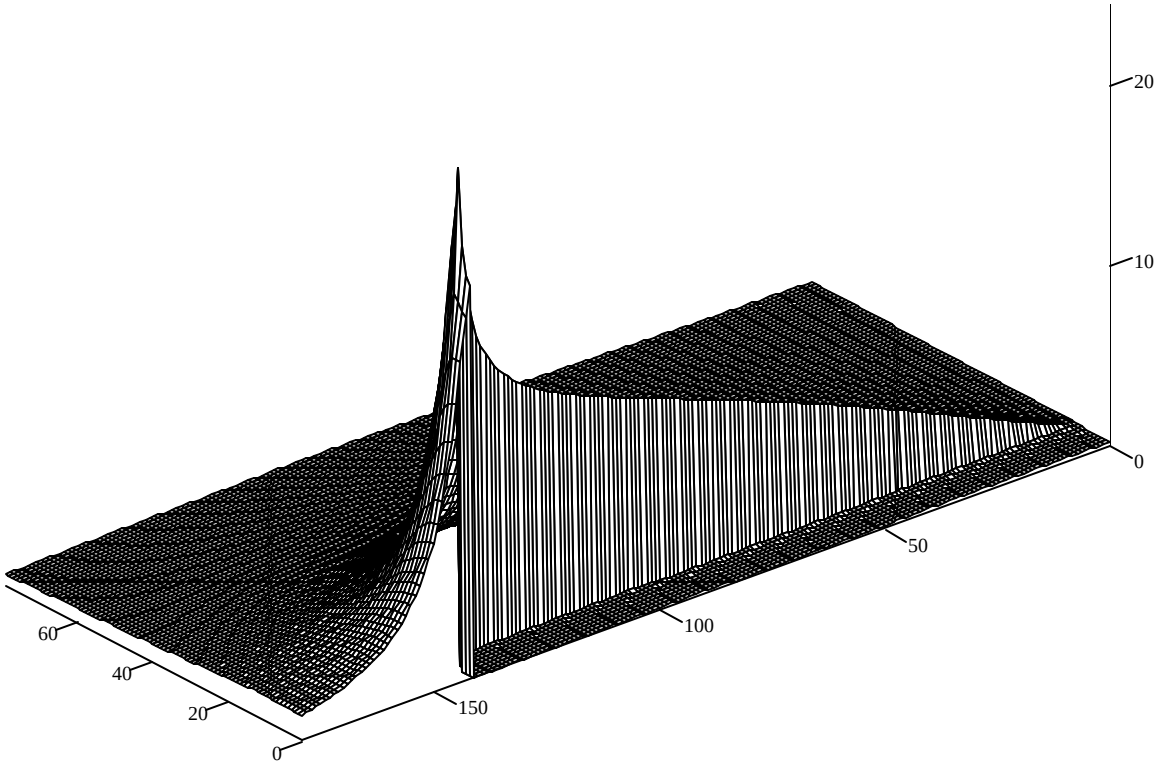

Fig.10.1. The spatial distribution of the microwave field amplitude $E(r,z)/E_0$ around the cylindrical body with semi-sphere on the tops of the perfect conductivity. λ=8.9 cm, the half length of the initiator L=2 cm, radius of the initiator a=0.1 cm. The numbers along the axis are the numbers of steps in the code.

The most accurate method of calculation of the Pocklington's equation was designed at 60-th of last century [3]. We have used this method for calculation of top field of very thin initiators.

Below the algorithm of computation of the current I(z) is represented by Eq. (10.2)

$$I(z) = P(z)\exp(ikz) + Q(z)\exp(-ikz) + J_0 \qquad (10.2)$$

where

$$J_0 = i\frac{c}{k}\frac{E_0}{2\ln\left(\frac{2i}{gka}\right)}$$

$$P = -J_0 f(L+z)\exp(ikL) - Wj(L+z)\exp(i2kL)$$

$$Q = -J_0 f(L-z)\exp(ikL) - Wj(L-z)\exp(i2kL)$$

$$W = -\frac{J_0}{D} f(2L)\exp(ikL)(1 - j(2L)\exp(i2kL))$$

$$D = \left(1 - (j(2L)\exp(i2kL))^2\right)$$

$$f(z) = \ln\left(\frac{-2}{g^2 q}\right)\Psi\left(\frac{kz}{q}, \frac{q}{2}\right)$$

$$j(z) = \ln\left(\frac{-1}{g^2 q}\right)\Psi\left(\frac{kz}{q}, q\right)$$

. **I k/c**

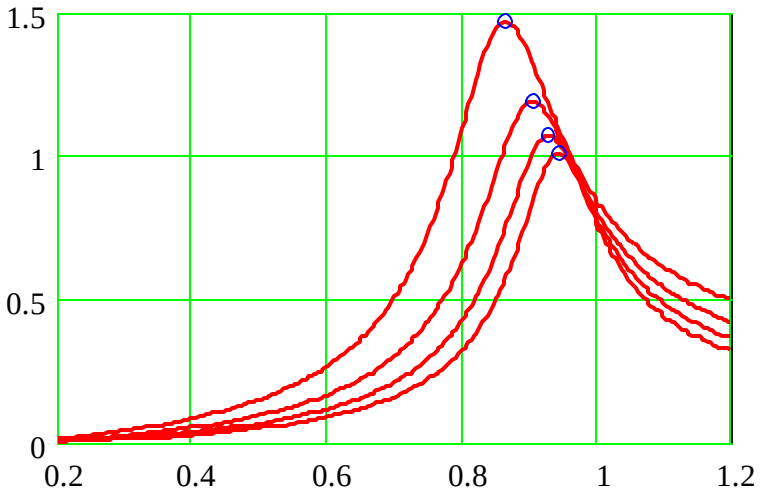

$$a \cdot k = \begin{bmatrix} 3.162 \cdot 10^{-3} \\ 7.499 \cdot 10^{-3} \\ 0.018 \\ 0.042 \\ 0.1 \end{bmatrix}$$

Fig.10.2. The maximum inducted current in dependence of the half length of initiator.

$$W = -\frac{J_0}{D} f(2L)\exp(ikL)(1 - j(2L)\exp(i2kL))$$

$$D = \left(1 - (j(2L)\exp(i2kL))^2\right)$$

$$f(z) = \ln\left(\frac{-2}{g^2 q}\right)\Psi\left(\frac{kz}{q}, \frac{q}{2}\right)$$

$$j(z) = \ln\left(\frac{-1}{g^2 q}\right)\Psi\left(\frac{kz}{q}, q\right)$$

$$\Psi(x,q)=\left(\begin{array}{l}\ln\left(\frac{i}{g^{\,2}q}\right)+(1-\exp(-i2qx))\ln(2gqx)-\\-(Ci(2qx)+i(Si(2qx)-p/2))\exp(-i2qx)\end{array}\right)^{-1}$$

$$q=(ka)^2$$

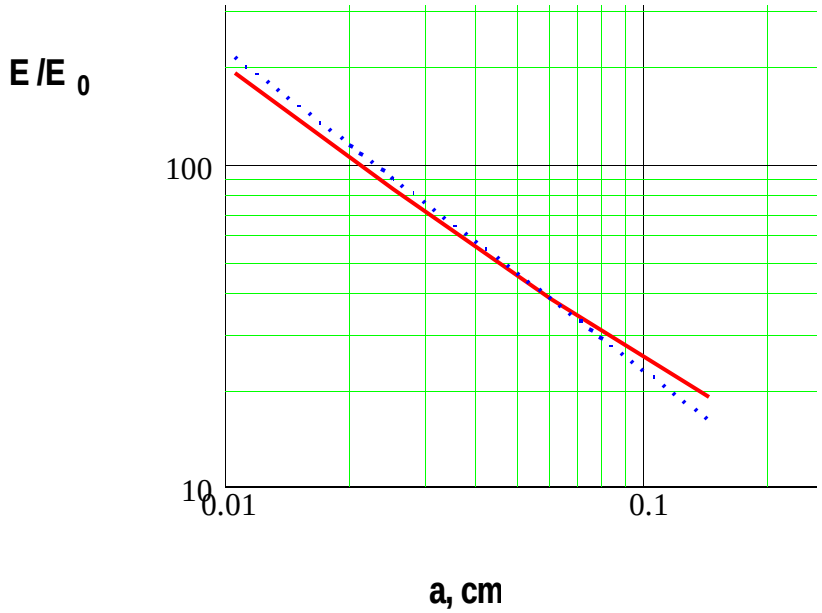

Fig.10.3. The relative field amplitude on the top of the initiator with resonant length in dependence of the radius. The red solid line – solution of Eq.(10.3), the blue dot line – estimation Eq. (4.8).

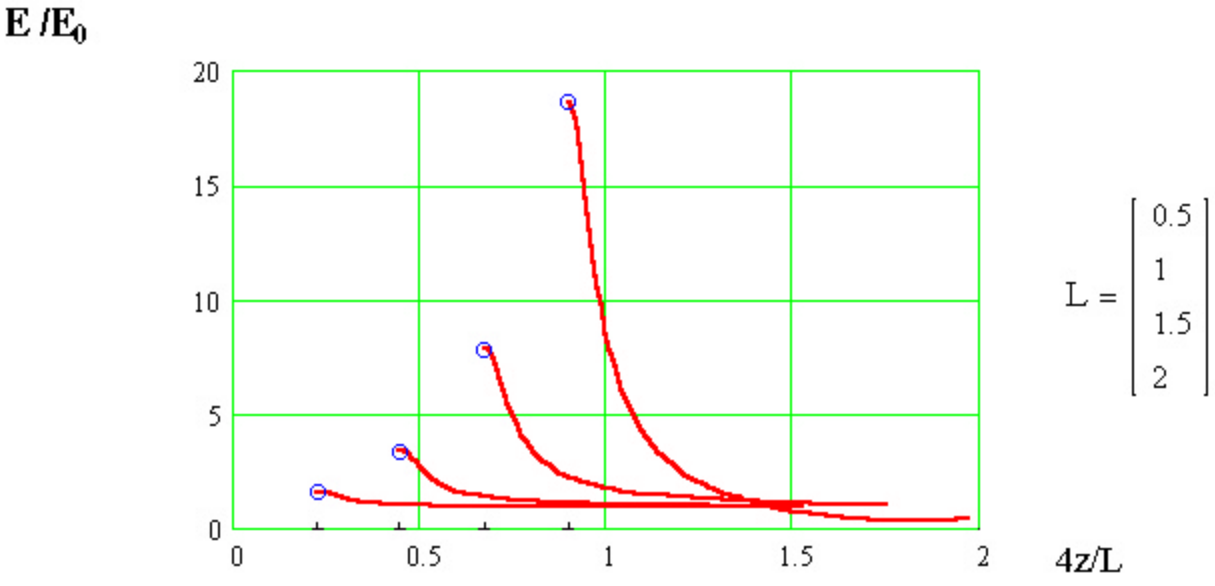

Fig.10.5. The field distribution along the initiator's axis aside the initiator's body at different length of it L, cm. λ=8.9 cm, a=0.01 cm.

The distribution of the microwave electric field amplitude along the initiator axis aside the bogy is defined by Eq. (10.3) where I(z) is solution of (10.2)

$$E(z) = E_0(z) + ik \int_{-kL}^{kL} I(z')G(z,z') \cdot dz' \qquad (10.3)$$

The solution of Eq.(10.2) and Eq.(10.3) is presented on Fig.10.2 and Fig.10.3.

The maximum field on the initiator's top corresponding to resonant length of initiator (see Fig.10.2) in dependence of the radius of the initiator calculated by means of Eq. (10.2) is shown on Fig.10.3. This solution is compared with the estimation Eq.(4.8). One can see the quite well consent.

The Fig.10.4 demonstrates the field distribution at the initiator axis near the top of initiator at different length of initiator with fixed radius a=0.01 cm

10.2. The calculation of the field at presence of the initiator and plasma channel

The modeling of the initiated discharge requests the solving of electrodynamic task which consists from finding of the field amplitude distribution in space fulfilled by arbitrary distributed electrical conductivity of plasma at presence of initiator. This task can be solved by means of Helmholtz's equation. The code [1] allows to do it. But it is too difficult way because it demands the much time of calculation. For more quick solving of this task the Pocklington's equation was modified into the integral equation of 2-nd kind for arbitrary distribution of conductivity in the channel. The application of this equation supposed that the conductivity is significant only in the thin channel. The initiated streamer discharge satisfies this demand.

The modified integral equation has a view (10.4)

$$E(z) = E_0(z) + ik \int_{-\infty}^{\infty} S(z')E(z')F(S(z'),a')G(z,z',a') \cdot dz', \qquad (10.4)$$

where

E(z) – electric field complex amplitude at axis (r=0),

$S = \frac{4ps}{w}$ - normalized conductivity

σ - electrical conductivity,

ω - circular frequency of microwave field, 1/s,

$F(S) = \frac{ka}{2\sqrt{1+iS}} \cdot J_1\left(\sqrt{1+iS}\right)$ - the function taking into account the skin –effect.

Function G(z,z',a) is the same as Eq.(10.1).

The Eq.(10.4) is being solved on each step of time together with the plasma-gas dynamic equations

10.3. The model of the plasma-gas dynamics

The plasma of discharge is not thermodynamically equilibrium. The electron temperature is defined by the relation of the electric field to gas density |E|/N so

that the two-temperature model must be used. The gas gynamic equations for dissociating and ionizating diatomic electronegative gas mix are strongly simplified. It is supposed that dissociation coefficient f_d is defined by the gas temperature by the Saha equation and the ionization coefficient f is the same for moleculas and atoms. The equations of continuity and movement is exchaged on the simple differential equations for channel radius a.

$$\frac{da}{dt} = V \tag{10.5}$$

$$\frac{dV}{dt} = \frac{P_0 - P}{r_0} \tag{10.6}$$

$$C_v(T_g, N)\frac{dT_g}{dt} = \tag{10.7}$$

$$= -(1 + f_d(T_g, N))(T_g + fT_e)\frac{2V}{a} + \frac{s(f, N, T_e, T_g)|E|^2 \Phi(s, a)}{N} - Q_{rec}(f, N, T_e)$$

$$\frac{dn}{dt} = N(K_i(T_e) - K_a(T_e))n + \frac{d}{dz}\left(D(N, T_e)\frac{dn}{dz}\right) \tag{10.8}$$

$$T_e = T_{e0}\frac{[E]}{E_{cr}(N)} \tag{10.9}$$

$$f = \frac{n}{N(1 + f_d(T_g, N))} \tag{10.10}$$

where

n-electron number density,

N =ρ/M, M – averaged molecular number of unperturbed gas mix.

10.4. The results of simulation

The system Eq. (10.5) – (10.10) has allowed to investigate the different regimes of the initiated discharges and the wind influence on them.

Below the three calculated variants present the typical regimes of the initiated discharges. All variants correspond to the same conditions: wave length λ=8.9 cm, air pressure p_g=760 Torr, the initiator's diameter 2a=0.2 cm and the wind velocity W=1 km/s. The variants differ one from another by the length of initiator 2L=4cm, 2.8 cm and 2 cm. These parameters of initiator correspond to values of a field increasing coefficient Q=21, 11 and 6. The electric field amplitude have been elected a bit more than breakdown in the presence of the given initiator. Correspondingly it was E_0=1.9 kV/cm, 3.3 kV/cm and 6.8 kV/cm. In accord with classification on the Fig. 5.7 these parameters relate to the deeply undercriirical (attached) discharge, boundary between both types of initiated discharges and the undercritical (separated) discharge. The results of modeling of attached discharge are presented on the Fig. 10.6 – 10.10. From all calculated variables only something are presented.

10.4.1. The deeply undercritical (attached) discharge

The Fig.10.6 - Fig.10.9 demonstrate the results of modeling of the discharge initiated in the room air by the initiator with almost resonant length 2L=4 cm and diameter 2a=0.2 cm at the wind presence. The wind velocity W=1 km/s is directed along the initiator. The external field amplitude is many times less than the critical one, E_0=2 kV/cm. According to the Fig.5.7 the mentioned conditions correspond to border between undercritical and deep undercritical discharges.

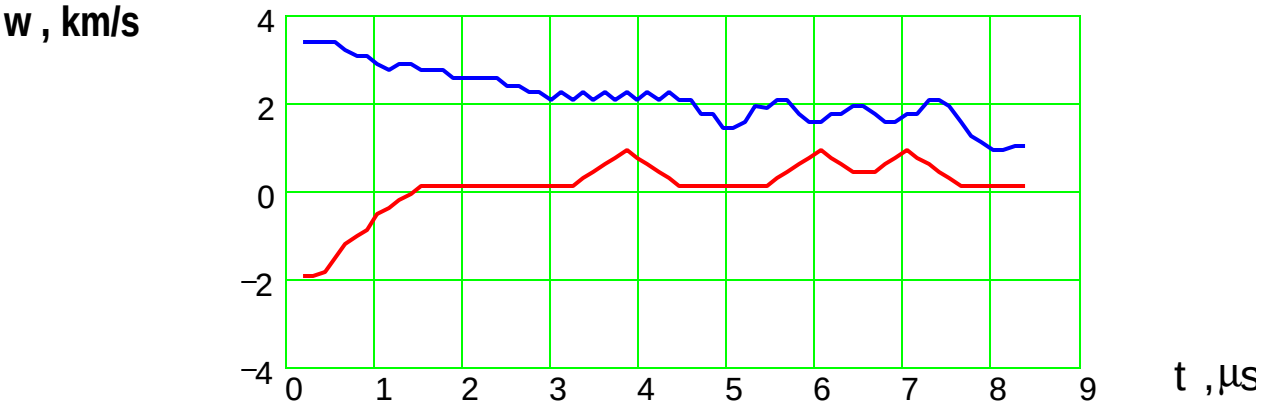

Fig.10.6. The streamer ends velocity w. The red line – velocity of the forward streamer, the blue line – velocity of the back streamer. λ=8,9cm, 2L=4cm, 2a=0.2cm, air pressure – 760 Torr, E_0=1.9 kV/cm, Q=21.

Initially the discharge arise on the both ends of the initiator. The plasma conductivity is not enough for field increasing aside the initiator. During the first microsecond the ionization front has some small velocity but than stops and begin to move with the wind flow (see Fig.10.6 and Fig.10.7).

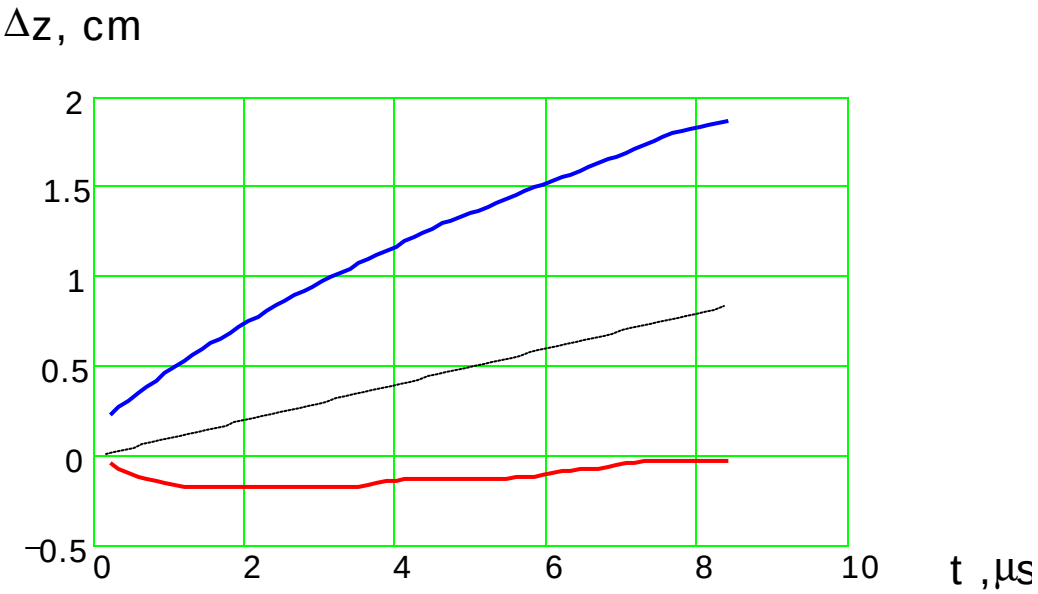

Fig.10.7. The streamer head outstanding from the initiator's end. The red line –of the forward streamer, the blue line –of the back streamer, dash line - W·t. λ=8,9cm,

2L=4cm, 2a=0.2cm, air pressure – 760 Torr, E_0=1.9 kV/cm, Q=21.

Through a couple of microseconds the discharge at the forward end of initiator being influenced by the wind is over. The Fig.10.6 shows the velocity of the streamer's ends in dependence upon time. On initial stage the streamer develops with the velocity more than 2 km/s during the time less than 1 μs. Then the forward streamer have stopped but back streamer is moving slowly with the wind flow on some distance being slowly cooled.

This process is viewed very well on the gas temperature distributions. The Fig.10.8 demonstrates the parameters distribution at the time t=3.2 μs.

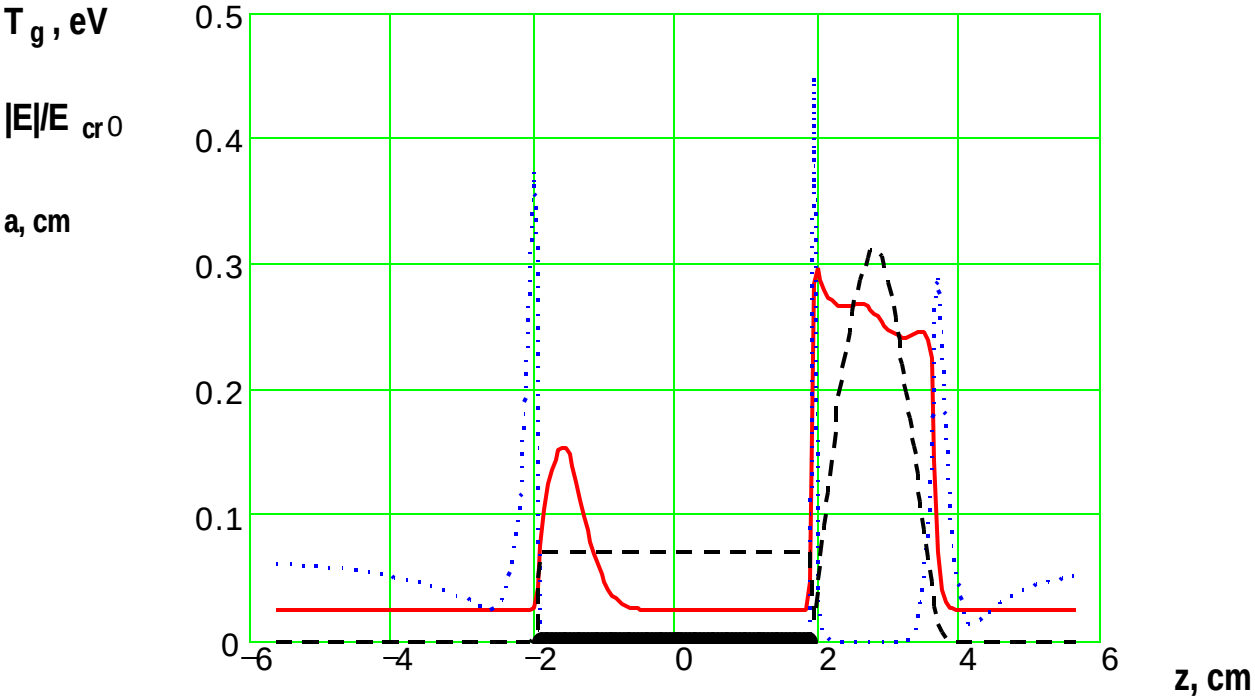

Fig.10.8 The gas mix temperature T_g (red solid line), microwave field amplitude $|E|/E_0$ (blue dot line) and the channel radius a (black dash line) distributions along axis z. The bold black solid line at the z axis is the initiator body. The wind velocity along the axis z - W=1 km/s. The time after discharge start - t=8.2 μs. λ=8,9cm, 2L=4cm, 2a=0.2cm, air pressure – 760 Torr, E_0=1.9 kV/cm, Q=21

The region of the heated gas exists only on the back end of the initiator in the wake of discharge which moves with the wind together. Let us point that the field amplitude at the ends of the initiator have maxima. The maxima are approximately the same. But the field at the forward end do not cause the ionization because the gas at this end is cold and density is near to normal so the parameter E_{max}/N is less than critical one. Other sytuation arise at the back end. There the gas is hot and its density is small enough (see Fig. 10.9.) so the parameter E_{max}/N is more than critical one and ionization continues despite of the wind. The heated gas expands so the radius of the hot channel can be more than initiator's one. Note that the gas temperature is maximum on the back top of the initiator and is able to excide the 3000-4000 K. So it must not surprise us that ends of the initiator is evaporating

during the discharge. Of course the wind cool the initiator that is doing the problem not such desperate.

The process development in the time is demonstrated by the Fig.10.10 where the spatial-temporal gas temperature distribution $T_g(z)$ is presented. One can see the boundary of the initiator and the hot gas regions development. The picture is not symmetry because the wind influence. The forward streamer is shorter than back one. The heated gas is going with wind flow but the wind do not break the discharge.

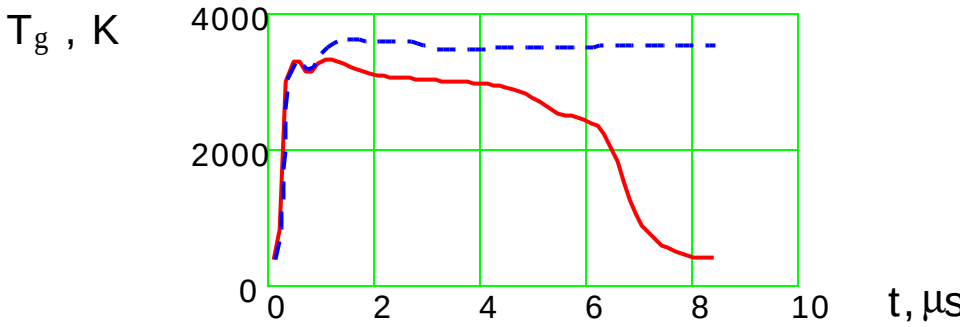

Fig.10.9. The gas temperature T_g near the top of the initiator. The red line – the forward end, the blue line – wake end. λ=8,9cm, 2L=4cm, 2a=0.2cm, E_0=1.9 kV/cm, air pressure – 760 Torr, Q= 21

One can see that the wind will bring out the discharge from the forward end and creates the long wake of the hot gas beside the back end. It is important to note that in the case of the attached deeply undercritical discharge which can be created in a very weak microwave field the gas temperature of the wake is quite high and possibly this hot wake will able to ignite a combustible mix in a supersonic flow.

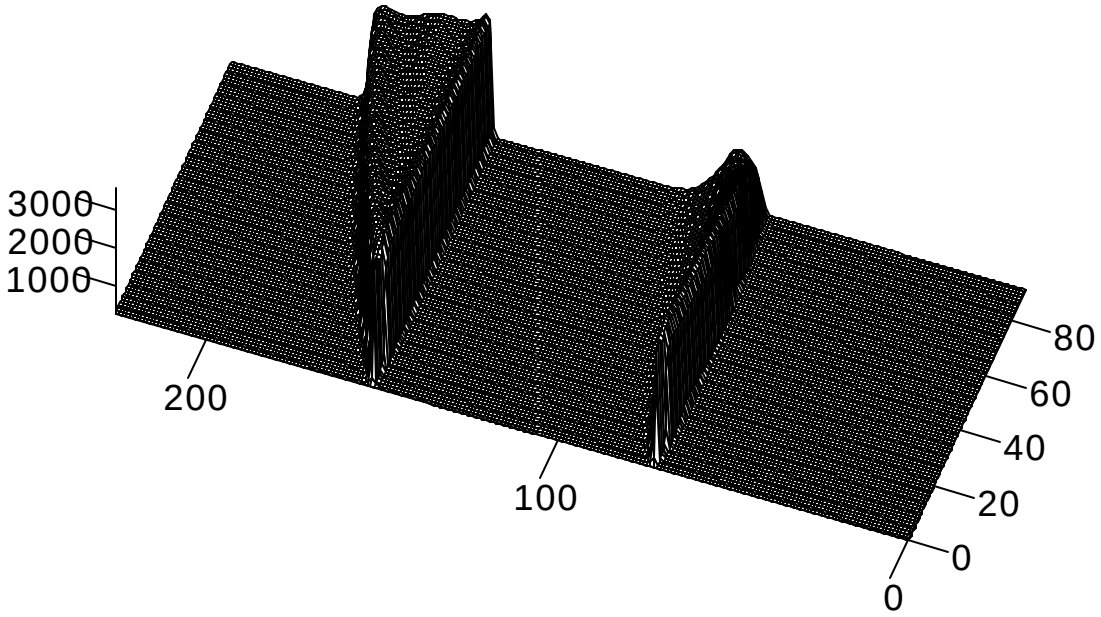

Fig.10.10 The spatial-temporal distribution of the air temperature T_g, K of the undercritical discharge. The numbers 0-90 –the number the time steps ($0<t<8.2$ μs). The numbers 0-226 – the numbers of the spatial steps (-5.7cm <z<5.7cm). λ=8,9cm, 2L=4cm, 2a=0.2cm, air pressure – 760 Torr, E_0=1.9 kV/cm, Q=21

Naturally the calculated "photograph by open lens" of the deeply undercritical discharge shows a single short bright spot near the back end of the initiator (see Fig. !0.11.).

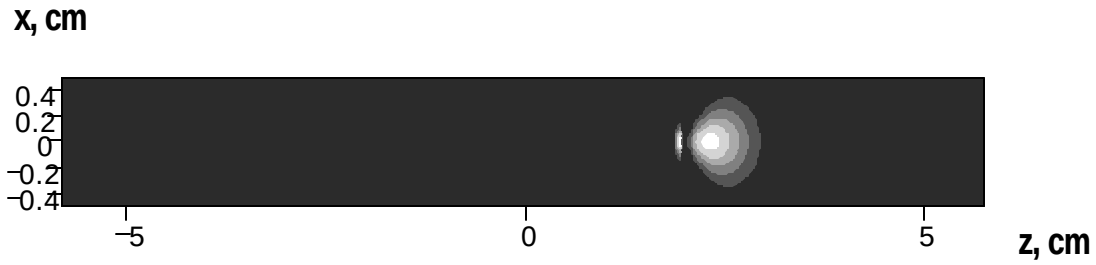

Fig.10.11. The calculated "photo by open lens" of the deeply undercritical discharge. λ=8,9cm, 2L=4cm, 2a=0.2cm, E_0=1.9 kV/cm, air pressure – 760 Torr, Q=21.

The Fig.10.11 represents the calculated "photo by the opened lens" of discharge. One can see the good consent with real image on the Fig.7.2a obtained for discharge in unmoving air.

The important result of the simulation is a high gas temperature T_g in the discharge and large radius of the channel (see Fig.10.8). Both parameters must be enough for the fuel mix ignition. It is important too that wind with velocity 1 km/s is not able to influence this high values of parameters of a deeply undercritical discharge.

10.4.2. The discharge which is intermediate between attached and separated

The same seria of the illustration are presented for the discharge that lays on the boundary between the attached and separated discharges (Fig.10.12 – Fig. 10.16). This boundary is seen on the Fig. 5.7. One can see that the streamer at the forward end of the initiator is not depressed but through 2 μs stoped by the wind at some distance from the end (Fig,10.13). The streamer at the back end of the streamer is continue to develop and creates the hot wake.

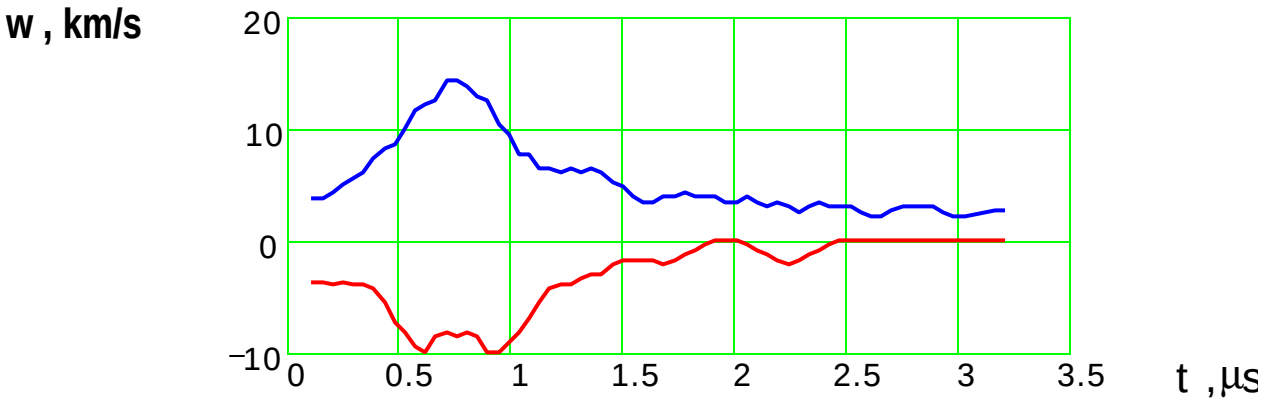

Fig.10.12 The streamer ends velocity w. The red line – velocity of the forward streamer, the blue line – velocity of the back streamer. λ=8,9cm, 2L=2.8cm, 2a=0.2cm, air pressure – 760 Torr, E_0=3.3 kV/cm, Q=11

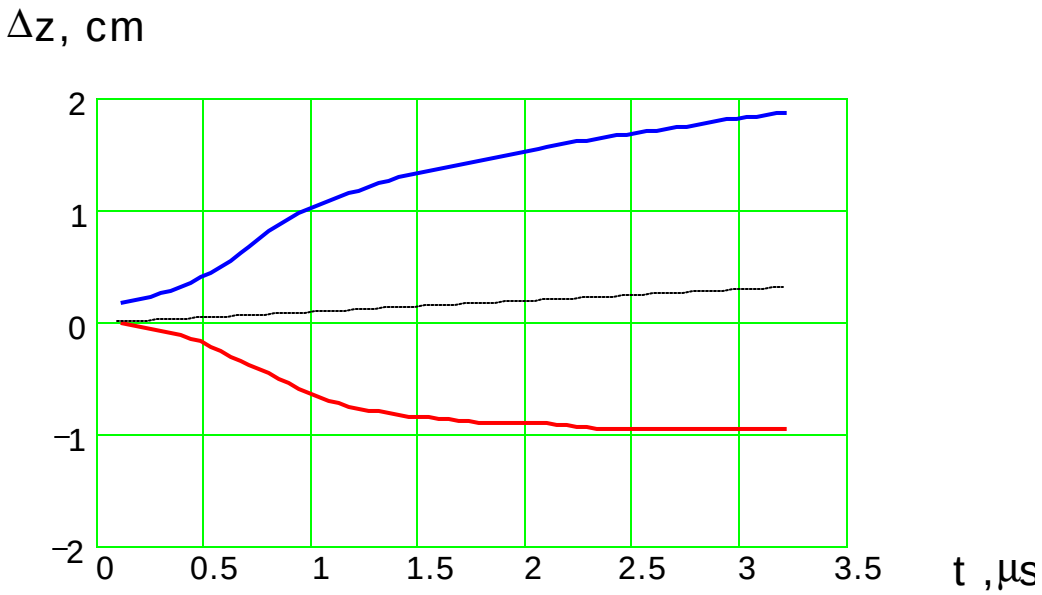

Fig.10.13. The streamer head outstanding from the initiator's end. The red line –of the forward streamer, the blue line –of the back streamer. λ=8,9cm, 2L=2.8cm, 2a=0.2cm, air pressure – 760 Torr, E_0=3.3 kV/cm, Q=11. The dot line -W·t.

The gas is being ionised on the heads of both streamers and at the back end of the initiator. The heating is maximum at this place (Fig.10.14 and Fig.10.15). Note that at this top of the initiator the temperature is higher than in the discharge and achieves the value about 9000 K.

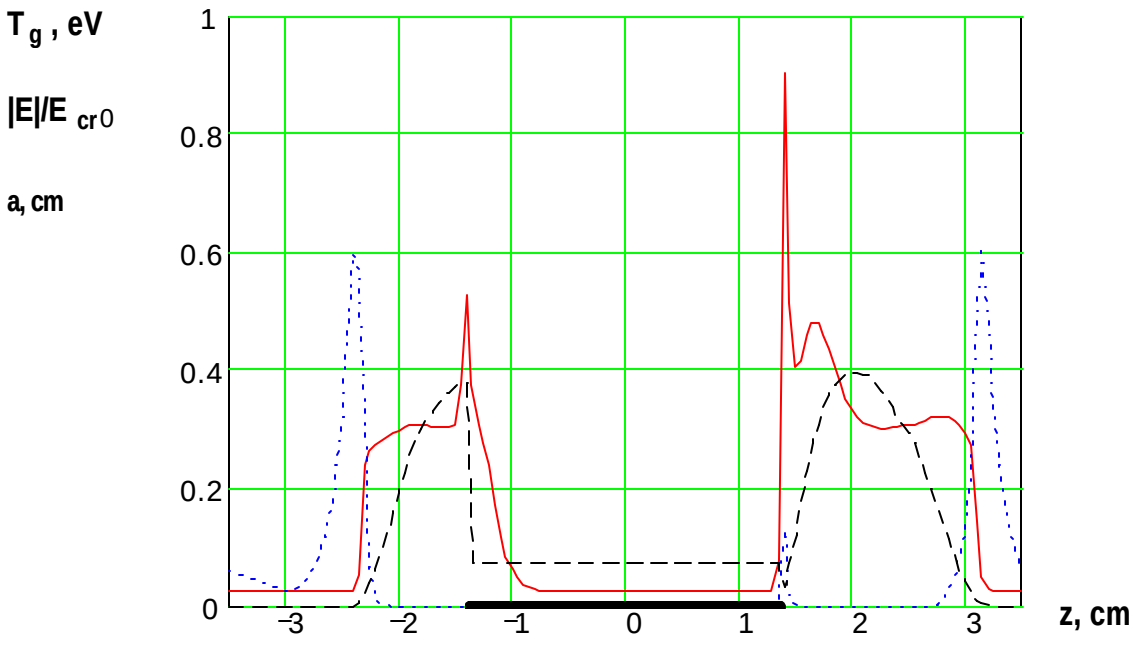

Fig.10.14. The gas mix temperature T_g (red solid line), microwave field amplitude $|E|/E_0$ (blue dot line) and the channel radius a (black dash line) distributions along axis z. The bold black solid line at the z axis is the initiator body. The wind velocity along the axis z W=1 km/s. The time after discharge start - t=3 μs. λ=8,9cm, 2L=2.8cm, 2a=0.2cm. The air pressure – 760 Torr, E_0=3.3 kV/cm, Q=11.

It is significantly more than the temperature of metal evaporating. It explains the fact that the discharge light spectrum contains the lines of the metal. Because the discharge at the forward end is sustained the slight light near this place can be seen at the calculated "photograph by open lens" (Fig.10.16).

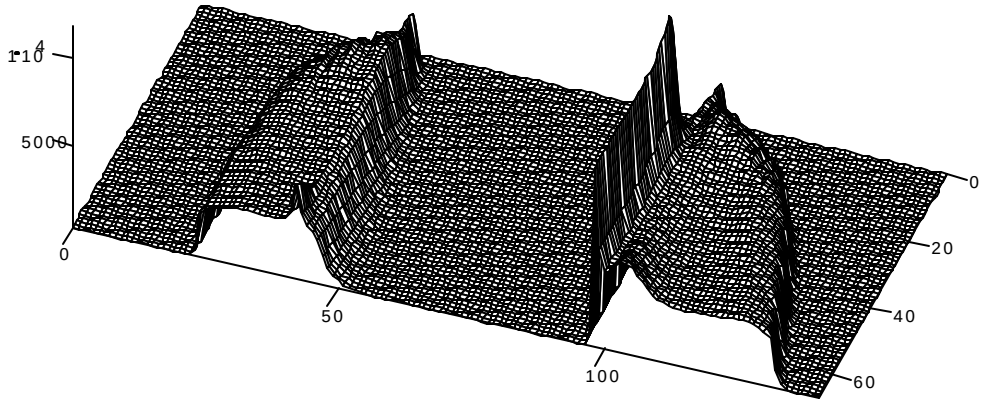

Fig.10.15 The spatial-temporal distribution of the air temperature T_g, K, of the undercritical discharge. The numbers 0-68 –the number the time steps (0<t<3.2 μs). The numbers 0-140 – the numbers of the spatial steps (-3.5cm <z<3.5cm). λ=8,9cm, 2L=2.8cm, 2a=0.2cm, air pressure – 760 Torr, E_0=3.3 kV/cm, Q=11

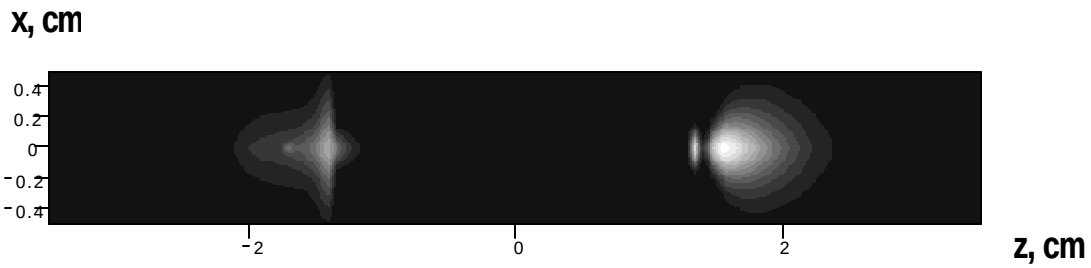

Fig.10.16. The calculated "photo by the opened lens" of deeply undercritical discharge. λ=8,9cm, 2L=2.8cm, 2a=0.2cm, air pressure – 760 Torr, E_0=3.3 kV/cm, Q=11

10.4.3. The undercritical (separated) discharge

This variant differs from the second by the circumstance that both streamers forward and back continue the development despite of the supersonic wind. On can see it on the Fig.10.17 – Fig. 10.21. The streamers stipped only after the momemt when sum of their length and length of the initiator have significantly excited the resonant value λ/2. Both streamers have the almost same length (Fig.10.19) and brightness of light (Fig.10.21). In the real process at this moment the next generation of the separated streamers goes away from the initiatorThe designed model is unable to describe these next steps of the process. It can only show that the streamers length is rising up to value that exceds the resonant value. The next step of the streamer development demand a more advanced model. But we may declare that the streamers of the next steps will have the same values of parameters that the streamers of first generation being born by initiator have.

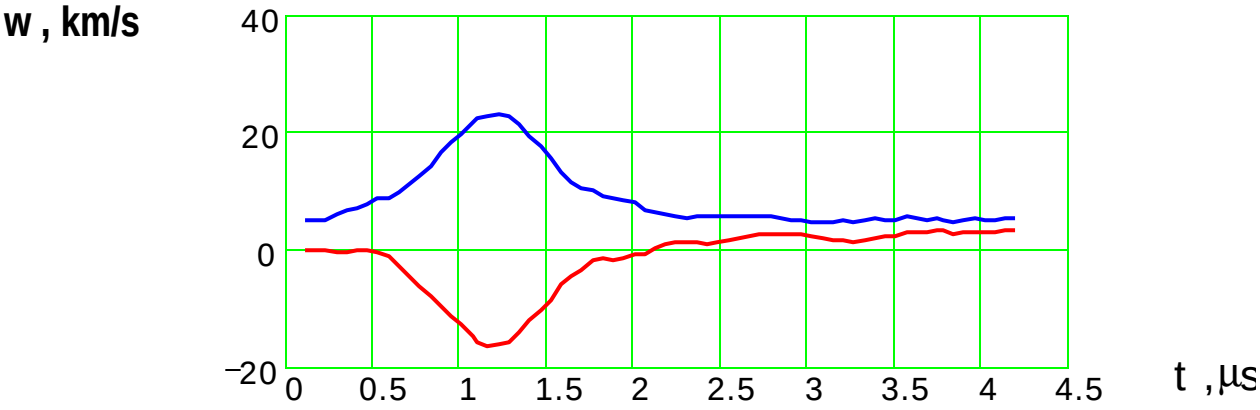

Fig.10.17. The streamer ends velocity w. The red line – velocity of the forward streamer, the blue line – velocity of the back streamer. λ=8.9cm, 2L=2cm, 2a=0.2cm, air pressure – 760 Torr, E_0=6.8 kV/cm, Q=6.

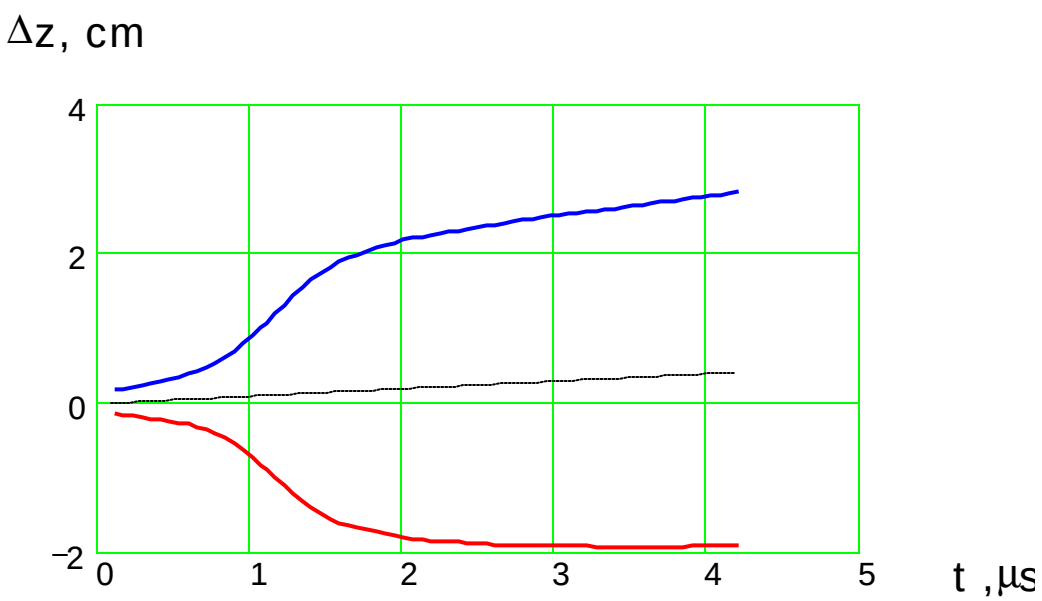

Fig.10.18. The streamer head outstanding from the initiator's end. The red line –of the forward streamer, the blue line –of the back streamer. λ=8,9cm, 2L=2 cm, 2a=0.2cm, air pressure – 760 Torr, E_0=6.8 kV/cm, Q=6.

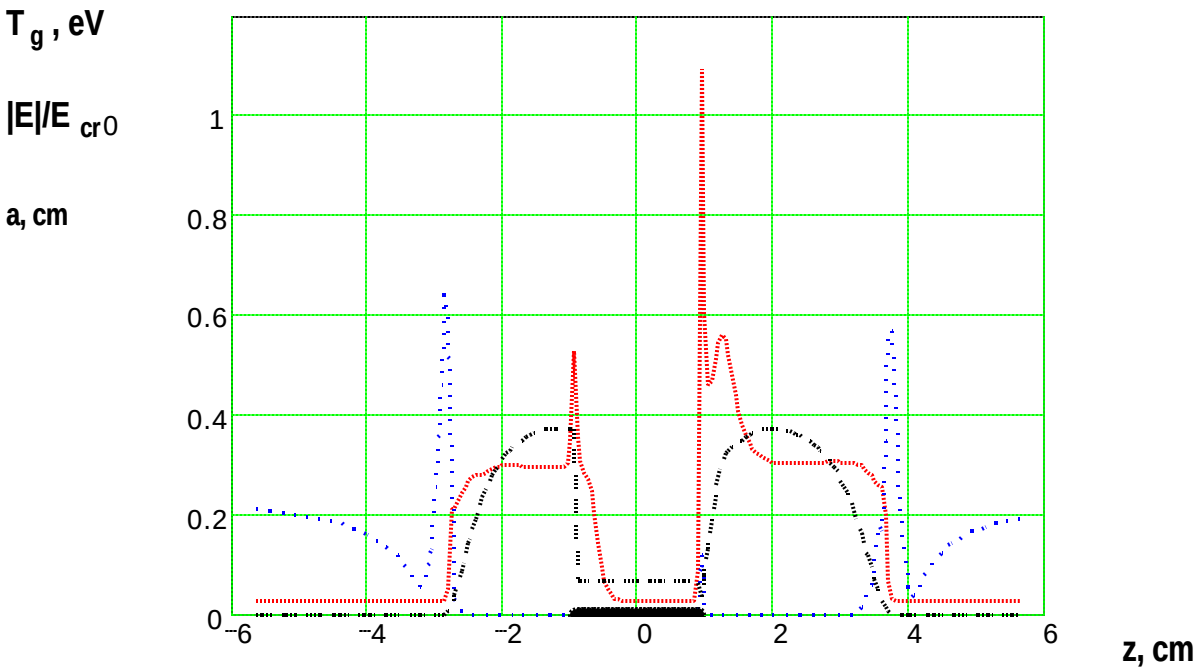

Fig.10.19. The gas mix temperature T_g (red solid line), microwave field amplitude $|E|/E_0$ (blue dot line) and the channel radius a (black dash line) distributions along axis z. The bold black solid line at the z axis is the initiator body. The wind velocity along the axis z W=1 km/s. The time after discharge start - t=4 μs. λ=8,9cm, 2L=2cm, 2a=0.2cm. The air pressure – 760 Torr, E_0=6.8 kV/cm, Q=6.

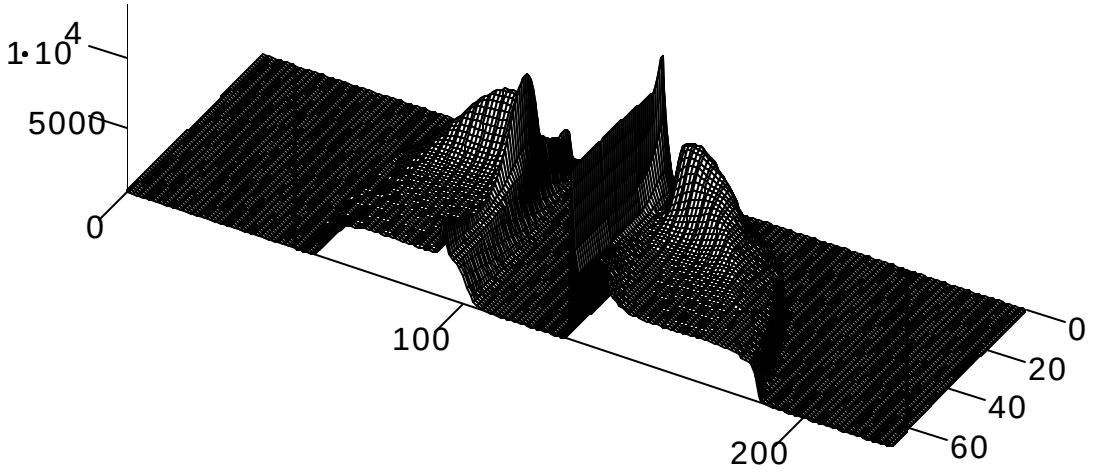

Fig.10.20. The spatial-temporal distribution of the air temperature T_g, K of the undercritical discharge. The numbers 0-70 –the number the time steps ($0<t<4.05$ μs). The numbers 0-226 – the numbers of the spatial steps (-5.7cm <z<5.7cm). λ=8,9cm, 2L=1cm, 2a=0.2cm, air pressure – 760 Torr, E_0=6.8 kV/cm, Q=6.

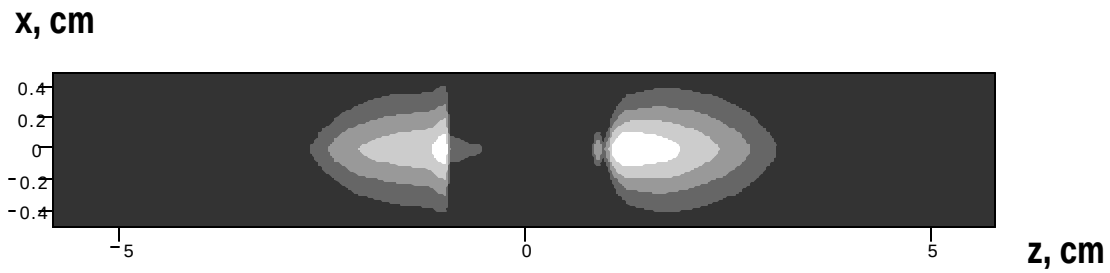

Fig.10.21. The calculated "photo by the opened lens" of deeply undercritical discharge. λ=8,9cm, 2L=2cm, 2a=0.2cm, E_0=6.8 kV/cm, air pressure – 760 Torr, Q=6.

10.5. Summary of modeling

The performed modeling allows to accept for farther designing that

1) gas temperature in the initiated discharge channel is more than 3000 K,

2) a supersonic wind with velocity 1 km/s do not cut the initiated discharge,

3) said properties relates to both types of discharge, separated and attached.

The point 1) is well correlate with the experimental fact that initiated discharge of both types ignites the combustable gas mix.

It must be noted that at start of the discharge the power of heating is relatively high and proportional to ~ E_0^2. But 3-4 ms later the power of heating equals to 3 kW approximately independently from type of discharge (Fig.10.22).

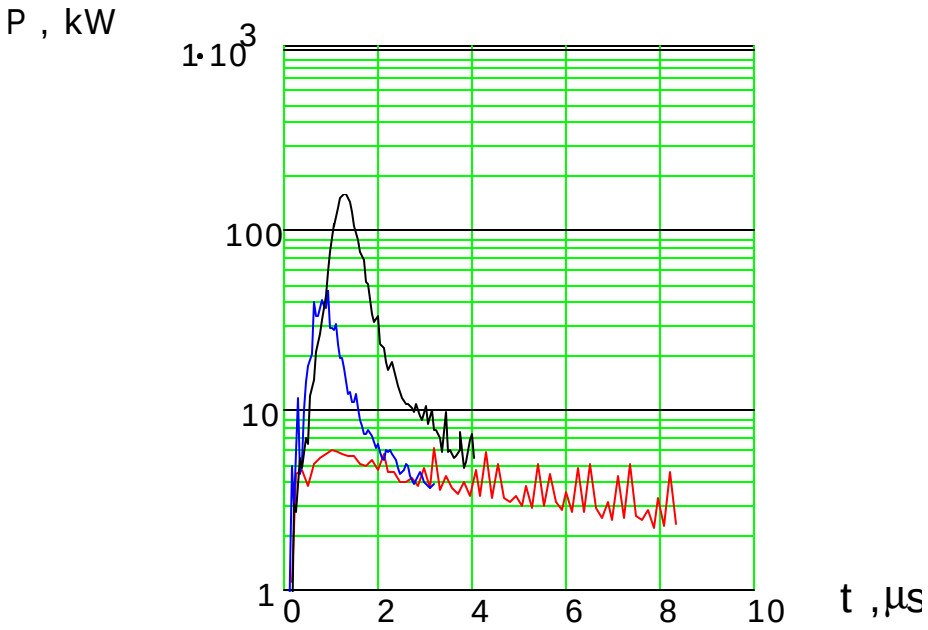

Fig. 10.22. The power included into the discharge, red line – variant with Q=21, blue line – variant with Q=11, black line – variant with Q=6.

The simple estimation gives the value of the hot wake radius in quasi-stationary regime for attached discharge:

$$a_{ch} = \sqrt{\frac{P}{p \cdot W \cdot w_0} \cdot \left(\frac{T_{g0}}{T_g} \right)^{g-1}} \qquad (10.11)$$

where W-wind velocity,
w_0 and T_{g0} – unperturbed gas enthalpy and temperature,
P – power of heating,
T_g – temperature of the heated gas in the wake.

The Eq. (10.11) gives for calculated power P = 3 kW at wind velocity W=1 km/s and temperature of the channel 3000 K the size of the radius 0.123 cm. This value of radius relates to far distance from the initiator for attached discharge.

11. Direction of future investigations

The achieved experimental and theoretical data on properties of the initiated microwave discharge and experimental confirmation of an opportunity of ignition of a combustible gas mix with the help of the initiated discharges of a various type allow to formulate the basic tasks of the following stage of works:

- the determination of requirements for the pulse duration and the flux level of the MW radiation needed for the combusting of the model mixture at the different share of fuel in the mixture;
- the demonstration of the possibility of the flammable mixture's ignition in a flow at the sub- and supersonic velocity and the investigation of the influence of the discharge regime on the mixture combustion characteristics.

The performance of first of them will give the data that is necessary for minimization of the energy cost of ignition. The performance of second task will give general views on burning ignition in a high-speed flow by the microwave discharge and on preferability of the various types of the initiated microwave discharge for further use.

11.1. Requirements to the discharge energy

Present investigations will be carried out by means of the described in Chapter 2.To investigate the threshold of a combustion initiation in dependence on the pulse duration and the microwave field level it supposed to execute the following experiments:

Experiments on the determination of the minimum duration of the microwave pulse $\mathbf{t_{pul}}$, ensuring the ignition of the model flammable mixture at the pulse regime of the generator with wave length 8.9 cm. In our set up there is the capability to vary $\mathbf{t_{pul}}$ in a range from 4 to 40 μs discretely with the period 4 μs and to change the field's level from E_0 = 6,5 kV/cm to $E_0 \cong$ 100 V/cm.

Experiments on the determination of the minimum level of the microwave field $\mathbf{E_0}$, ensuring the ignition of the model flammable mixture at continuous regime of the generator with wavelength 12.5 cm.

11.2. Set up description for undertaking of experiments in a flow

The experimental demonstration of the combustion ignition in a high-speed flow of the model flammable mixture will be carried out in the setup GDS which scheme is represented in the Fig.11.1. The photos of its external view from different points of view are in the Fig.11.2 and 11.3.

The set up consists of the fore chamber of 0.15 m^3 volume, cylindrical working chamber of 0.7 m diameter and 1 m length and receiver of the volume approximately equal to 0.15 m^3. All these elements are connected into the united hermetic volume that can be pumped out by the fore vacuum pump up to p = 3 ?orr. The microwave generator at λ = 12.5 cm, described above, will be included into the set up. The radiation from its outlet can be introduced into the working chamber by the waveguide.

The air from the atmosphere will leak into the preliminary pumped out volume through an electric valve with the pass cross section of 56 mm diameter and the controlled throttle. the maximum velocity of the leak in is 40 Torr/s. The air from the fore chamber will be leaking into the working chamber through the accessory nozzles. During the work at the subsonic velocities the Vitoshinsky nozzles will be used, during the work at the supersonic velocities will be used the Laval nozzles. Their minimum cross sections will be of the size not exceeding 50 mm.

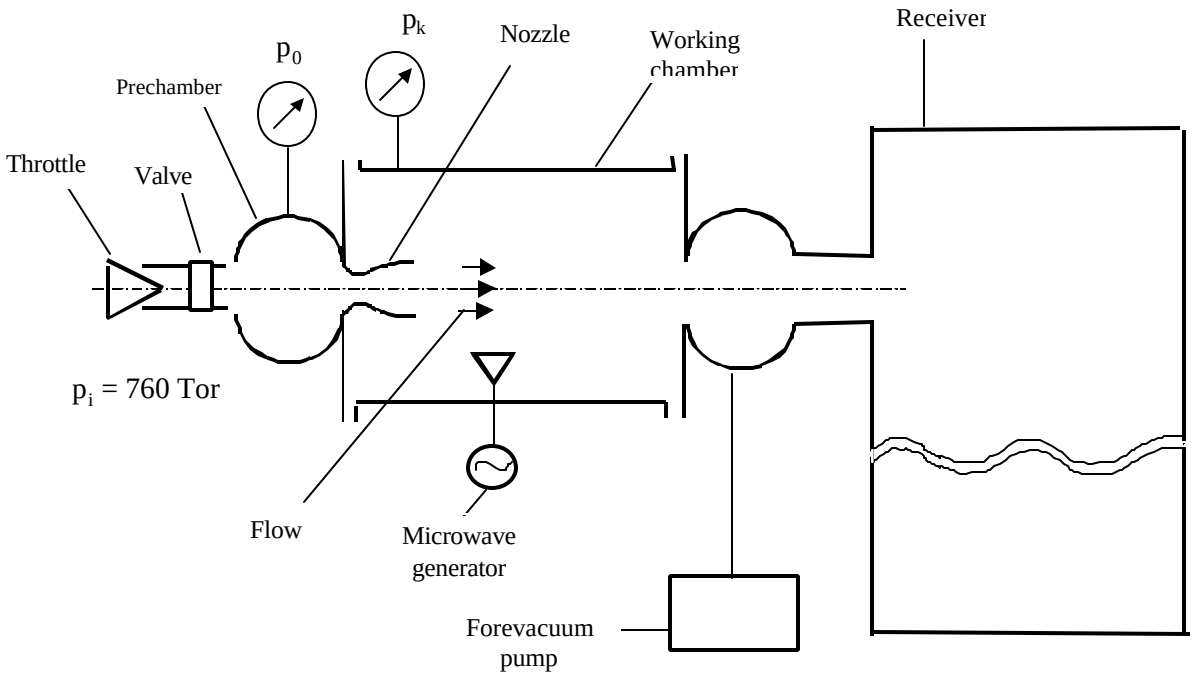

Fig.11.1. The scheme of the setup GDS for investigation of the combustion initiating in the high-speed flow.

We suppose to carry out experiments at the supersonic velocities at the Mach number up to M=2. The submerged jets or flows in pipes will be formed in the working chamber as it is shown in the Fig. 11.4.

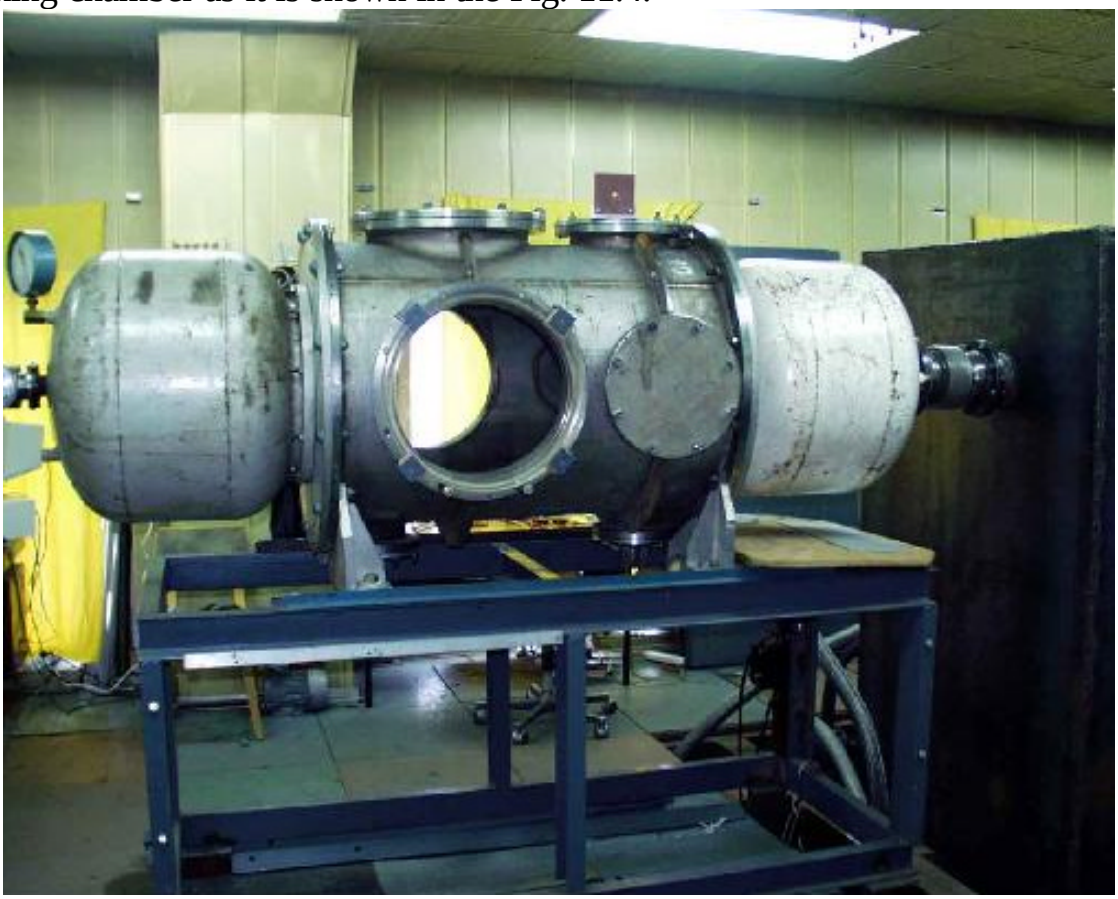

Fig.11.2 The view of the setup GDS from the side of the diagnostic window.

Fig.11.3. The view of the setup GDS from the side of the air injection.

During some experiments we plan to locate the wedge-type dielectric pylon in the flow as it is represented, for example, in the Fig.11.5. It can be used for inputting of the fuel into a flow and for discharge initiating vibrator's fastening.

11.3. Schemes of experiments

The combustion initiating is supposed to realize at two variants:

Variant 1. The speedy flow is being formed of the beforehand prepared mix.

The initiation of the mix combustion is executed in the spatial homogeneous combustible mix.

One of the possible experimental schemes with the flammable mixture's flow is represented in the Fig. 11.4a. In this case the discharge initiating microwave vibrator is located in the flow by means of the streamlined support.

During an experiment it will be possible to determine the minimum field level that ensures the ignition of the flammable mixture and the velocity of the flame propagation across the flow will be determined. In the same experiment the velocity of the flammable mixture's combustion in respect to the microwave energy field's level inputted to the discharge can be determined by the measurement of the flow static pressure along the wall of the dielectric pipe. All the experiments can be carried out at different concentrations of the fuel in the airflow at different velocities of the flow, both in subsonic and supersonic conditions, and at different values of the jet's static pressure.

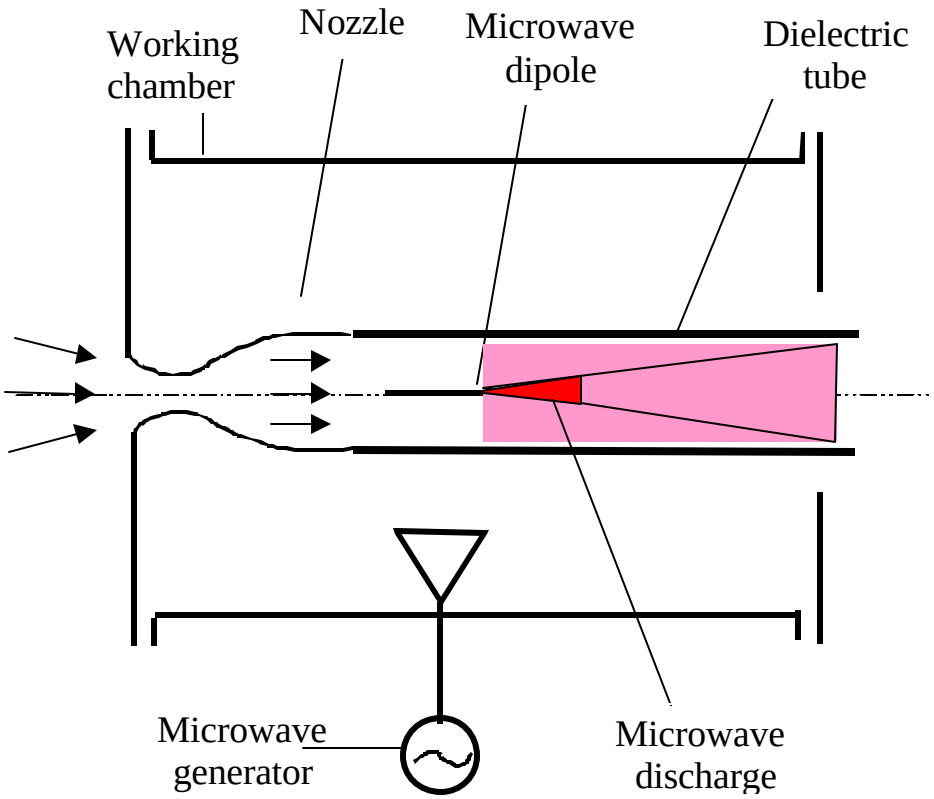

Fig.11.4. The scheme of the experiments with the combustion initiating of the spatial homogeneous combustible mix.

The ignition of the flammable mixture's flow could be studied by the scheme represented in the Fig.11.5 as well. In this case the dielectric wedge is applied for the discharge initiating microwave vibrator's fastening. The discharge can be ignited in the base part of the wedge in the stagnation flow's region (Fig.11.5a), or directly in the flow (Fig.115b).

Variant 2. The fuel is being injected into the high-speed flow of air.

The initiation of the combustion is being executed near the place of the fuel injection into the airflow. The dielectric wedge can be used for the local feeding of the fuel or the flammable mixture to airflow. One of the possible schemes of such feeding of the fuel to the flow is represented in the Fig.11.6a. In this case the fuel goes to the flow axis throw the hole drilled in the wedge perpendicularly to its triangle cross section. Another perpendicular hole leads the fuel to the base part of the wedge.

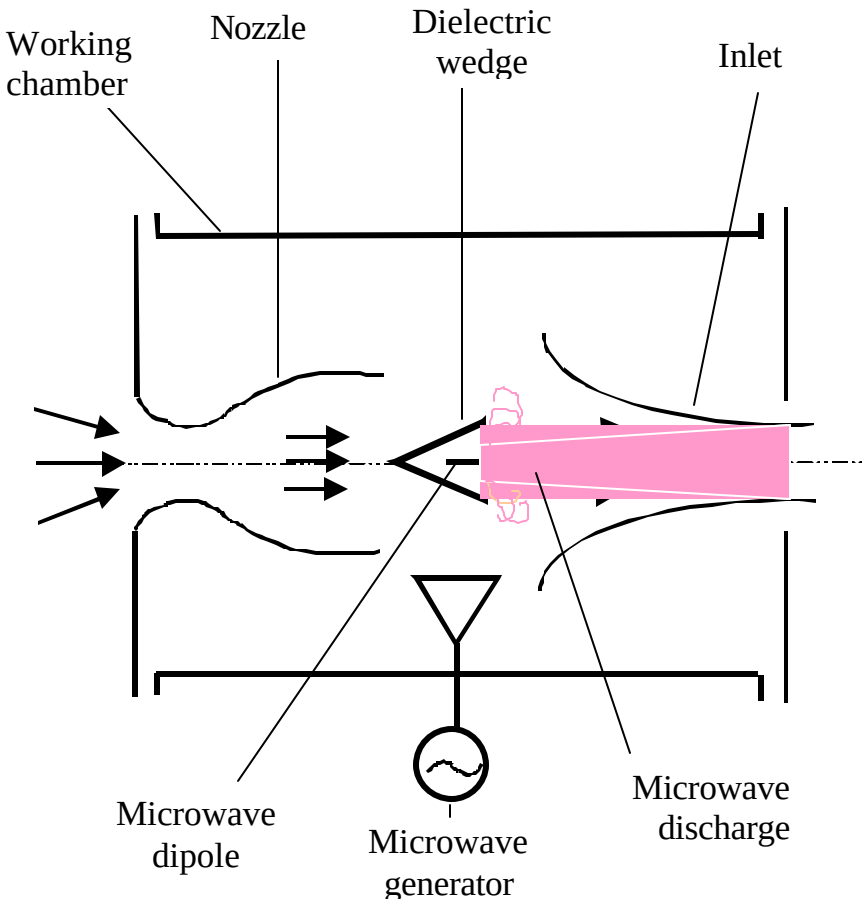

Fig.11.5a. The scheme of the experiments with the combustion initiating at the bottom part of the wedge-shaped support.

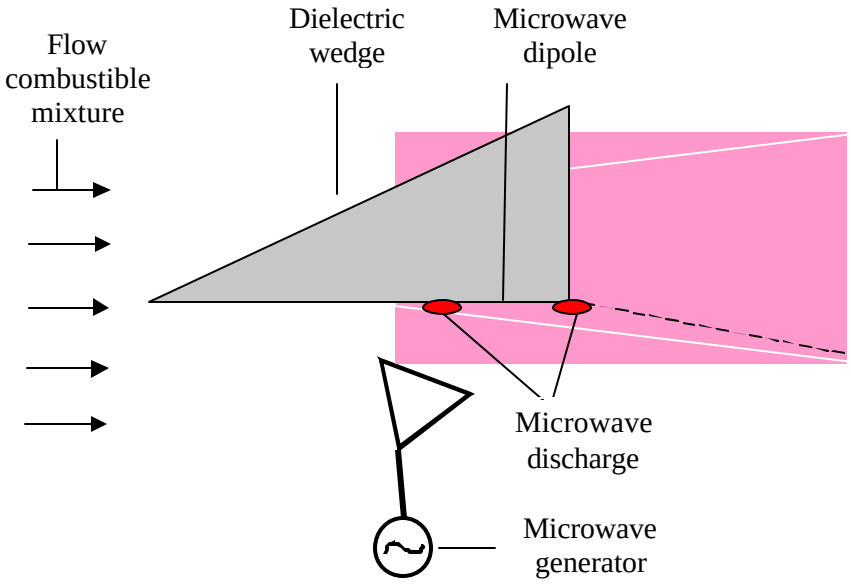

Fig.11.5b. The scheme of the experiments with the combustion initiating at the lateral part of the wedge-shaped support.

The metallic pipe is located in the same hole it simultaneously presents the discharge initiating microwave vibrator. In such a scheme not only the possibility of the ignition can be investigated but the process of the fuel-air mixing as well.

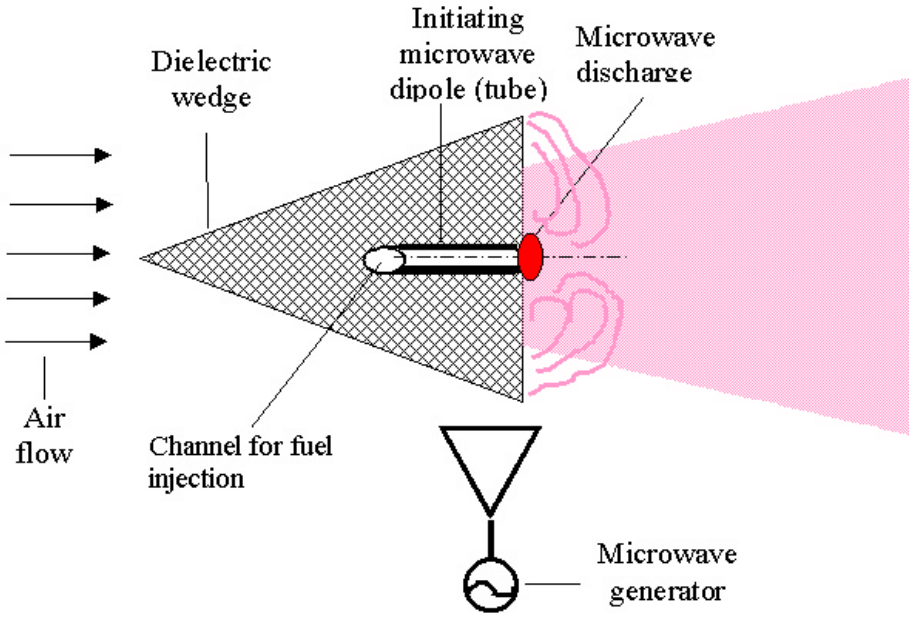

Fig.11.6a. The scheme of the experiments with the fuel injection at the bottom part of the wedge and the combustion initiating at the same place.

The fuel can be injected from the side of the weigh, for example, as it is shown on Fig.11.6b. In this case the vibrator initiating discharge is located below along the flow than the place of the fuel injection.

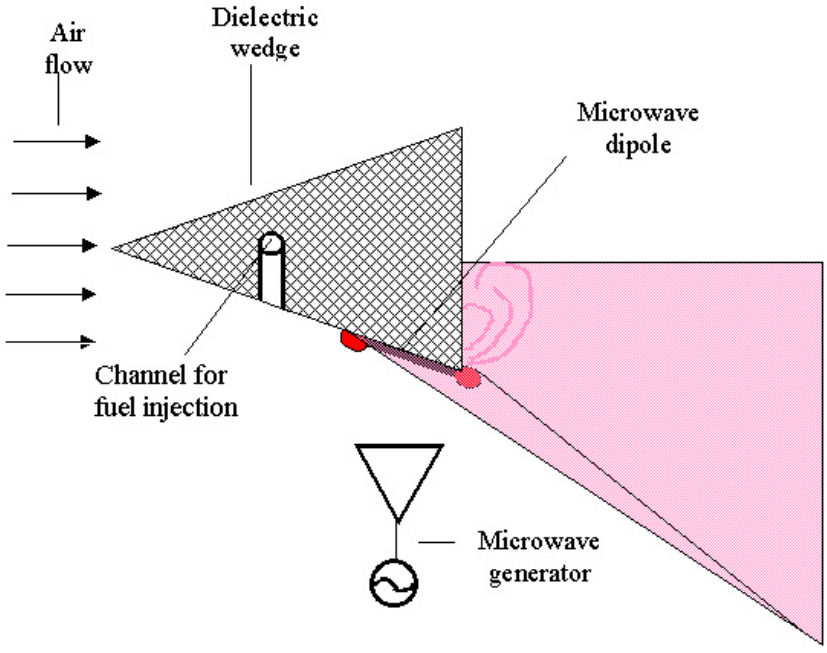

Fig.11.6b. The scheme of the experiments with the fuel injection at the lateral part of the wedge and the combustion initiating below along the flow.

Conclusion

In the frame of the present Project during the first stage of works the experimental setup was considerably modernized. It was previously used in the frame of the special Project SPS-97-4003. The setup was additionally equipped by the microwave generator at $\lambda = 12.5$ cm, by the pulsed supersonic wind tunnel, and by the device of the model flammable mixture's feeding to the discharge region.

The fulfilled experimental program included the following main investigation directions:

1. Investigations of the generator at $\lambda = 12.5$ cm characteristics and of the quasi-optic beam of the travelling electromagnetic wave.
2. Works on the local absolute measurements of the field's amplitude in the quasi-optic microwave beam.
3. Refinement of properties of free localized streamer undercritical discharge and of deeply undercritical initiated microwave discharge in the "separating" and the "attached" forms as well.
4. Determination of the boundary between undercritical and deeply undercritical discharges in respect to air pressure and to the level of the microwave field.
5. Investigations of properties of streamer undercritical and deeply undercritical discharges in the supersonic airflow.
6. Determination of the electromagnetic field's wavelength influence the characteristics of streamer initiated discharges.
7. Refinement of the gas temperature in the streamer channels of the microwave discharges in the "separating" and the "attached" forms.
8. The demonstration of the model flammable mixture's ignition at the application of the initiated undercritical and deeply undercritical microwave discharges.

In the frame of the theoretical support of the experimental program and of the summarizing of obtained results the investigations were carried out in the following directions:

1. The calculations of the field increasing coefficient for initiators with subresonant and resonant length.
2. The calculation of the undercriticality. coefficient in presence of the initiating bodies in the form of a ball or of the thin vibrator with the electron diffusion influence taking into account.
3. The design of the theory model of the microwave discharge at the any value of the parameter of undercriticality and speed of the flow.
4. The executing of the numerical investigation of the properties of initiated discharge of attached and separated form.

The following main results were obtained during the undertaken experiments:

The region of the realization of the undercritical "separating" discharges in respect to the field's level becomes wider with the rise of the pressure. For

example, such a discharge at the atmospheric pressure can be ignited at the under criticality field level up to the value equal to 17. In this case the microwave beam power can be decreased more than by 300 times in comparison with the power of the beam necessary for the ignition of the non initiated discharge. Deeply undercritical initiated discharge in the "attached" form can be ignited at the under criticality level equal to several hundreds at the total beam's power of kilowatts.

Properties of the undercritical discharge practically does not change during its realization in the airflow at velocities about several hundreds meters per second. Deeply undercritical discharge can be ignited in such high-speed flow. In this case some of its properties change so it requires the future investigation.

Experimentally was demonstrated that discharges in the "separating" and the "attached" forms ignite the model flammable mixture.

The results of the theoretical investigations have agreed with the experimental observations quite well and significantly have added of them. In particular:

1. The simulation results allow to forecast that the initiated discharges of both attached and separated form are able to be sustained in the stream moving with velocity up to 1 km/s.
2. The channel temperature in the high-speed flow finding by the modeling is more than 3000K. It allows to suppose that the initiated discharge is able to ignite the combusting mix moving with high velocity.

On the basis of the fulfilled works the proposal on the application of the undercritical microwave streamer discharge for the fuel ignition in the jet engine has been developed. From the point of view of the device it is first of all connected with the realization of the model mixture's ignition in the high-speed flow including the supersonic case. From the ideological point of view it is connected with the determination of the minimum duration and field's level insuring the ignition of the model mixtures. It includes the investigation of the possibility of the ignition in the high-speed flow in itself, the investigation of the discharge influence the characteristics of the model flammable mixture's combustion in a flow, and the investigation of the possible discharge influence the mixing characteristics of the fuel and the oxidizer.[4]

References

1. O.Woskoboynikova. Preprint of tThe Keldysh Applied Mathematics Institute RAS. 1998 #

2. H.C.Pocklingnon. Camb. Phil. Soc. Proc., 9, 324 (1897)

3.L.A.Winestein. The waves of current in a thin cylindrical conductor. Part II.. Zhurnal tehnicheskoy fiziki 1959, No. 6, p. 689-699. Part III. Zhurnal tehnicheskoy fiziki 1961, No.1, p. 29-44.